Broadband Microstrip Antennas with Switchable Polarizations

by

Bombale Uttam Laxmanrao

A Thesis submitted in partial fulfillment of the requirements for the degree of

Doctor of Philosophy

in

Information and Communication Technology

of

Dhirubhai Ambani Institute of Information and Communication Technology

July 2010

Declaration

This is to certify that

(i) the thesis comprises my original work towards the degree of Doctor of Philosophy in Information and Communication Technology at DA-IICT and has not been submitted elsewhere for a degree,

(ii) due acknowledgement has been made in the text to all other material used.

Bombale Uttam Laxmanrao

(200321001)

Signature of Student

Certificate

This is to certify that the thesis work entitled “Broadband Microstrip Antennas with Switchable Polarizations” has been carried out by Bombale Uttam Laxmanrao (ID: 200321001) for the degree of Doctor of Philosophy in Information and Communication Technology at this Institute under my supervision.

Sanjeev Gupta
Thesis Supervisor

Abstract

Microstrip antenna consists of a patch of metallization on grounded substrate. These are low profile, lightweight antennas, most suitable for aerospace and mobile application. They are replacing many conventional antennas used in defense and commercial applications. They have got certain drawbacks such as narrow bandwidth, low gain, and low power handling capability and polarization impurity. Many researchers are trying to overcome these drawbacks.

In this thesis also some efforts have been done to overcome certain drawbacks of microstrip antenna. One of the serious limitations of the microstrip antennas is its narrow bandwidth. The impedance bandwidth of MSA is around 1% only for thin substrates. The bandwidth of the MSA can be increased by increasing thickness of the substrate. If the thickness is increased it creates problems for impedance matching, produces radiations from the feed and distortions in the radiation patterns due to higher order modes. Therefore to avoid these problems thicker substrate is not used. The common techniques to improve bandwidth are Planner multiresonator configurations, Electromagnetically coupled MSA; Aperture coupled MSAs, Impedance matching networks for broad band MSAs & Log periodic MSA configurations. It is advantageous to use Electromagnetically coupled MSA because of its small size and no back radiations. Therefore Electromagnetically coupled MSA is used to design the antenna. The MSA gives linear polarization. Many times we need circular polarization with low cross polar level (generally below 10-12 dB). This circular polarization is obtained in this antenna using a shorting pin. This is the major achievement. Many papers discuss about bandwidth only, a few papers discuss just about polarizations using shorting pins.

Many times we need large bandwidth, desired polarization and high gain. In order to obtain high gain we have to form an array of antennas. It is convenient to feed the array elements using microstrip feed. Therefore the Electromagnetically coupled MSA is fed using a microstrip line as described in chapter 4. Some times we need right circular or

left circular or linear polarization depending on situation. These polarizations can be obtained using two shorting pins instead of one as described in chapter 4.

In satellite TV transmission vertical and horizontal polarizations (Eθ and EΦ) are used. In order to minimize adjacent channel interference they are placed alternately on vertical and horizontal polarizations. These additional Eθ, EΦ polarizations as well as RHCP and LHCP are obtained using additional shorting pins as described in chapter 4. for satellite TV transmission we need high gain around 30 dB. This can be obtained using an array of above elements. The design is given in chapter 4. Various feeding techniques, transmission lines, bends, power dividers and quarter wave transformers are discussed. Spacefed microstrip antennas are also designed, simulated and studied in chapter 5.

Recently fractal antennas are becoming very popular because of their small size, multiband response and high efficiency. The basic types of fractal antennas are designed and simulated in chapter 6. Bandwidth is the major problem in microstrip antennas. In chapter 7, it is discussed how do we get large bandwidth, and the concept is used to obtain very large or ultra-wide bandwidth using rectangular microstrip antenna. The same concept is used to obtain very large bandwidth using sierpinski fractal antennas.

Acknowledgements

The author would like to express his gratitude to Prof. Sanjeev Gupta, for his valuable guidance, assistance and tolerance throughout the course of this research work.

In addition, the author is most grateful to the Director, DA-IICT for his permission to pursue this research at DA-IICT. Thanks are due to Prof. Samaresh Chatterji, Prof. V.P. Sinha, Prof. Deepak Ghodgaonkar, Prof. C. Vijaykumar, Prof. Hemant Patil for their cooperation and encouragement during this research work.

The author also acknowledges the support of DA-IICT for providing financial assistance and making available various resources required to carry out this research work. The author is also thankful to his parent Institute, Terna Engineering College, Navi Mumbai for granting study leave for this research work.

Further the author would like to express particular thanks to his family members for their continued patience and understanding.

List of Publications

In International Journals:

[1] Uttam L. Bombale and Sanjeev Gupta., "Broadband Planar Array with Switchable Polarizations"**,** *Microwave and Optical Technology Letters,* Volume 49, Issue 10, 27 July 2007, pp. 2415 – 2419.

[2] Uttam L. Bombale and Sanjeev Gupta., "Compact Broadband Planar Array For C-Band Applications", *Submitted to International Journal of Electronics.*

[3] Uttam L. Bombale and Sanjeev Gupta., "Broadband High Efficiency Planar Array For C-Band Applications", *Submitted to Springer.*

[4] Uttam L. Bombale and Sanjeev Gupta, "Design of Wideband Microstrip Antenna Using Smaller Size Ground than the Radiating Patch", *Submitted to IEEE Transactions on Antennas and Propagation.*

[5] Uttam L. Bombale and Sanjeev Gupta, "Multi-Polarization Planar Array for C-Band", *Submitted to IEEE Transactions on Antennas and Propagation.*

In International Conferences:

[1] Uttam L. Bombale and Sanjeev Gupta, "A Compact Broadband All Polarization Microstrip Antenna", *Proceedings of 2nd International Conference on Microwaves, Antenna, Propagation and Remote Sensing (ICMARS-2004)*, Jodhpur, India, November 23-25, 2004.

[2] Bombale, U.L. and Gupta, S., "Multi-polarization Planar Array for Satellite TV Reception**",** *Proceedings of IEEE International Symposium on Microwave, Antenna, Propagation and EMC Technologies for Wireless Communications, 2005 (MAPE-2005),* August 8-12, 2005, pp. 273 – 276.

[3] Uttam L. Bombale and Sanjeev Gupta, "Wide Band Multi-Polarization Planar Array" *Proceedings of Twelfth National Conference on Communications (NCC-2006)*, IIT Delhi, New Delhi, India, January 27-29, 2006, pp. 429-433.

[4] U.L. Bombale and S. Gupta, “Design of Ultra Wideband Microstrip Antenna” *Proceedings of 2006 IEEE AP-S International Symposium on Antennas and Propagation and USNC/URSI National Radio Science Meeting*, Albuquerque, New Mexico, USA, July 9 - 15, 2006, pp. 3705-3708.

Contents

Page No.

List of Principal Symbols

λ	Wavelength
μ	Permeability of a medium
θ	Angle
c	Velocity of light
C	Capacitance
E	Electric field
h	Height
H	Magnetic field
I	Current
k	Boltzmann's constant
k_o	Propagation constant in free space
Y	Admittance
Z	Impedance
ϵ	Dielectric constant
ϵr	Effective dielectric constant
Ω	Angular frequency
φ	Azimuth angle
θ	Elevation angle
D	Directivity of the antenna
f_0	Resonant frequency
G	Gain of the antenna
H	Height of the substrate
k_{mn}	Free space wave number
L	Length of the square patch
W	Width of the patch

Other minor symbols are defined at first occurrence; where necessary some symbols are redefined in the text.

Acronyms

DC	Direct Current
GaAs	Gallium Arsenide (Semiconductor Material)
MSA	MicroStrip Antenna
BW	Bandwidth
VSWR	Voltage Standing Wave Ratio
CP	Circularly Polarized
LHCP	Left Hand Circularly Polarized
RHCP	Right Hand Circularly Polarized
AR	Axial Ratio
RMSA	Rectangular Microstrip Antenna
SMSA	Square Microstrip Antenna

List of Figures

List of Tables

Page No.

Index

Page No.

1 Introduction

1.1 Introduction

There are many emerging applications, such as mobiles, pagers, wireless local loops, weight sensitive vehicles, rockets, missiles, satellites, radars, communication and navigational systems etc. which require broadband, high gain and properly polarized radiations. For such applications, microstrip antennas are particularly attractive due to their low profile, light weight, and easy fabrication. They have got certain drawbacks such as narrow bandwidth, low gain, and low power handling capability and polarization impurity. But above applications require broad bandwidth.

The impedance bandwidth of Microstrip Antenna (MSA) is around 1% only for thin substrates. The bandwidth of the MSA can be increased by increasing thickness of the substrate. If the thickness is increased, it creates problems for impedance matching, produces radiations from the feed and distortions in the radiation patterns due to higher order modes. Therefore to avoid these problems thicker substrate is not used. The common techniques to improve bandwidth are planar multi-resonator configurations, electromagnetically coupled MSAs, aperture coupled MSAs, Impedance matching networks for broad band MSAs & Log periodic MSA configurations. It is advantageous to use electromagnetically coupled MSA because of its small size and no back radiations. Therefore electromagnetically coupled MSA is used to design the antenna.

The MSA gives linear polarization. Many times, circular polarization with low cross polar level (generally below 12 dBs) is required. This circular polarization is obtained in this antenna using a shorting pin. This is the major achievement in this work. Many papers discuss about bandwidth only. Electromagnetically coupled microstrip antenna, as shown in Figure 1.1, can be used to obtain wide bandwidth. A few papers discuss just about polarizations using shorting pins where we get various polarizations but very narrow bandwidth around 1% only as shown in figure 1.2. There is no reported work which gives wide bandwidth as well as desired polarization. Figure 1.3 shows the

antenna which gives wide bandwidth as well as the desired circular polarization. It is the combination of figures 1.1 and 1.2. This is the novel design and major achievement in this work.

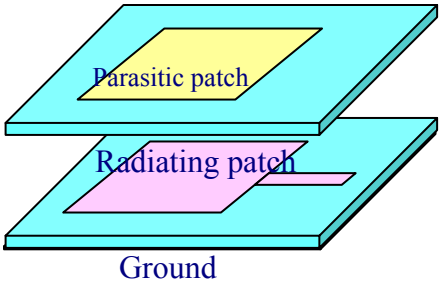

Figure 1.1 Electromagnetically coupledmicrostrip fed MSA (for wide bandwidth only)

+

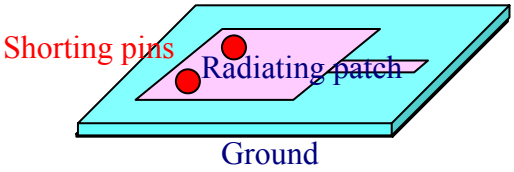

Figure 1.2 Ordinary MSA (for desired polarization only)

=

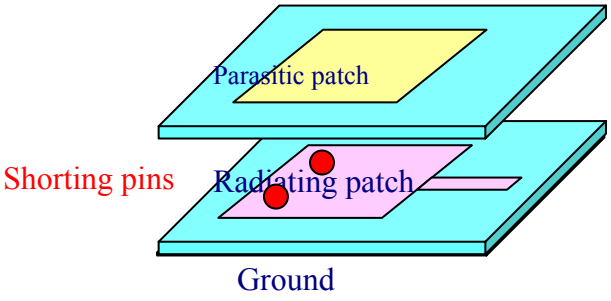

Figure 1.3 Electromagnetically coupled microstrip fed MSA (for wide bandwidth & desired polarization)

By increasing the number of shorting pins in the above design, one can obtain horizontal, vertical, RHCP or LHCP. One can get more gain by forming the array of above antennas. With this array, wide bandwidth, switchable polarizations and high gain could be achieved [1]. These are the important properties of an antenna system. Antenna system with these capabilities can also be used in smart antennas [2-11].

Small size multiband antennas are very important in mobile communication. These antennas are also designed and analysed even to obtain wide band operation.

1.2 Organisation of the Thesis

Microstrip antenna consists of a patch of metalization on grounded substrate. These are low profile, lightweight antennas, most suitable for aerospace and mobile application. They are replacing many conventional antennas used in defense and commercial applications. They have got certain drawbacks such as narrow bandwidth, low gain, and low power handling capability and polarization impurity. Many researchers are trying to overcome these drawbacks.

In this thesis also, some efforts have been made to overcome certain drawbacks of microstrip antenna. The motivation behind the thesis is described in the first chapter. In this thesis various types of patch antennas and arrays are developed which can be used in smart antennas as well as other applications. Chapter 2 describes the basics of microstrip antennas, its advantages, drawbacks and various methods to overcome the drawbacks.

Chapter 3 describes design of a compact wideband antenna. A patch of 25×30 mm^2 gives very wide bandwidth. The actual design and the theoretical results are presented in this chapter. It also describes design of compact wideband patch antenna, which covers the frequency range from 3.7 to 4.5 GHz. The actual design, theoretical results and radiation pattern with polarization levels are presented in this chapter.

Chapter 4 describes compact broadband electromagnetically coupled microstrip antenna which produces linear, right circular and left circular polarization. The actual design, simulated results and radiation pattern with polarization levels are presented in this chapter.

In satellite TV transmission, vertical and horizontal polarizations (Eθ and EΦ) are used. In order to minimize adjacent channel interference, these are placed alternately on vertical and horizontal polarizations. These additional Eθ, EΦ polarizations as well as RHCP and LHCP are obtained using additional shorting pins for satellite TV transmission where high gain of the order of 30 dB is required. This can be obtained using an array of above elements. The design of patch antenna, design of array and the theoretical results are also given in chapter 4. Various feeding techniques, transmission lines, bends, power dividers and quarter wave transformers are discussed.

Space-fed microstrip antennas are also designed, simulated and studied in chapter 5. Now a days, fractal antennas are becoming very popular because of their small size, multiband response and high efficiency. The basic types of fractal antennas are designed and analysed. Bandwidth is the major problem in microstrip antennas. In chapter 6, it is discussed how do we get large bandwidth, and the concept is used to obtain very large or ultra-wide bandwidth (UWB) using rectangular microstrip antenna. The same concept is used to obtain very large bandwidth using sierpinski fractal antennas. These antennas are designed and analysed in this chapter.

2 Microstrip Antennas

2.1 Introduction

The rapidly growing communication industry demands for smaller and low profile antennas have put the microstrip antennas (MSA) to the forefront [12-16]. An MSA in its simplest form consists of a radiating patch on one side of a thin dielectric substrate backed by a ground plane. The radiating patch could be of any arbitrary shape but generally regular shapes are considered for ease of analysis and design. One of the simplest and widely used configurations is rectangular MSA as shown in figure 2.1. A rectangular patch is defined by its length L and width W. for a simple microstrip line the width is much smaller than the wavelength. However, for the RMSA, the width is comparable to the wavelength to enhance radiation from edges. The thickness is much smaller than the wavelength.

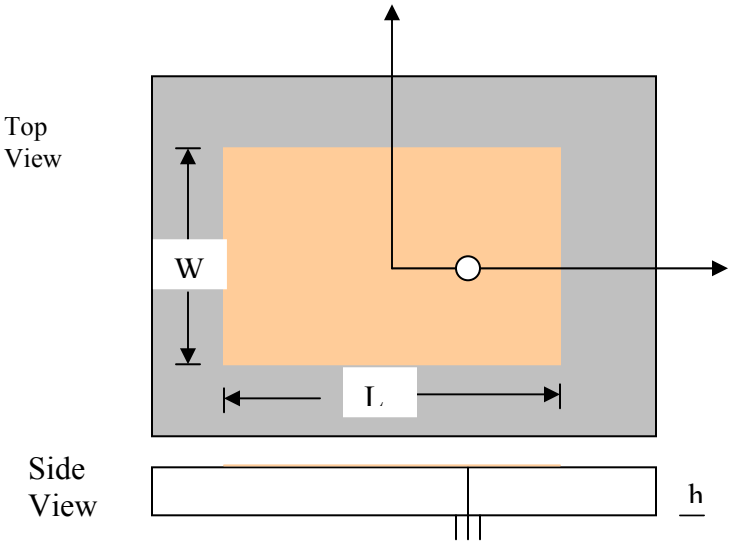

Figure 2.1 Mircostrip antenna

For the fundamental TM_{10} mode, the length L should be slightly less than $\lambda/2$, where λ is wavelength in dielectric medium. $\lambda=\lambda_0/(\epsilon_e)^{0.5}$, where λ_0 is free space wavelength and ϵ_e is the effective dielectric constant. The value of ϵ_e is slightly less than ϵr, because the fringing fields around the periphery of the patch are not confined in the dielectric substrate but are also spread in air as shown in figure 2.2.

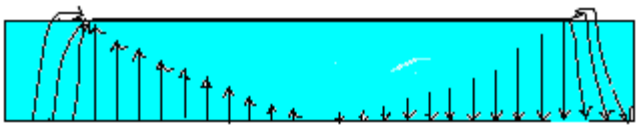

Figure 2.2 Fields in mircostrip antenna

The fundamental mode TM_{10} implies that the field varies one $\lambda/2$ cycle along the length, and there is no variation along the width of the patch. Along the width of the patch, the voltage is maximum and current is minimum due to the open end. It may be observed from figure 2.2 that the vertical components of the electric field at the two edges along the width are in opposite directions and hence cancel one another in the broadside direction, whereas the horizontal components are in same direction and hence combine in the broadside direction. Therefore edges along the width are termed as radiating edges. The fields due to the sinusoidal distribution along the length cancel in broadside direction, and hence edges along the length are known as non-radiating edges [17]. The fringing fields along the width can be modeled as radiating slots as shown in figure 2.3.

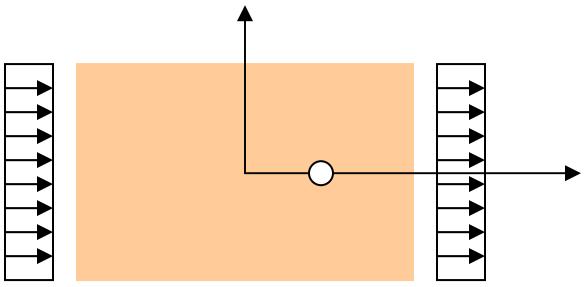

Figure 2.3 Radiating edges of microstrip antenna

2.2 Advantages of Microstrip Antennas

The main advantages of microstrip antennas are:

a) The microstrip antennas are lightweight and have small volume and low profile planar configuration.

b) They can be made conformal to the host surface.

c) Their ease of mass production using printed circuit technology leads to a low fabrication cost.

d) They are easier to integrate with other MIC's on the same substrate.

e) They allow to both linear and circular polarization.

f) They can be made compact for use in personal mobile communication.

g) They allow for dual and triple frequency operation.

2.3 Drawbacks of Microstrip Antennas

The main drawbacks of microstrip antennas are:

a) They are narrow band.

b) They are having low gain.

c) They are having low power handling capability.

d) They do not offer polarization purity.

In this thesis, efforts have been made to overcome above drawbacks using proper techniques. One of the serious limitations of the microstrip antennas is its narrow bandwidth. The impedance bandwidth of MSA is around 1% only [19] for thin substrates. The VSWR or impedance bandwidth of the MSA is defined as the frequency range over which it is matched with that of the feed line within specified limits. The bandwidth of the MSA is inversely proportional to its quality factor Q and is given by

$$BW = \frac{(VSWR - 1)}{Q\sqrt{VSWR}}$$

In order to increase the bandwidth, Q should be decreased. The required value of Q can be obtained by varying dielectric constant ϵ_r and thickness h. The Q increases with increase in dielectric constant ϵ_r. It decreases with increase in h. In order to increase the bandwidth, simply increasing the substrate height keeping dielectric constant low, will create following problems [18]:

1) Substrates thicker than $0.11\lambda_0$ for $\epsilon_r = 2.2$ make the impedance locus of the probe fed patch antenna increasingly inductive in nature, resulting in impedance matching problem.

2) Thick substrate with microstrip edge feed will give rise to increased spurious radiation from the microstrip step in width and other discontinuities. Radiation from probe feed will also increase.

3) Higher order modes along the thickness may develop, giving rise to distortions in the radiation patterns and impedance characteristics. This is a limiting factor in achieving octave bandwidth.

Therefore to avoid above problems thicker substrate is not used to obtain wide bandwidth. The common techniques to improve bandwidth are as follows:

a) Planar multi-resonator configurations: The planner multiresonator gives bandwidth around 20%. The drawback of this configuration is its large planner size[20].

b) Electromagnetically coupled MSA: With this configuration we can obtain 10% to 30% bandwidth. The increase in the bandwidth is obtained due to increase in the overall height of the antenna, a decrease in the effective dielectric constant ϵ_e and the multi-resonator effect [17].

c) Aperture coupled MSAs : Aperture coupled elements have been demonstrated with bandwidths up to 10 - 15% with a single layer[22]-[24], and up to 30-50% with a stacked patch configuration [25]-[28].

d) Impedance matching networks for broad band MSAs: The complexity and losses of the matching network generally limit the achievable bandwidth of the antenna to about 10% to 30% [18, 29]

e) Log periodic MSA configurations.

2.4 Wave Polarization

Microstrip antennas are having many advantages as compared to the conventional antennas.they are having few drawbacks such as narrow bandwidth, high cross polarization levels or low polarization purity, low gain and low power handling capability. How to increase bandwidth of microstrip antenna is already discussed in the previouse chapter. In this chapter we shall discuss about polarization, the types of polarization and the various methods to achieve these polarizations.

Antenna polarization is a very important consideration when choosing and installing an antenna. Most communications systems use either vertical, horizontal or circular polarization. Knowing the difference between polarizations and how to maximize their benefit is very important to the antenna user. A linear polarized antenna produces linearly polarized wave, a circular polarized antenna produces circularly polarized wave. Recently, the microstrip antenna with switchable polarizations [30-37] has received much attention because it is useful for some specific application in wireless communication, such as multi-system operation, frequency reuse and reducing multipath fading. The various types of wave polarizations are explained in detail in the following section.

An important property of an electromagnetic wave is its polarization, a quantity describing the orientation of the electric field E [38]. Consider a plane wave traveling out of the page (positive z direction), as in Figure 2.4, with the electric field at all times in the *y* direction. This wave is said to be linearly polarized (in the *y* direction). As a function of time and position the electric field of a linearly polarized wave, as in Figure 2.9(a), traveling in the positive z direction (out of the page) is given by

$$E_y = E_2 \sin(\omega t - \beta z)$$

In general, the electric field of a wave traveling in the z direction may have both a *y* component and an x component, as suggested in Figure 2.4 (b). In this more general situation the wave is said to be *elliptically polarized.* At a fixed value of z the electric

vector E rotates as a function of time, the tip of the vector describing an ellipse called the *polarization ellipse.* The ratio of the major to minor axes of the polarization ellipse is called the *axial ratio* (AR). Thus, for the wave in Figure 2.4 (b), $\mathrm{AR} = \mathrm{E}_2/\mathrm{E}_1$. Two extreme cases of elliptical polarization correspond to *circular polarization,* as in Figure 2.4 (c), and *linear polarization,* as in Figure 2.4 (a). For circular polarization $E, = E_2$ and AR = 1, while for linear polarization $E, = 0$ and AR = ∞.

In the most general case of elliptical polarization the polarization ellipse may have any orientation, as suggested in Figure 2.5. This elliptically polarized wave may be expressed in terms of two linearly polarized components, one in the x direction and one in the *y* direction. Thus, if the wave is traveling in the positive z direction (out of the page), the electric field components in the x and *y* directions are

$$E_x = E_1 \sin(\omega t - \beta z) \tag{2.1}$$

$$E_y = E_2 \sin(\omega t - \beta z + \delta) \tag{2.2}$$

where E_1 = amplitude of wave linearly polarized in x direction

E_2 = amplitude of wave linearly polarized in *y* direction

δ= time-phase angle by which E_y leads E_x

Combining (2.1) and (2.2) gives the instantaneous total vector field **E**:

$$\mathbf{E} = \boldsymbol{x}\, E_1 \sin(\omega t - \beta z) + \mathbf{y}\, E_2 \sin(\omega t - \beta z + \delta) \tag{2.3}$$

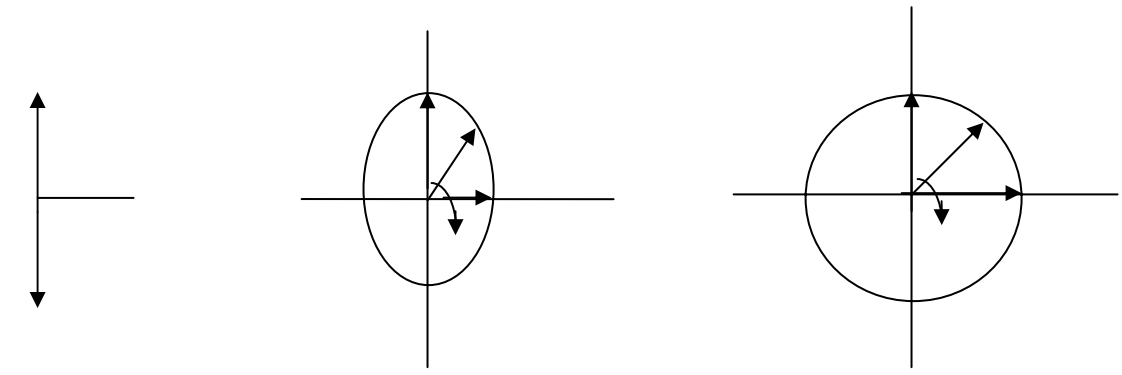

(a) Linear polarization (b)Elliptical polarization (c) Circular polarization

Figure 2.4 Linear, Elliptical and Circular polarization for wave propagation out of page

$$\text{At z} = 0,\ E_x = E_1 \sin(\omega t - \beta z) \text{and}\ E_y = E_2 \sin(\omega t - \beta z + \delta) \tag{2.4}$$

Expanding E_y yields

$$E_y = E_2(\sin \omega t \cos\delta + \cos \omega t \sin\delta) \tag{2.5}$$

From the relation for we have $\sin \omega t = E_x / E_1$ and $\cos \omega t = \sqrt{1 - (E_x / E_1)^2}$

Introducing these in (2.4) eliminates *rot,* and on rearranging we obtain

$$\frac{E_x^2}{E_1^2} - \frac{2E_x E_y \cos\delta}{E_1 E_2} + \frac{E_y^2}{E_2^2} = \sin^2\delta \tag{2.6}$$

$$\text{Or}\ \ aE_x^2 - bE_x E_y + cE_y^2 = 1 \tag{2.7}$$

$$\text{where } a = \frac{1}{E_1^2 \sin^2\delta} \qquad b = \frac{2\cos\delta}{E_1 E_2 \sin^2\delta}$$

$$c = a = \frac{1}{E_2^2 \sin^2\delta}$$

Equation (2.7) describes a (polarization) ellipse, as in Figure 2.4. The line segment *OA* is the semi major axis and the line segment *OB* is the semi minor axis. The tilt angle of the ellipse is τ . The axial ratio is

$$AR = \frac{OA}{OB} \qquad (1 \le AR \le \infty) \tag{2.8}$$

For $E_1 = 0$, the wave is linearly polarized in the *y* direction. For $E_2 = 0$, the wave is linearly polarized in the x direction. If $\delta = 0$ and $E_1 = E_2$, the wave is also linearly polarized but in a plane at an angle of 45° with respect to the x axis

$(\tau = 45^0)$

For $E_1 = E_2$ and $\delta = \pm 90^0$ the wave is circularly polarized. When $\delta = +90^0$ the wave is *left-circularly polarized,* and when $\delta = -90^0$ the wave is *right-circularly polarized.* For the case $\delta = +90^0$ and for $z = 0$ and $t = 0$ we have from (2.1) and (2.2) that

$E = \hat{y}E_2$, as in Figure 2.6 (a). One-quarter cycle later ($\omega t = 90^0$) $E = \hat{x}E_1$ as in Figure 2.6(b). Thus, at a fixed position ($z = 0$) the electric field vector rotates clockwise (viewing the wave approaching). According to the IEEE definition, this corresponds to left-circular polarization. The opposite rotation direction ($\delta = -90^0$) corresponds to right-circular polarization.

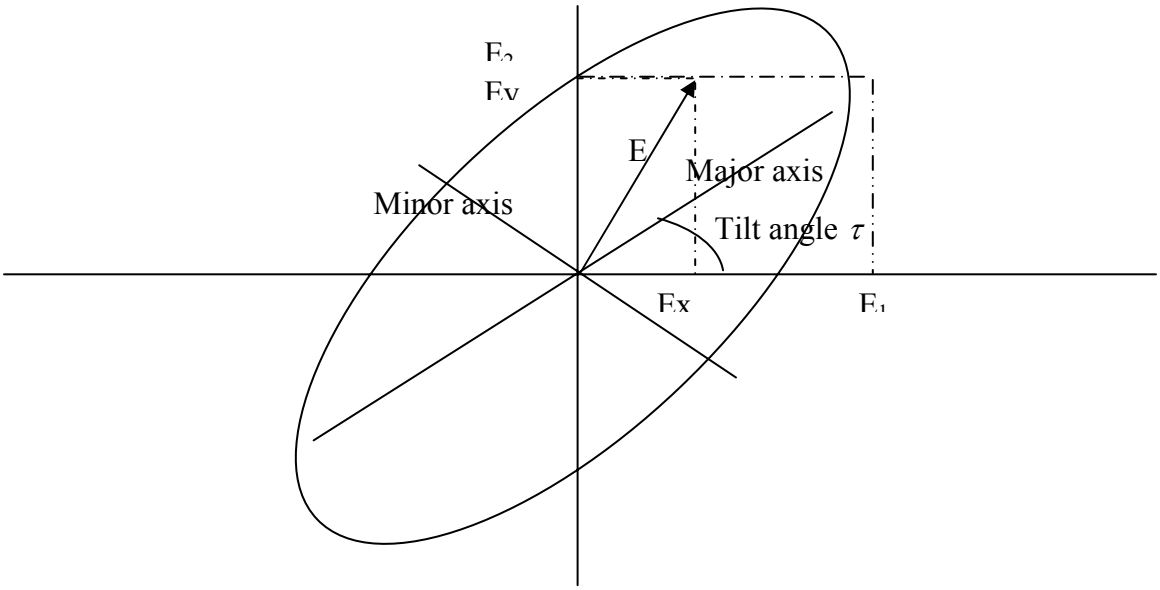

Figure 2.5 Polarization ellipse at tilt angle τ showing instantaneous components E_x and E_y and amplitudes (or peak values) E_1 and E_2.

Polarization ellipses, as a function of the ratio E_1 / E_2 and phase angle δ (wave approaching), are shown in Figure 2.6. In special cases, the ellipses become straight lines (linear polarization) or circles (circular polarization).

If the wave is viewed receding (from negative *z* axis in Figure 2.6), the electric vector appears to rotate in the opposite direction. Hence, clockwise rotation of E with the wave approaching is the same as counterclockwise rotation with the wave receding. Thus, unless the wave direction is specified, there is a possibility of ambiguity as to whether the wave is left- or right-handed. This can be avoided by defining the polarization with the

aid of helical antennas. Thus, a right-handed axial-mode helical antenna radiates (or receives) right circular (IEEE) polarization. A right-handed helix, like a right-handed screw, is right-handed regardless of the position from which it is viewed. There is no possibility here of ambiguity.

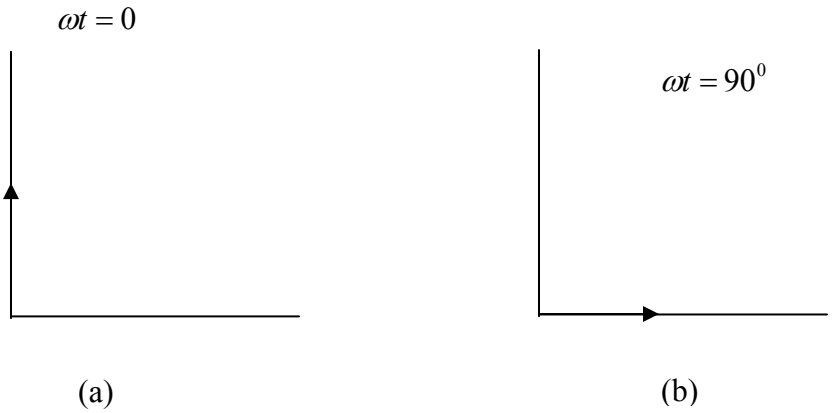

Figure 2.6 Instantaneous orientation of electric field vector *E* at two instants of time for a left-circularly polarized wave which is approaching (out of page).

Following section describes applications of microstrip antennas and how to produce various types of polarizations using the microstrip antennas.

2.5 Loaded Microstrip Antenna

Modern communication systems, such as those for satellite links (GPS, vehicular-Jar, etc.), for mobile communication, and for emerging applications, such as Wireless local-area networks (WLANs), often require compact antennas at low cost [12-16] Further, due to their lightness, microstrip antennas are well suited for airborne applications, such as synthetic aperture radar (SAR) systems and scatterometers. In addition to compactness, the antenna may be required to provide circular polarization as in satellite links. In some applications, operation at two or more discrete bands and an

arbitrary separation of bands is desired. Further, all bands may be required to have the same polarization, radiation Pattern, and input impedance characteristics.

It may not be possible to achieve these objectives from the basic microstrip antennas having regular shapes that have been discussed in earlier chapters. The range of applications of micros trip antennas and their performance can be improved considerably by suitably loading them. Some examples of loaded microstrip antennas are given in next chapters, where loadings of the basic shape was used to obtain circular polarization, frequency tuning, broadbanding, impedance matching, higher gain, and so on. It is the goal of this chapter to discuss loading in a general way to obtain characteristics such as size reduction, dual-frequency operation, polarization control, radiation pattern control, and frequency agility [18].

A survey of various papers published on the applications of microstrip antennas shows that shorts, stubs, and slot loadings have been used for the most part. Therefore, we consider only the effect of these loadings although loading can take various forms such as stub loading, slot or notch loading, short circuits or vias, parasitic coupling, substrate loading, superstrate cover, resistors, capacitors, and diodes.

A microstrip antenna can easily be made to resonate at many frequencies associated with various modes. The characteristic of each mode is different and is determined by the resonant frequency, radiation pattern, polarization, bandwidth and so on. For a given feed location, if the patch is now loaded with a short, the field and current distributions for various modes will be disturbed and therefore their characteristics will change. This change will depend on the amount of load and the mode under consideration. For example, a short placed at the nodal line of a mode will hardly affect its characteristics, whereas another mode with electric field maximum at the short will experience the maximum change. If used properly, the loading effect can be used to obtain a desirable change in the antenna characteristics.

First, some applications of loaded microstrip antennas to realize polarization diversity, frequency agility, and radiation pattern control are discussed. Next, loading will be used to reduce the size of circularly polarized antennas, and dual-frequency operation antennas. Various types of compact antennas are listed. The planar inverted-F antenna, a compact antenna suggested, is described in detail.

2.6 Polarization Diversity Using Microstrip Antennas

Polarization diversity [25] of reception is important to counter the effect of fading in communications, especially in mobile communications. The polarization of a microstrip antenna can be selected by making a proper choice for the feed location. For example, the square microstrip antenna shown in Figure 2.7 [39] can be used to transmit or receive vertical polarization or horizontal polarization depending on which feed is used and which shorting posts are not used. The two polarizations are associated with the modes (l, 0) and (0, 1) excited by the respective feeds. Simultaneous operation in two polarizations at the same frequency is possible if both feeds are used. If the square patch is replaced by a rectangular patch antenna, then it is possible to have dual-frequency and dual-polarization operation. The square patch antenna of Figure 2.7 when loaded with posts as indicated can be used for generating desired circular polarization by a proper selection of feed. The posts located along the diagonal help in the excitation of both the modes with a single feed. Proper location of the posts ensures equal amplitude and a phase difference of 90° for the two modes.

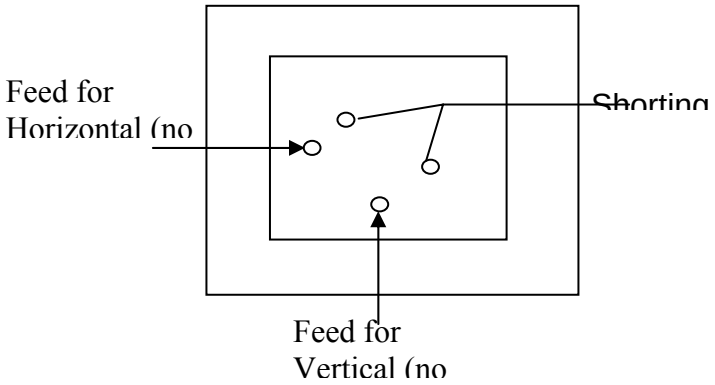

Figure 2.7 dual-feed antenna for horizontal and vertical.[39]

It is also possible to obtain four different polarizations-horizontal, vertical, right-hand circular, and left-hand circular-with a single feed. This is shown in Figure 2.8 for a square patch antenna. The feed is located along the diagonal and the shorting pins are located along the center lines. The polarization of the signal is decided by the selection of the shorting pins, and can be explained on the basis of change in resonant frequency produced by the loading effect of the short.

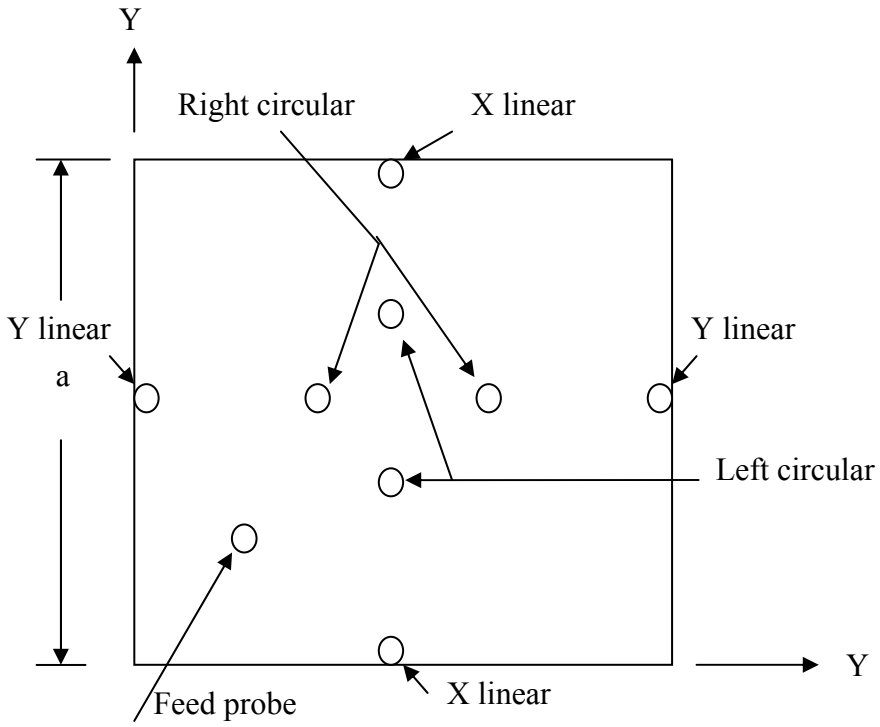

Figure 2.8 Single-feed square patch antenna with four pairs of posts for obtaining four different polarizations.

The square patch, without shorting pins, supports both the (1, 0) and (0, 1) modes with x-oriented and y-oriented polarizations. The resonant frequency for both the modes is the same. Because the feed probe is located along the diagonal, both the modes are excited with equal amplitude and phase. By adding shorting pins along the center line $x = a/2$ (Figure 2.8), the resonant frequency of the (0, 1) or y-oriented mode can be raised without affecting the other mode. Therefore, the mode with desired polarization (x or y) can be selected by shifting the resonant frequency of the undesired mode far above that of

the desired mode. The required large frequency shift is obtained by placing the shorting pins at or near the edges of the patch as shown in the figure.

Circular polarization is obtained by exciting both the *x*- and y-polarized modes with equal amplitude and 90° phase difference. This can be accomplished by raising the resonant frequency of one mode slightly above the other and operating at a frequency midway between the two frequencies. Then the input impedance of one mode is inductive and the other mode is capacitive. By adjusting the difference between the resonant frequencies, both the modes can be excited with equal amplitude and 90° phase difference.

The pair of posts inside the patch raises the resonant frequency of one of the modes only. Figure 2.9 [39] shows the measured axial ratio of a typical patch antenna as the separation between a pair of shorting posts is varied.

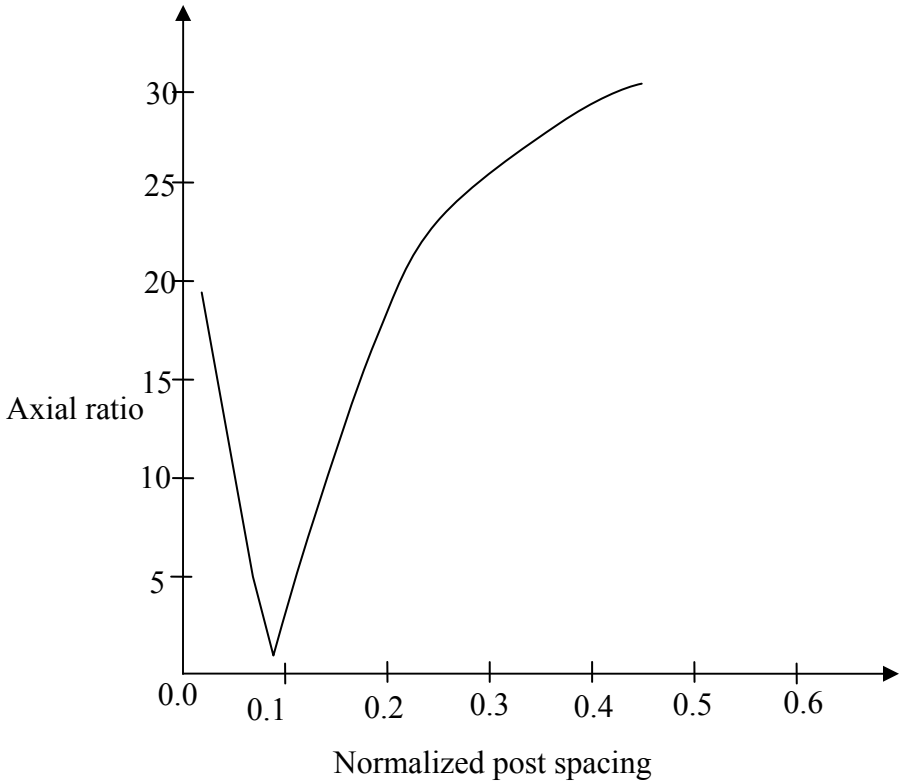

Figure 2.9 Measured axial ratio as a function of post spacing [39] *s/a* for a square patch antenna on a 1.6-mm Teflon fiberglass substrate.

When *s/a* = 0, the posts are at the center and they don't affect either mode. Because both the modes are excited with equal amplitude by the diagonal feed, the polarization is linear oriented along the feed diagonal. When *s/a* = 0.09, the resonant frequencies of the two modes are offset enough to obtain a phase difference of about 90° and the antenna is circularly polarized. As the posts are moved further apart, that is, as they approach the respective edge, the resonant frequency of the vertically polarized mode is further increased and the polarization of the antenna becomes horizontal linear with large axial ratio as shown in the figure. The input impedance of the antenna changes with the movement of the posts, but the VSWR remains good for all senses of polarization. Although one post is sufficient to raise the resonant frequency of any mode, two symmetrically located posts are used so that the antenna structure is symmetric with respect to loading, and the cross-polarized component in the radiation pattern due to loading is minimized. The shorting posts can be realized by microwave switching diodes for precise control of the resonant frequency and polarization switching applications.

2.7 Single-Feed Circularly Polarized Microstrip Antennas

For a circularly polarized radiation, a patch must support the orthogonal fields of the equal amplitude but in phase quadrature. This requirement is accomplished by slightly perturbing a patch at appropriate locations with respect to the feed. However, these perturbation configurations have very narrow axial ratio (AR) and voltage standing wave ratio (VSWR) bandwidths. However, a successful attempt has been made in the present work to improve the axial ratio within the impedance bandwidth for VSWR ≤ 2. In this chapter, we discuss the analysis and optimized designs of single-feed modified square microstrip antennas for enhancement of axial ratio and VSWR bandwidths. The effect on the input impedance and axial ratio for different values of width by keeping length constant of nearly square microstrip antenna is described. Improvement in the axial ratio and VSWR bandwidths on thick dielectric substrate with different values of probe diameter is investigated in the present work. Our analysis is along the lines of the discussions in [40] on the singly-fed microstrip antennas for circularly polarized radiation.

2.7.1 Diagonally-Fed Nearly Square Microstrip Antenna

In this section, a method for designing a circularly polarized microstrip antenna with singly-fed is presented. Depending upon the perturbation the feed location is either on the x or y-axis, or the feed is placed on the diagonal axis of a patch. Note that the feed is always located diagonal to perturbation segments that are appropriately selected to produce two orthogonally degenerate modes in the patch for circularly polarized radiation. Nearly square microstrip antenna is one of the simplest configurations to generate circularly polarized radiation with feed location along the diagonal as shown in Figure 2.10 (a).

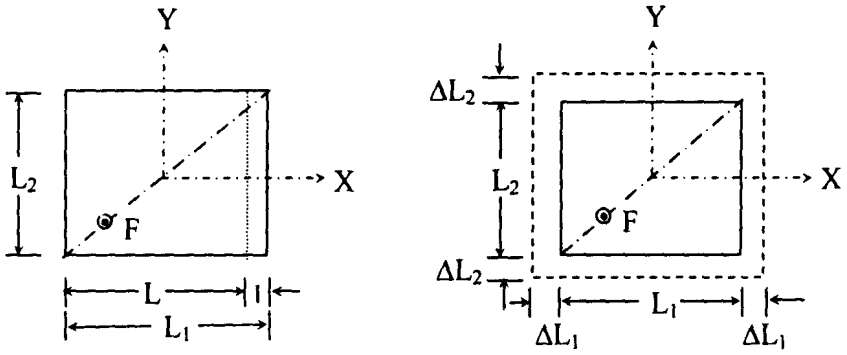

Figure 2.10 (a) Diagonally fed nearly square microstrip antenna, and (b) equivalent diagram of nearly square microstrip antenna in the presence of fringing fields

The patch length (L = L+l), and width (L_2 = L) determines the orthogonal resonant frequencies, and are critical parameters in design because of inherent narrow bandwidth of the patch. In practice, the fields are not confined to the patch. A fraction of the fields lie outside the physical dimension of the patch. This is called the fringing field. Considering the effect of the fringing fields, the effective dimensions of diagonally fed nearly square microstrip antenna are different from the physical dimensions. The extension of the dimension of nearly square microstrip antenna due to the fringing field is shown dotted lines in Figure 2.10 (b). For the fundamental TM_{10} mode, the L_1 should be slightly less than $\lambda/2$, where λ is the wavelength in the dielectric medium. The

fundamental TM_{10} mode implies that the field varies one $\lambda/2$ cycle along the length, and no variation along the width of the patch. A nearly square microstrip antenna operating at TM_{10} mode can be visualized as a transmission line, because the field is uniform along the width and varies sinusoidally along the length. Their equivalent capacitance and the radiation resistance model the fringing fields along the edges and the radiation from the slots. To account for the fringing fields, instead of adding the capacitor at the edges, the dimensions around the periphery of the patch can be extended outwards. This can be explained in terms of the parallel rectangular plates of dimensions L_1 and L_2, which are separated by a dielectric substrate of thickness h. If the fringing fields along the periphery are ignored, then the capacitance of the two parallel plates will be

$$C = \varepsilon_0 \varepsilon_r \frac{L_1 L_2}{h} \tag{2.9}$$

However, due to the fringing capacitance, the effective capacitance C_e of the two parallel plates increases. One of the ways to account for the fringing capacitance is to extend the dimensions of the plate outward, and the value of C_e is calculated from

$$C_e = \varepsilon_0 \, \varepsilon_r \frac{L_{1e} L_{2e}}{h} \tag{2.10}$$

where, L_{1e} and L_{2e} are the effective dimensions and are equal to:

$$L_{1e} = L_1 + 2\Delta L_1 \tag{2.11}$$

And

$$L_{2e} = L_2 + 2\,\Delta L_2 \tag{2.12}$$

The ΔL_1 and ΔL_2 are the extensions along the L_1 and L_2, respectively.

The edge extensions are calculated using the empirical formula [41]:

$$\Delta L_1 = 0.412h \frac{\varepsilon_{re1} + 0.300}{\varepsilon_{re1} - 0.258} \frac{u + 0.264}{u + 0.813} \tag{2.13}$$

where $u = L_2 / h$

$$\varepsilon_{re1} = \frac{\varepsilon_r + 1}{2} + \frac{\varepsilon_r - 1}{2}\left(1 + \frac{10}{u}\right)^{-ab} \tag{2.14}$$

where

$$a = 1 + \frac{1}{49}\ln\left\{\frac{u^4 + (u/52)^2}{u^4 + 0.432}\right\} + \frac{1}{18.7}\ln\left\{1 + \left(\frac{u}{18.1}\right)^3\right\}$$

$$b = 0.564\left(\frac{\varepsilon_r - 0.9}{\varepsilon_r + 0.3}\right)^{0.053}$$

and

$$\Delta L_2 = 0.412h\frac{\varepsilon_{re2} + 0.300}{\varepsilon_{re2} - 0.258}\frac{v + 0.264}{v + 0.813} \tag{2.15}$$

where $v=L1/h$

$$\varepsilon_{re2} = \frac{\varepsilon_r + 1}{2} + \frac{\varepsilon_r - 1}{2}\left(1 + \frac{10}{v}\right)^{-ab} \tag{2.16}$$

where

$$a = 1 + \frac{1}{49}\ln\left\{\frac{v^4 + (v/52)^2}{v^4 + 0.432}\right\} + \frac{1}{18.7}\ln\left\{1 + \left(\frac{v}{18.1}\right)^3\right\}$$

$$b = 0.564\left(\frac{\varepsilon_r - 0.9}{\varepsilon_r + 0.3}\right)^{0.053}$$

The calculated values of ΔL_1 or ΔL_2 fit the measured resonant frequency within ± 1.6% [42]. It is expected that the use of (2.13) and (2.15) should result in a better fit. The resonant frequency f_{10} or the effective length L_{1e} for the dominant TM_{10} mode of a nearly square microstrip antenna is related by the following simple formula [43]

$$f_{10} = \frac{c}{2L_{1e}\sqrt{\varepsilon_{re1}}} \qquad \text{or} \qquad L_{1e} = \frac{c}{2f_{10}\sqrt{\varepsilon_{re1}}} \tag{2.17}$$

where c is the velocity of the light.

Similarly the resonant frequency f_{01} or the effective length L_{2e} for the orthogonal TM_{01} mode of a nearly square microstrip antenna is related as

$$f_{01} = \frac{c}{2L_{2e}\sqrt{\varepsilon_{re2}}} \qquad \text{or} \qquad L_{2e} = \frac{c}{2f_{10}\sqrt{\varepsilon_{re2}}} \tag{2.18}$$

Using (2.7) and (2.18), the lengths of nearly square microstrip antenna are calculated. From Figure 2.10 (a), the perturbation area of a nearly square microstrip antenna, $\Delta S = 1L$, and square microstrip antenna area with out perturbation $S = L^2$. The empirical design equation for diagonally fed nearly square microstrip antenna is given as [44]:

$$\left|\frac{\Delta S}{S}\right| = \frac{1}{Q_0} \tag{2.19}$$

where Q_0 is unloaded quality factor of the microstrip antenna. The design of the patch with perturbation requires Q_0, which depends on the dimensions, substrate thickness *h*, and the substrate dielectric constant ε_r. For the given substrate parameters, the substrate depended quality factor is approximately calculated as [44]:

$$Q_0(\varepsilon_r) = \frac{Q_0\sqrt{\varepsilon_r}}{\sqrt{2.55}} \tag{2.20}$$

For better accuracy, Q_0 should be selected to ensure better radiation efficiency of the microstrip antenna. The amount of perturbation required for circularly polarized radiation is calculated from (2.13). The location of the feed on the diagonal axis is selected for 50Ω impedance match or the quarter wave transformer is used for the matching purpose. The sense of circularly polarized radiation changes by switching the feed to the orthogonal diagonal axis. The ratio of the two orthogonal dimensions L_1 / L_2 of nearly square microstrip antenna should be generally in the range of 1.01 to 1.10 depending upon the substrate parameters. When the patch is fed along the diagonal, then the two resonance modes corresponding to lengths L_1 and L_2 are spatially orthogonal. The circularly polarized radiation is obtained at a frequency between the resonance frequencies of these two modes, where the two orthogonal modes have equal magnitudes and are in phase quadrature. In this section, the effect on the input impedance for different values of L_2 by keeping L_1 constant has been studied. Nearly square microstrip antenna of length, L_1 = 30 mm, relative dielectric constant, ε_r = 2.55, the substrate height,

h = 1.59 mm, and loss tangent, tan δ = 0.001, which is fed along the diagonal at feed location F, the input impedance, voltage standing wave ratio and axial ratio plots for three values of L_2 = 0.967 L_1, 0.973 L_1, and 0.983 L_1 are shown in Figure 2.11 (a) - (c).

In singly-fed microstrip antennas, the kink in the impedance plot represents that the two orthogonal modes are excited with equal amplitude and 90^0 phase difference. At the kink frequency minimum axial ratio is obtained. Instead of a kink, a small loop or the absence of the loop in the impedance plot yields poor axial ratio at center frequency. The loop in the impedance plot implies that the separation between the two orthogonal modes is large, and hence it is to be reduced to obtain better axial ratio. If there is only a slight bend in the impedance plot without any kink or loop, then the separation between the two modes is to be increased. For the diagonally fed nearly square microstrip antenna, we observed that as the length L_2 increases, the loop in the impedance plot becomes a kink, and then it disappears as L_2 increases further. The criticality of the dimension is to be noted. Even though, larger VSWR bandwidth of 4 % is obtained for L_2 = 0.967 L_1 mm due to the loop in the impedance plot, the minimum axial ratio is 4 dB at resonant f_0 = 3.01 GHz. For L_2 = 0.973 L_1, the loop becomes kink, hence the VSWR bandwidth is reduced to 3 %, but the minimum axial ratio is improved to 0.5 dB. In this case, the bandwidth for axial ratio $\leq$ 3 dB is 0.8 %. The value of L_1/L_2= 1.027 implies separation of 2.7 % between the two resonant lengths, which is slightly greater than the VSWR bandwidth (1.8 %) of the square patch of length L. A lower value of axial ratio could be obtained by fine-tuning the length L_3 For the feed location shown in Fig. 2.15, left hand circularly polarized radiation is obtained, and if the feed is shifted to the other diagonal, then right hand circularly polarized is obtained.

The axial ratio and VSWR bandwidths are improved by increasing the substrate thickness. When the substrate height is doubled, larger ratio of L_1 / L_2 = 1.06 is taken because bandwidth increases with increase in the substrate thickness. The input impedance and axial ratio variations with frequency are shown in Figure 2.12. For the SMA connector (probe diameter d = 1.2 mm), the kink in the input impedance plot is formed in the inductive region of the Smith chart, which is due to the larger probe

inductance of increased substrate thickness. The probe inductance is reduced by increasing its diameter to 2.0 mm, which shifts the kink towards the center of the Smith chart as shown in Figure 2.12, thereby improving the VSWR bandwidth and also the axial ratio at the kink. The change in the probe diameter changes the resonance frequency slightly. For the thicker probe, the impedance bandwidth for VSWR $\leq$ 2 is 7.4 % and the axial ratio bandwidth for AR $\leq$ 3 dB is 1.7 %.

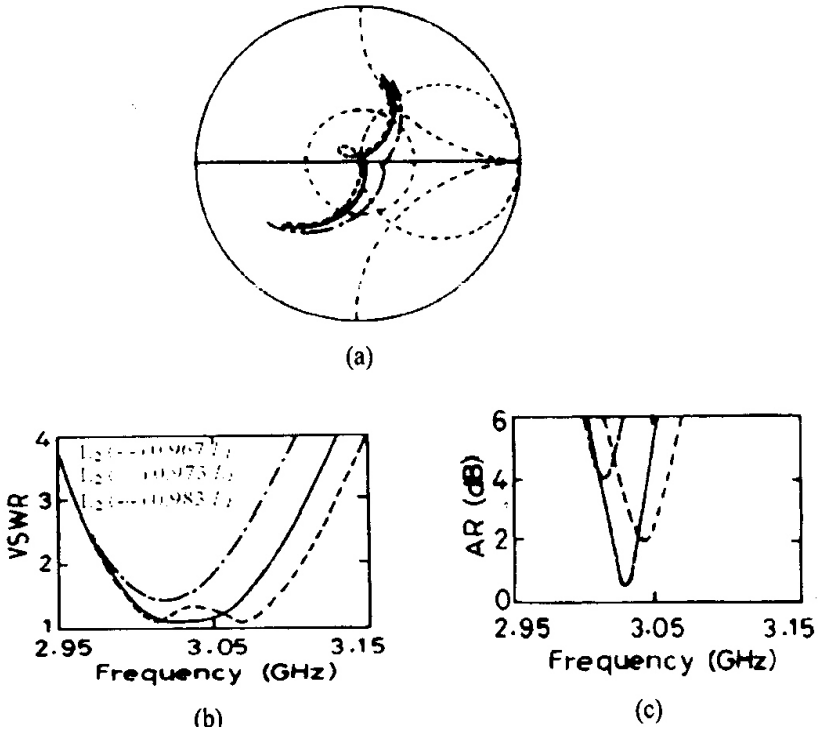

Figure 2.11 (a) Input impedance (b) VSWR, and (c) axial ratio variation of diagonal fed nearly square microstrip antenna.

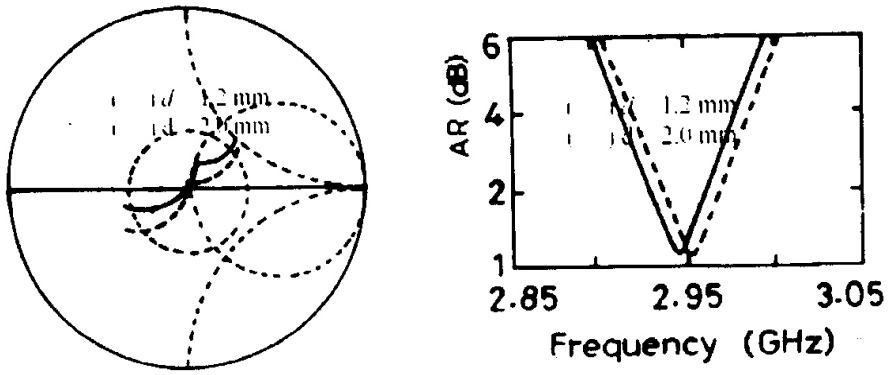

(a) (b)

Figure 2.12 (a) Input impedance, and (b) axial ratio variation of singly-fed nearly square microstrip antenna for the substrate height *h=3.18 mm.*

The axial ratio bandwidth is improved further when thicker substrate with low dielectric constant is used. In this case, a thicker probe diameter of 4.0 mm is taken to reduce the probe inductance, so that the kink in the impedance plot is within VSWR = 2 circle. VSWR and axial ratio variation with low dielectric constant on thick substrate is shown in Figure 2.13. The bandwidths for VSWR $\leq$ 2 and axial ratio $\leq$ 3 dB are 14 % and 2.8 %, respectively. Notice that the bandwidth of the microstrip antenna is limited by its axial ratio and not by its voltage standing wave ratio.

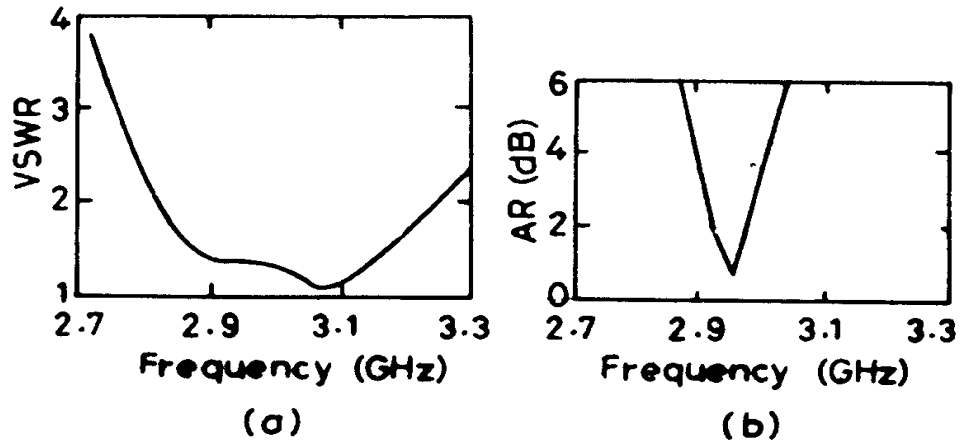

Figure 2.13 (a) VSWR, and (b) axial ratio variation with frequency of nearly square microstrip antenna on thick substrate (h = 5 mm) with low dielectric constant (ε_r = 1.01).

2.8 Square Microstrip Antenna with Modified Edge

Instead of using the nearly square microstrip antenna, the edges of the square microstrip antenna are modified by adding stubs or by cutting slots as shown in Figure 2.14. By adding only one stub or by cutting one notch, circularly polarized radiation can also be obtained, but then the configuration is not symmetrical. However as long as the total effective areas of these perturbations are of the same order, the performance of one edge modified is similar to that of two edges modified square microstrip antenna. The approximate value of the total perturbation area is $\Delta S = 2l^2$ for square microstrip antenna with symmetric stubs or notches. The amount of perturbation required for circularly polarized radiation is calculated from (2.14). ΔS represent the total sum of perturbation segments. The amount of perturbation of individual stub or notch is calculated as $\Delta S_1 = \Delta S_2 = \Delta S/2$.

A square microstrip antenna of length L = 30 mm and two square stub of length l = 0.083 L with substrate parameters dielectric constant, ε_r = 2.55, substrate thickness or substrate height, h = 1.59 mm, and loss tangent, tanδ = 0.001, yield right hand circularly

polarized radiation when fed at F. Similarly with two square notch of length $l = 0.083\ L$ on the same substrate parameters, yield left hand circularly polarized radiation. For both the configurations the bandwidth for AR $\leq$ 3 dB and VSWR $\leq$ 2 are 0.7 % and 3.2 %. In these cases, the values of axial ratio and VSWR bandwidths are similar to that of the nearly square microstrip antenna. We observed that the perturbation area of the stub or the notch is very critical to yield lower axial ratio value, just as in the case of nearly square microstrip antenna, where L_1 / L_2 ratio is very critical to yield circularly polarized radiation. The advantage of these configurations is that trimming the stub or notch can easily do the fine-tuning.

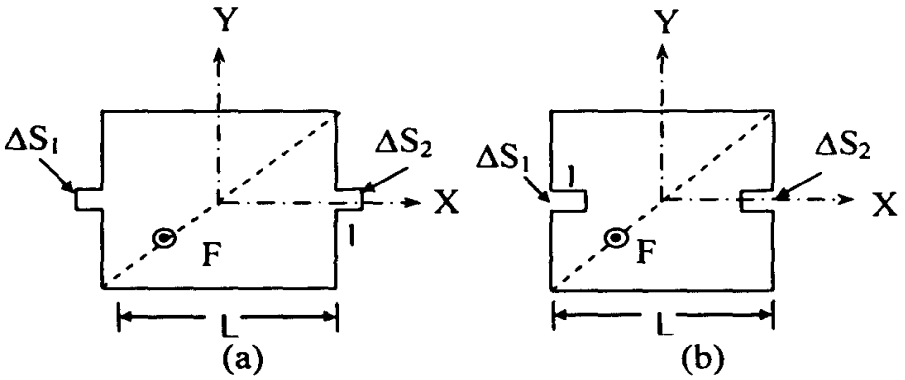

Figure 2.14 Diagonal fed square microstrip antenna with (a) two stubs, and (b) two notches along its opposite edges.

2.9 Square Microstrip Antenna with Modified Corner

Square microstrip antenna with modifying corners is also used to produce two orthogonally degenerate modes for circularly polarized radiation. Small isosceles right angle triangular patches or small square patches are removed from the diagonally opposite corners of the square patch shown in Figure 2.15. Chopping of two diagonally opposite corners makes the resonance frequency of the mode along this diagonal to be higher than that for the mode along the un-chopped diagonal. The patch is fed along the central axis so that the orthogonal modes are generated. Instead of chopping the corners, small square patches could be added at the corners as shown in Figure 2.15 to obtain

circularly polarized radiation. For these configurations the perturbation area is calculated using the following relation:

$$\left|\frac{\Delta S}{S}\right| = \frac{1}{2Q_0} \tag{2.21}$$

In all these configurations, only one corner could be modified to yield circularly polarized radiation. Since two corners modified configurations are symmetrical, the details are given for only these cases. The perturbation area of corners chopped square microstrip antenna is $\Delta S = l^2$. When isosceles right angle triangular patches of side length $l = 0.12\ L$ are removed from the two corners, left hand circularly polarized radiation is obtained for the feed at F. The axial ratio and the VSWR bandwidths are 1 % and 3 % for AR $\leq$ 3 dB and VSWR $\leq$ 2, respectively.

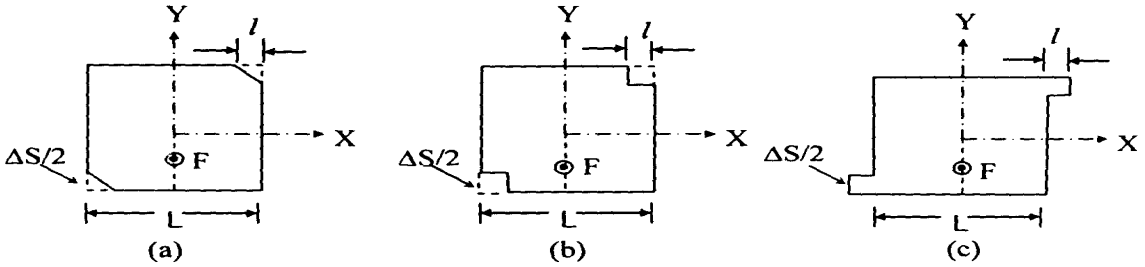

Figure 2.15 square microstrip antennas with modified diagonally opposite corners (a) small isosceles right angle triangles removed (b) small squares removed, and (c) small squares added.

The perturbation area of square microstrip antenna with small squares added or removed from the corner is $\Delta S = 2l^2$. When a small square of length $l = 0.083\ L$ is removed from the two corners of square the perturbation area, left hand circularly polarized radiation is obtained for the feed at *F*. When a small squares of length $l = 0.067$ *L* is added at the two corners of the square the perturbation area as shown in Figure 2.20 (c), right hand circularly polarized radiation is obtained for the feed at F. In the letter case, the resonance frequency and axial ratio bandwidth are slightly smaller than that of the corner chopped cases, because of its larger patch area.

2.11 Square Microstrip Antenna with a Diagonal Slot

A square microstrip antenna with a rectangular diagonal slot and the feed along its central axis is shown in Figure 2.16. The difference in the resonance frequencies of the orthogonal modes is caused by the rectangular slot, which makes the path lengths of the two diagonals unequal. In this case, the ratio of length and width of the slot governs the circularly polarized radiation characteristics of the antenna for given substrate specifications. The perturbation area of rectangular slot is $\Delta S = l \times w$. Square microstrip antenna of length L = 30 mm with rectangular slot of length l = 0.25 L and width w = 0.07 L, fed at F, left hand circularly polarized radiation is obtained. The axial ratio and VSWR bandwidths are 1 % and 3 %, respectively. These theoretical results follow the same trend as observed in the measured results [45].

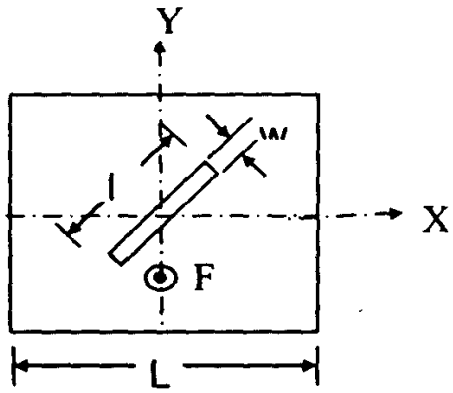

Figure 2.16 Square MSA with a diagonal slot

In the entire singly-fed modified square microstrip antennas, the ratio of the two orthogonal modes is very critical to yield circularly polarized radiation with minimum axial ratio at the resonance frequency. Due to the design limitations and fabrication error (tolerance in the patch dimensions and the substrate parameters), it is possible that the results may not be optimum and fine-tuning of the dimensions is required. Whether to increase or decrease the dimensions could be determined by looking at the input impedance plot. By fine-tuning the dimensions, lower axial ratio can be obtained with larger axial ratio bandwidth. In this regard, stub configurations are more suitable as fine tuning can be easily done.

2.12 Matlab based free software for antenna simulation

Matlab based free software for antenna design and simulation is developed by Sergey N Makarow. It is not fully developed like other commercial software such as ADS or IE3D. It is not much more user friendly and while using it one has to write many codes to analyze the required antenna. I have used this software. I have written some codes of my own, designed a microstrip patch antenna for 2.5 GHz. and simulated. The codes are not included in this report. The simulated results are given in following figure 2.17 to 2.19.

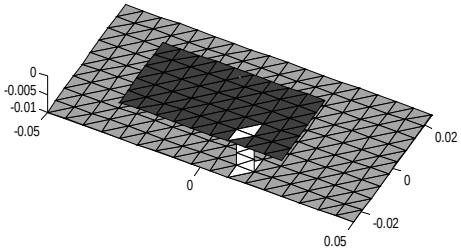

Figure 2.17 microstrip patch antenna for 2.5 GHz

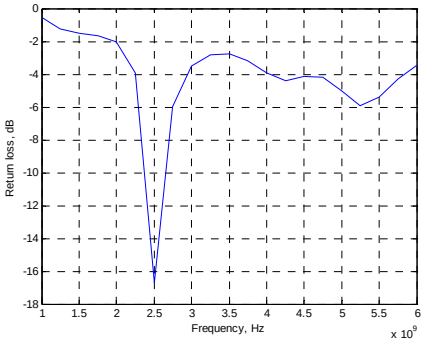

Figure 2.18 S_{11} Versus Frequency plot

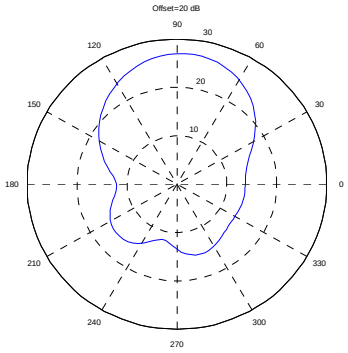

Figure 219 S_{11} Versus Frequency plot

3 Compact Broadband Antenna Design and Analysis

3.1 Introduction

Microstrip patch antennas are very narrow band antennas. There are various methods to improve the bandwidths of such types of antennas, for example using parasitic elements, impedance matching networks and stacked multiresonators [17] etc. But the design of such antennas become complex and can yield maximum 30% bandwidth. In this paper an easy method is described to obtain large (up to 95%) bandwidth. A single layer C shape micro strip patch suspended (5 mm) above ground plane gives the large bandwidth. It is a compact. Radiates in a narrow and a wide band. The design is simulated using ADS2003A software.

3.2 Design

It is a C shape patch having overall dimensions 34.5x22.9 mm. The slot dimensions are 10x10.6 mm. This radiating patch is prepared on one side of the PCB (printed circuit board) of 1.6 mm thickness, having 4.4 dielectric constant and loss tangent of .001. The copper of the other side of PCB is removed (or one can use single sided PCB). This C shape acts as radiating patch. It is suspended 5 mm above the ground plane with the help of non-conductive pins and foam. For the ground plane one can use a metal sheet or a single sided or a double sided PCB as shown in Figure 3.1.

Here the ground plane is assumed as infinite plane. Therefore the dimensions of the ground plane should be around 50 mm x 40 mm (around 40% more than the dimensions of radiating patch) [46]. The feed point is located at 14.5 mm from left and 3.8 mm from top as shown in Figure 3.2. The slot is at the center of the edge of the patch.

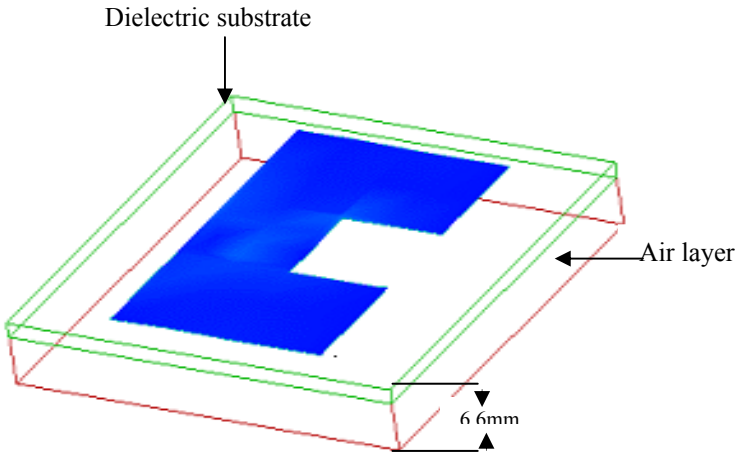

Figure 3.1 C shape microstrip antenna

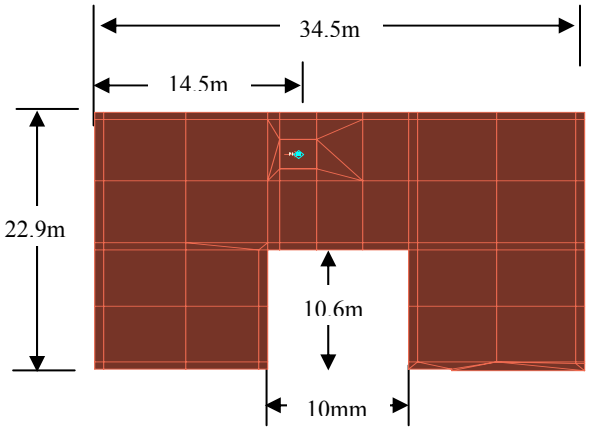

Figure 3.2 Microstrip antenna with feed details

3.3 Measurements

In this paper a C shape patch is used. If a simple rectangular patch is used, the continuous wide band from 3.7 GHz to 5.3 GHz is not achieved. In this band, there would be small non-radiating band, as shown in figure 3.4 by the red color response. To avoid

this non-radiating band and to obtain continuous band, some kind of resonating structure is necessary. In this antenna, rectangular slot is used as resonating structure, due to which this patch is converted into C shape patch. It is not necessary that the size of the rectangular slot should be exactly the same as shown in figure 3.2. The size should be chosen in such a way that it would bring down the non-radiating band (which is present in 3.7-5.3 GHz) below by –10 dB. In this antenna, the slot size is chosen sufficiently large so that it will help to make the pass band continuous from 3.7 GHz to 5.3 GHz as well as it will radiate at ISM (2.45 GHz.) band. It gives a bandwidth of 40 MHz at ISM band. In these bands, the S_{11} is less than –10 dB or the VSWR is less than 2. The variations in S_{11} with frequency are plotted in figure 3.3 by blue color.

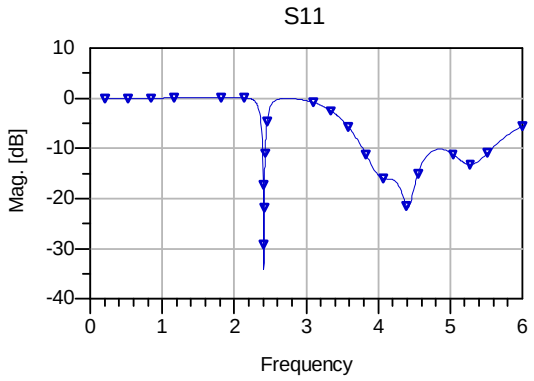

Figure 3.3 S_{11} plot for C shape antenna

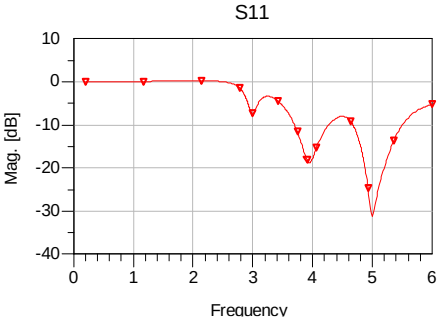

Figure 3.4 S_{11} plot for rectangular antenna

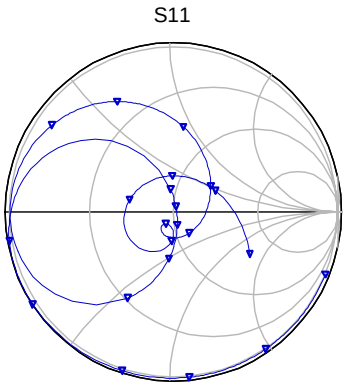

Figure 3.5 S_{11} plot for C shape antenna on smith chart

The variations in S_{11} with frequency are also plotted on the Smith chart as shown in figure 3.5. The wide band response in figure 3.3 is produced due to the loop in figure 3.5 near the centre of the Smith chart. The bandwidth of the wide band can be increased by taking the loop exactly at the centre of the Smith chart. This can be done by adjusting the feed point location. The bandwidth (40MHz) and the response (the maximum peak in negative direction at 2.45 MHz) can be adjusted (increased) by passing the circle exactly through the centre of the Smith chart. This also could be done by adjusting the location of feed point shown in figure 3.2. In practice, if we try to maximize the bandwidth and the response of the wideband by adjusting the location of feed point, the bandwidth and the response of the narrow band may be affected and vice-verse. Therefore the feed point should be selected in such a way that both the responses are within acceptable limit.

As the distance between the radiating patch and ground plane increases, the response improves a little bit. This improvement or increase in the bandwidth is very small. If we double the separation (10 mm) then also the bandwidth will not increase even by 5% (or total bandwidth will not become even 40%) [47]. By further increasing the distance beyond 15 mm, then again the response starts deteriorating.

One can design wide band antenna for frequencies less than 3.7 GHz by increasing the size of the patches and the separation between the patches. In this case, wide bandwidth even up to 95% is achieved. The wide band antenna at higher frequencies can be designed using smaller patch size and smaller separation or without air gap.

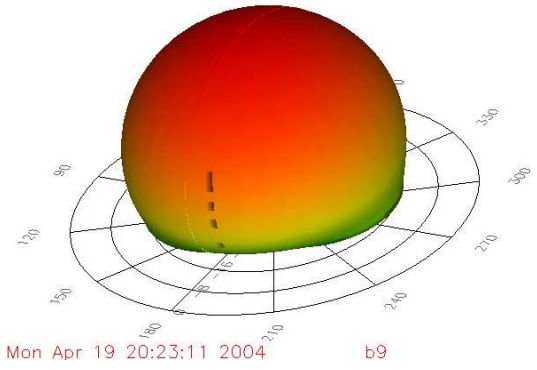

Figure3.6 Three dimensional radiation pattern of C shape antenna

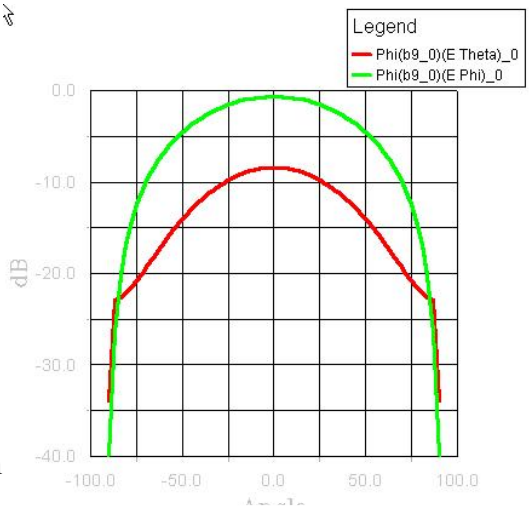

Figure 3.7 Radiation pattern

The three dimensional radiation pattern of the patch is shown in figure 3.6. The three dimensional far field cut E-fields are shown in figure 3.7. From this figure, it is clear that the directivity of this patch antenna is around 8 dB. It offers wide bandwidth as a result of various factors.

1) The use of air as a dielectric medium.

2) The large height of the elements 0.077λ at the lower and 0.1166λ at the higher end.

3) The separation between ground plane and radiating plane at higher frequency is 0.1166λ. It is comparable with wavelength. The ground plane acts as reflector giving wide bandwidth.

3.4 Conclusion

It is easy to design such type of antenna for any desired frequency band and is also easy to fabricate, cost effective. It gives very good performance (wide bandwidth). In future, it can be widely used in the frequency range 1 GHz to 7 GHz.

3.5 Design of compact broadband microstrip fed electromagnetically coupled MSAs

The major advantages of micro strip antennas (MSAs) are lightweight and small size, low fabrication cost and that they can be made conformal to the host surface. The limitations of MSAs are narrow bandwidth, difficult to achieve polarization purity, low gain and low power handling capability.

In this section, efforts have been made to overcome the above limitations to develop a microstrip fed wideband and circularly polarized patch antenna. Generally in MSAs, bandwidth around 3% only is achieved [18]. In this section, electromagnetically coupled stacked parasitic patch is used. It gives around 20% bandwidth [17]. Circular polarization is obtained using a shorting pin at one edge of the patch. The microstrip feed

makes the antenna suitable for forming an array to obtain high gain and high power handling capability.

There are total five methods to increase the bandwidth as described in chapter 2. Out of these five methods, the method which makes an antenna most compact with no back radiations is Electromagnetically coupled MSA. In this section the broadband antenna is designed using this method.

3.6 Design

This antenna consists of a ground plane, a radiating patch and a parasitic patch as shown in figure 3.8. The substrate used to support the radiating patch and the parasitic patch are of the same type. It has thickness of 1.6 mm. and dielectric constant of 2.2. The parasitic patch is suspended 3 mm above the radiating patch with the help of foam and non-conductive pins.

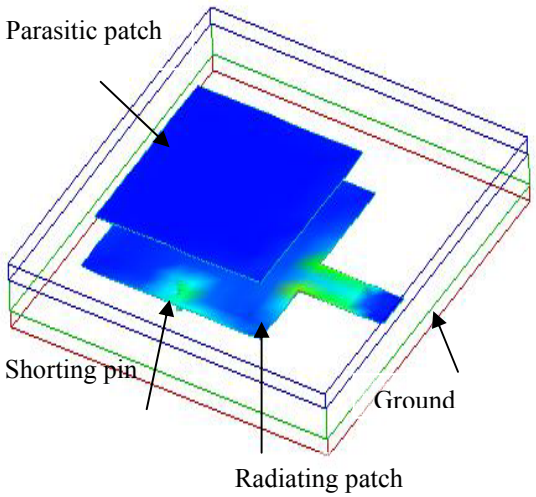

Figure 3.8 Electromagnetically coupled microstrip antenna

The separation between the parasitic patch and radiating patch is 3.0 mm (air) + 1.6 mm (dielectric) [48].

Figure 3.9 shows the top view of the antenna. The size of the ground plane should be around 40% larger than the size of the radiating patch. In order to obtain polarization purity, the size of the parasitic patch should around 5% less than the size of the radiating

patch. The actual sizes of the square patches are shown in the figure. The width of the feed patch is 4.6mm. The shorting pin is having diameter of 0.6 mm. It is placed approximately at the middle of the patch edge, 1.5 mm from the edge.

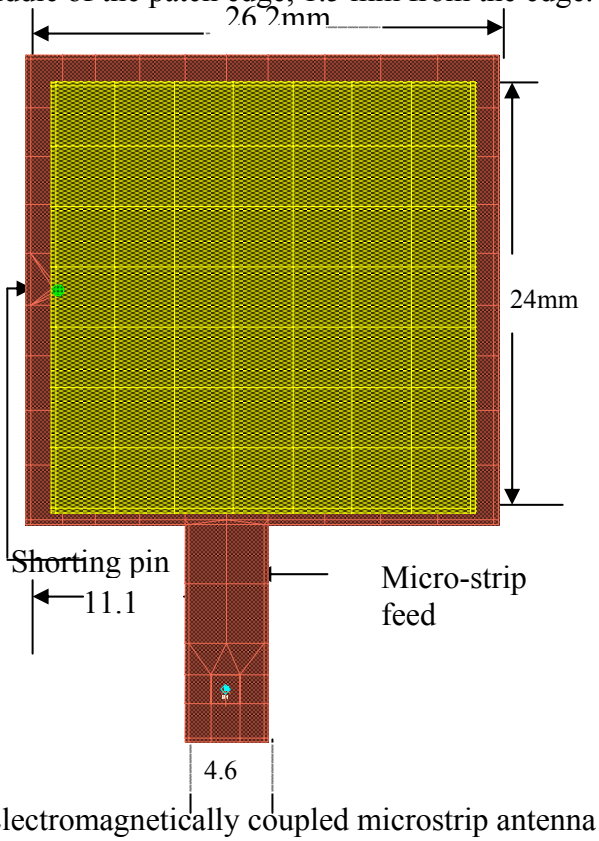

Figure 3.9 Electromagnetically coupled microstrip antenna With feed and shorting pin details.

3.7 Measurements and Discussion

This patch antenna is designed by keeping the view in mind that one should be able to design an array easily using the patch. The patch to be used in an array 1) should provide sufficient bandwidth 2) should be microstrip fed 3) should radiate with polarization purity.

In order to obtain wide bandwidth electromagnetically coupled parasitic patch is used. Advantages of this method are a) sufficient bandwidth (10%-30%) [49-55], b) compact planar size c) high front-to-back ratio.

The choice of the parasitic patch is perfectly suited for the antenna. The antenna gives wide bandwidth even if the size of the parasitic patch is less or more by 20% (or equal) as compared to the size of the radiating patch. But for all above sizes of parasitic

patch we don't get polarization purity. Polarization purity is achieved only if the size of the parasitic patch is less than the size of radiating patch.

As we go on decreasing the size, the polarization purity goes on increasing. If the size is decreased by 20%, 6 dB difference between right and left polarizations is observed. If we try to decrease the size further, bandwidth is affected. In this design, the size of the parasitic patch is kept approximately 10% less than the size of the radiating patch. Therefore to maximize polarization purity, shorting pin at one of the radiating edge is used, as shown in figure 3.9. The shorting pin shorts just the radiating patch (not the parasitic patch) with the ground. After shorting, the frequency band shifts towards lower frequencies. To obtain the required the frequency band, resizing of both the patches should be done.

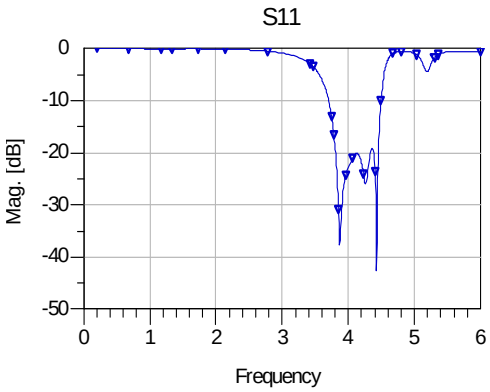

Figure 3.10 S_{11} plot for electromagnetically coupled microstrip antenna (ECMSA)

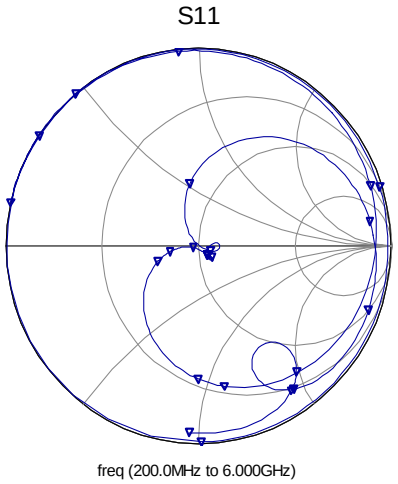

Figure 3.11 S_{11} plot on smith chart for electromagnetically coupled microstrip antenna (ECMSA) on smith chart

After putting the short and resizing the patches, again exact location of feed point is to be determined. The bandwidth and the polarization purity are checked at every 1.0 mm from the left. At the extreme left, the bandwidth as well as polarization are worst. As one starts moving towards right, the bandwidth starts increasing. Polarization also starts improving. When the feed point is at 11.0 mm from the left, the maximum difference (-16dB) between right & left circular polarization level is obtained. The left circular

polarization level is –16 dB down than the right circular polarization level. It means that for this feed position, the right circular polarized wave is obtained.

Figure 3.10 shows the variation in S11 with frequency. The –10 dB bandwidth (for which VSWR is less than 2) ranges from 3.7 GHz to 4.44 GHz [56]. Here, a bandwidth of 744 MHz is achieved. The variations in S_{11} with frequency are also plotted on the Smith chart as shown in figure 3.11. The tight knots at the center of the Smith chart indicate larger bandwidth. These knots are very close to the center of smith chart and indicate very good value of S_{11} or very low VSWR.

The polarization purity plots are shown in figure 3.12. The plot shown by blue color indicates the level of left circular polarization. It is –16 dB down than the level of right circular polarization (RCP) indicated by the outer most red color. It means the antenna produces right circularly polarized (RCP) waves. The Eθ and Eϕ plots are shown by the two middle curves (red & green).

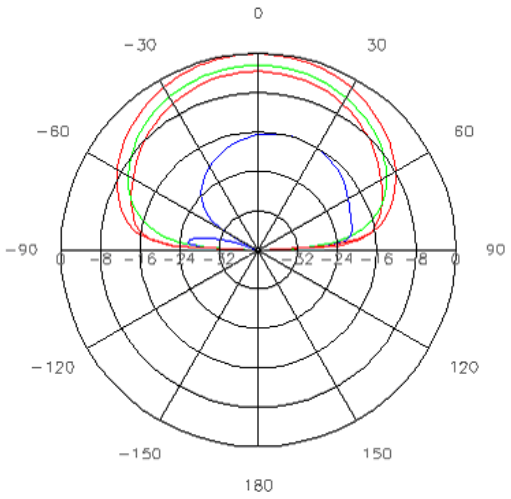

Figure 3.12 Various polarization levels

The difference between the levels of the two is very less. Therefore it is clear that the antenna doesn't produce linearly polarized waves.

If one starts shifting the feed point from the present position to towards right the level of rcp starts decreasing. The level of lcp starts increasing. When the feed point is at 6.1 mm away from right side edge, the patch produces lcp.

Following figure 3.13 shows the axial ratio versus frequency plot of the antenna. Axial ratio is the ratio of major axis and the minor axis as explained in figure 2.10. The ideal value of the axial ratio is 1 or 0 dB. Practically the acceptable values are from 0 dB to 1.44. from the following figure it is clear that the axial ratio is in the acceptable limit in the entire band. All the antennas of chapter 3 and 4 were designed and simulated using ADS software in which axial ratio versus frequency plots were not included. Inorder to include the axial ratio versus frequency plots of all the antennas, they are again designed and simulated in IE3D software as ADS was not available in the nearby Institutes where I am working now. All the results of got by simulating the antennas using ADS and IE3D are matching.

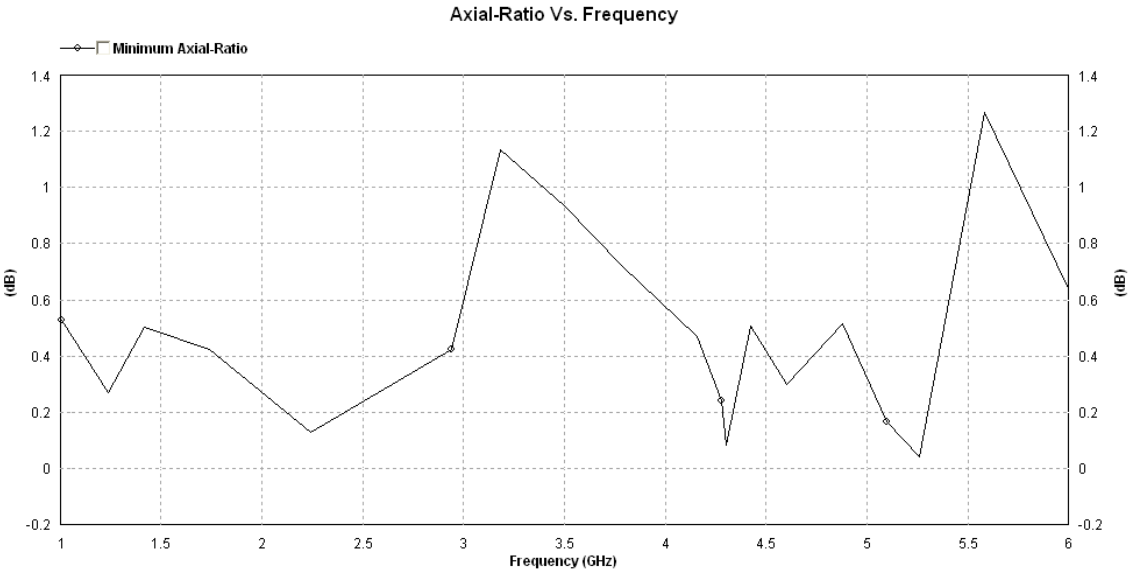

Figure 3.13 Axial ratio versus frequency

3.8 Conclusion

This antenna is compact and broadband. This antenna can produce right as well as left circularly polarized waves. It uses microstrip feed therefore it can be easily used in an array or any other application.

4 Broadband Planar Antenna Array with Switchable Polarizations

4.1 Introduction

In case of a microstrip antenna, the most important factors are wide bandwidth, polarization purity, high gain and high power handling capability. These demands can be fulfilled using an array of wideband antennas. Apart from these factors, some times various types of polarizations schemes are important to handle the problems of fading, co-channel interference, etc. In this chapter, design and analysis of a compact broadband microstrip antenna are presented. This antenna gives wide bandwidth and all types of polarizations such as linear, left and right circular polarizations.

4.2 Design

This antenna consists of a ground plane, a radiating patch and a parasitic patch as shown in figure 4.1. The dielectric material used to support the radiating patch and the parasitic patch are of same type. The dielectric material has thickness of 1.6 mm and dielectric constant of 2.2. The parasitic patch is suspended 3.0 mm above the radiating patch with the help of foam and non-conductive pins.

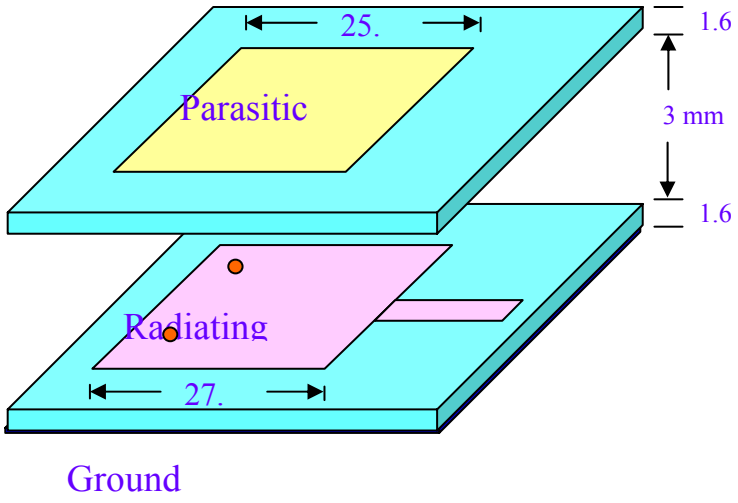

Figure 4.1 Electromagnetically coupled microstrip fed MSA

The separation between the parasitic patch and radiating patch should be around 0.1λ for maximum bandwidth. In this antenna, it is 3.0 mm (air) + 1.6 mm (dielectric) which is approximately 0.1λ [48].

Figure 4.2 shows the top view of the antenna. The size of the ground plane should be around 40% larger than the size of the radiating patch. In order to obtain (circular) polarization purity the size of the parasitic patch should be around 5% less than the size of the radiating patch. The actual sizes of the square patches are shown in the figure. The width of the feed patch is 5.0 mm.

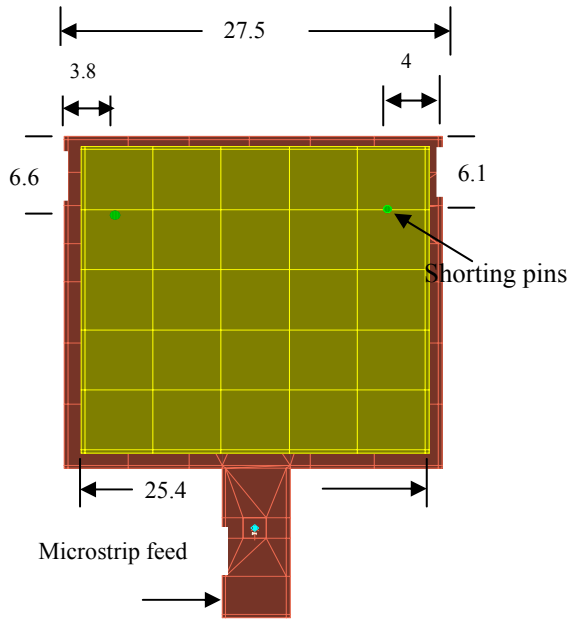

Figure 4.2 ECMSA with feed and shorting pins

The diameter of the shorting pins is 0.6 mm. The two pins (or shorting diodes) are fixed approximately along the diagonals near the top corners. If both the diodes are open-circuited or the shorts are removed, the patch produces linearly polarized waves. If the short at the left top corner is placed, the patch produces left circular polarization. If

the short at the right top corner is placed it produces right circularly polarized waves.

4.3 Measurements and Discussion

This patch antenna is designed with the intention that it can be used in an array to produce high gain wide bandwidth, and any desired polarization.

In order to obtain wide bandwidth, an electromagnetically coupled parasitic patch is used. Advantages of this method are a) sufficient bandwidth (10%-30%) [49-55], b) compact planar size, c) high front-to-back ratio. The patch is microstrip fed and is most suitable for an array.

The exact dimensions of the square parasitic patch and the square radiating patch are shown in the figure 4.2. In order to obtain all polarizations from the patch, the feed is applied at the center.

4.3.1 Linear Polarization

In the absence of the shorting pins (or the shorting diodes are in reverse bias), we get linear polarization. In order to increase bandwidth, the resonance frequency of the radiating and the parasitic patch should be adjusted close to each other. In order to achieve this, the size of the parasitic patch is kept around 8% less than the size of the radiating patch. In this situation, the bandwidth from 3.715 GHz to 4.192 GHz is achieved This is the maximum bandwidth which one can obtain for the above combination with center feed. The variations in S_{11} with frequency are plotted in figure 4.3.

The variations in S_{11} with frequency are also plotted on the Smith chart as shown in figure 4.4. Whenever there is a knot at the center of the Smith chart, wide bandwidth is obtained [56]. The patch is fed from bottom; it produces electric field varying mainly in horizontal direction (i.e. in the direction of Φ). The field in the direction of θ is very less. The relative levels of the two fields are shown in figure 4.5. The level of E_Φ is indicated

by the green color. The level of E_θ is indicated by the red color. E_Φ is greater than E_θ by 30 dB.

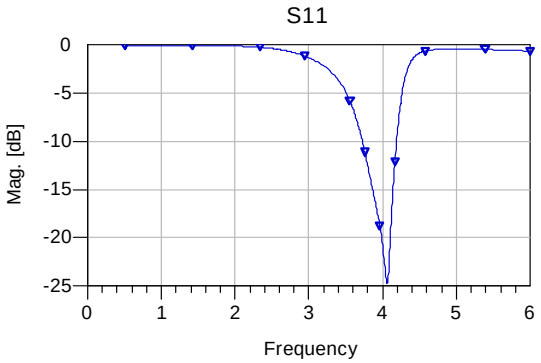

Figure 4.3 S_{11} plot for linear polarization

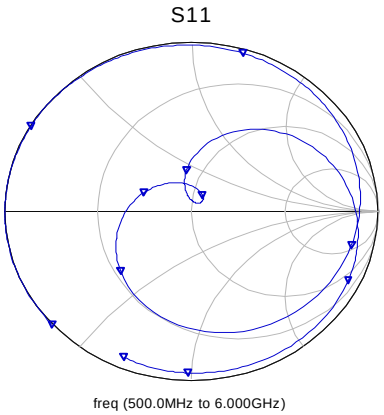

Figure 4.4 S_{11} plot on smith chart for linear polarization

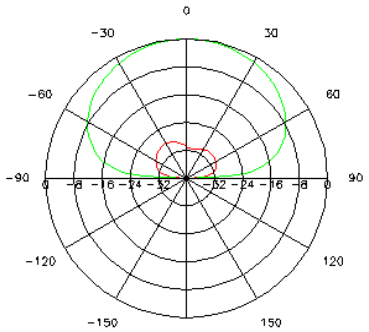

Figure 4.5 Polarization plot for EΦ
Green --- EΦ Polarization
Red --- Eθ polarization

4.3.2 Left Circular Polarization

Left circular polarization can be obtained using a shorting pin at the left top corner as shown in figure 4.2. Instead of shorting pin, it is advisable to use a diode. If this diode is forward biased, the patch produces left circular polarization. Figure 4.6 shows the variation in S_{11} with frequency.

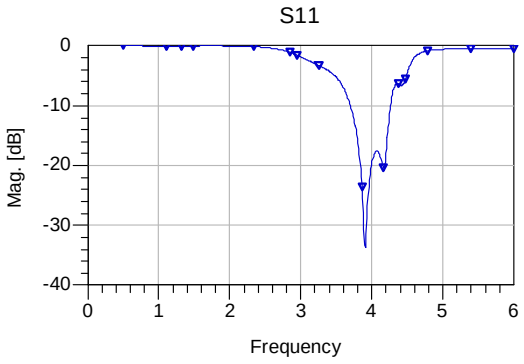

Figure 4.6 S_{11} plot for left circular polarization

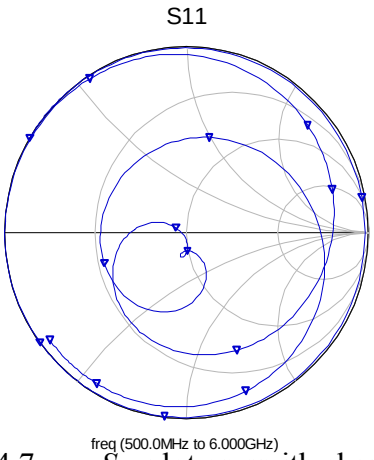

Figure4.7 S_{11} plot on smith chart for left circular polarization

In this case, more bandwidth (from 3.65 GHz to 4.23 GHz) is obtained due to the use of short at the left top corner. The variations in S_{11} with frequency are plotted on Smith chart as shown in figure 4.7. In this case, more bandwidth is obtained as compared to the previous case of linear polarization. This also can be confirmed with the help of the knots near the center of the Smith chart [56]. In case of the linear polarization the knot is relatively loose and therefore the bandwidth obtained is less.

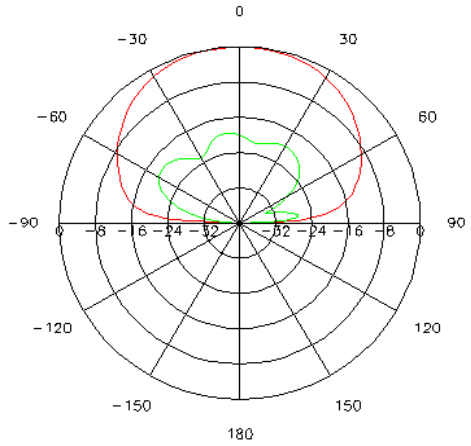

Figure 4.8 left circular Polarization plot
Red --- lcp
Green --- rcp

The polarization levels for right and left circular are plotted in figure 4.8. The levels of the left and right circular polarization are indicated by red and green curves respectively. The level of the left cp is higher than the right cp by 20 dB. Hence it produces left circular polarization.

4.3.3 Right Circular Polarization

In order to produce right circular polarization, a shorting pin should be placed at the top right corner of the patch. Instead of physical short, if shorting diodes are used, the diode in the left top corner should be reverse biased and the diode in the right top corner should be forward biased. In this case, approximately we get bandwidth from 3.65 GHz to 4.23 GHz. The polarization level of right cp is higher than left cp by 20dB. The plots of S11 with frequency and polarization levels are similar to the plots obtained previously for left circular polarization case; these are not presented here to avoid repeatability.

The shorting pins could also be placed at the left and right bottom corners. Instead of only one shorting pin, one can use two diagonally opposite shorting pins also but this method does not yield any additional benefits.

4.4 Conclusion

This antenna is compact and broadband. It can produce linear and right as well as left circularly polarized waves. It uses microstrip feed and therefore it can be easily used in an array.

4.5 Broadband Planar Array with Switchable Polarizations (EΘ, EΦ, Right and Left Circular)

In this section, microstrip planar array of 8 elements is designed and simulated. It operates in the frequency range from 3.7 to 4.2 GHz. It gives gain of 17 dB. It can produce many types of polarizations such as Eθ, EΦ, right and left circular. In all these polarizations, the cross-polar level is around 20 dB lower than the co-polar level (except for Eθ, for which it is around 10 dB). The novel microstrip antenna element used in this paper is constructed using parasitic patch and shorting pins. It gives wide bandwidth and various polarizations due to parasitic patch and shorting pins respectively.

In some communication systems applications, microstrip antennas are usually designed for single-mode operation that radiates mainly linear polarization [57]. In some applications, such as satellite communications, however, a circularly polarized system is more suitable because of its insensitivity to transmitter and receiver orientations [58]. In this regard, integrated systems with different communication networks have attracted significant attention. To achieve such multi-operation, numerous researchers have investigated microstrip antennas with switchable polarization. The switchable property allows the user to roam any existing network and have only a single handset to access a great number of services. Therefore, they can be utilized to realize frequency reuse [59]. Polarization diversity of reception is important to counter the effects of fading in communication, especially in mobile communication [60]. In addition, a microstrip antenna with switchable polarization is very important because many current communication and sensor systems require a high degree of polarization control to optimize system performance [61]. Practical applications of this technique have been described in [59], [60], and [62].

The band from 3.7 to 4.2 GHz (C-band) is widely used for satellite communication. In order to receive the signals from the satellite, it requires high gain antenna (of around 32 dB). There are various types of antennas such as parabolic dish, planar arrays, etc that can give the required gain of around 32 dB. The drawback of parabolic dish at C-band is its large size and can not be made conformal to the host surface.

In this paper, efforts have been made to design planar array. The planar array is formed using microstrip antennas (or patches). These microstrip antennas should provide sufficient bandwidth. Unfortunately the microstrip antennas have very narrow bandwidth due to the fact that they are very thin. If thickness is increased to increase the bandwidth, the cost of the patch will rise and the radiation efficiency will decrease. Therefore other techniques are used to increase bandwidth. These are described below.

One technique is to use stacked multi-resonators or multi-layers. The upper parasitic layer is electro magnetically coupled to obtain high bandwidth. The design is simple, gives high front-to-back ratio and enough bandwidth around (30%).

In the present design, electromagnetically coupled microstrip antenna is used. It gives bandwidth of 500 MHz (from 3.7 GHz to 4.2 GHz) or 20%.

The planar array should be compact one. The array can be compact if number of patches in the array is less or minimum. In order to achieve this, the gain of the individual patch should be increased. Gain of the patch can be increased using 1) superstrates [63-64], 2) stacked patches. If superstrates are used to increase the gain, following difficulties are encountered at this frequency:

1) Thicker superstrate should be used which degrades efficiency.
2) It affects bandwidth.
3) By doubling number of patches gain does not double.

The last two difficulties are encountered in case of stacked patches [48].

Electromagnetically coupled microstrip antenna is used in this paper. The single patch gives gain of 8.2 dB and bandwidth of 500 MHz (from 3.7 to 4.2 GHz). In order to obtain high gain of 32 dB, it requires such 256 patches. These patches are to be properly spaced and inter connected using appropriate matching networks. The size of this antenna array is 1 square metre.

4.6 Design

4.6.1 Design of Patch Antenna

The patch antenna consists of a ground plane, a radiating patch and a parasitic patch as shown in figure 4.9. The dielectric material used to support the radiating patch and the parasitic patch is of same type. The dielectric material has thickness of 1.6 mm. and dielectric constant of 2.2. The parasitic patch is suspended 4.0 mm above the radiating patch with the help of foam and non-conductive pins [65].

4.6.1.1 Effect of the distance between radiating and parasitic substrate

The separation between the parasitic patch and radiating patch should be around 0.1λ for maximum bandwidth [38]. In this antenna, it is 4.0 mm (air) + 1.6 mm (dielectric) which is approximately 0.108λ [20]. If the distance between the radiating and parasitic patch is 4.0 mm, we get just sufficient bandwidth (3.7 to 4.2 GHz). The bandwidth and the VSWR goes on improving slowly for the distance from 4.0 to 8.0 mm. If the distance between the substrates is increased to 14.0 mm or more, the bandwidth starts decreasing.

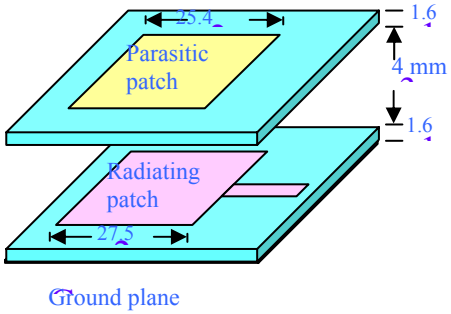

Figure 4.9 Structure of the antenna

4.6.1.2 Shape and size of the patches

In order to obtain all types of polarization and the required bandwidth, square patches (both radiating as well as parasitic) are used. The size of the parasitic patch is kept around 8% less than the size of the radiating patch. The optimized dimensions of the patches are shown in figure 4.9.

4.6.2 Design of shorting pins

Shorting pins are used to obtain various types of polarizations. Four shorting pins are used in this design. All the shorting pins are having diameters of 0.6 mm. Instead of shorting pins, one can use PIN diodes also. The exact positions of the shorts on the patch are shown in figure 4.10.

4.6.2.1 Pθ shorting pins

The group of four shorting pins placed at the left top corner of the radiating patch produces Eθ polarization when other three shorting pins (diodes) Prcp, Plcp and PΦ are open.

4.6.2.2 PΦ shorting pins

The two PΦ shorting pins placed at the right side of the radiating patch produces EΦ Polarization.

4.6.2.3 Plcp shorting pins

If this shorting pin is placed and all other are open, it produces left circular polarization (Plcp).

4.6.2.4 Prcp shorting pins

If this shorting pin is placed and all other are open, it produces right circular polarization.

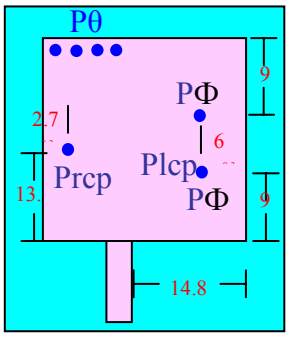

(All dimensions are in mm)

Figure 4.10 Positions of shorting pins

4.7 Results obtained using various shorting pins

Required polarization can be obtained using the corresponding pin(s) as follows.

4.7.1 Eθ Polarization

In order to obtain Eθ polarization, the three shorting pins Prcp, Plcp and EΦ are removed. The Pθ shorting pins (four shorting pins at the top) should be placed as shown in figure 4.10. Instead of shorting pins, if PIN diodes are used, the Pθ diodes should be forward-biased and remaining diodes should be reverse-biased. In the entire band, the cross polar level is around 10 dB lower than the co-polar polar level. The bandwidth obtained in this case is approximately 700 GHz (from 3.5 GHz to 4.2 GHz). The variation in return loss (S11) with respect to frequency and the polarization plots are shown in figures 4.11 and 4.12(a) respectively. Figure 4.12(b) shows the axial ratio versus frequency plot.

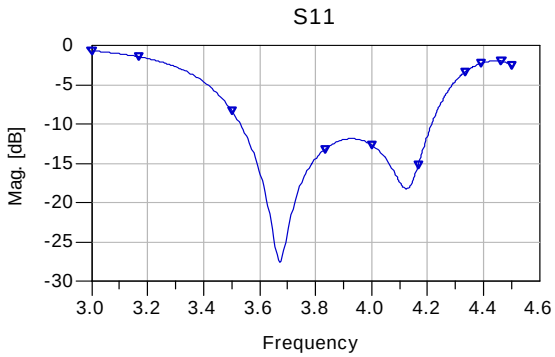

Figure 4.11 Return loss for Eθ polarization

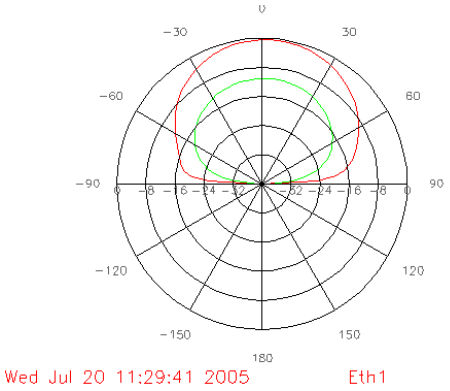

Figure 4.12(a) Polarization plot for Eθ
Red --- Eθ polarization
Green --- EΦ Polarization

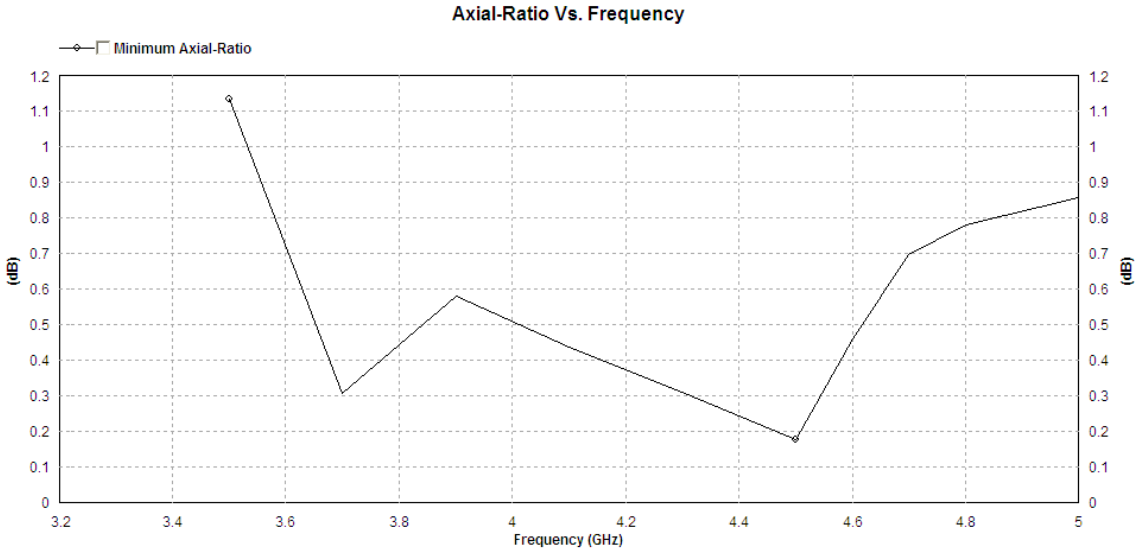

Figure 4.12(b) Axial ratio versus frequency

4.7.2 EΦ Polarization

In order to obtain EΦ polarization, the two shorting pins Prcp and Eθ (the four shorting pins at the top) are removed. The PΦ and Plcp shorting pin should be placed as shown in figure 4.10. Instead of shorting pins, if PIN diodes are used, the PΦ and Plcp diodes should be forward-biased. In this case, we get bandwidth of around 500 GHz (3.6 GHz to 4.1 GHz.). The EΦ level is higher than Eθ by around 20 dB. The variation in return loss (S_{11}) with respect to frequency and polarization plots are shown in figures

4.13 and 4.14a respectively. Figure 4.14(b) shows axial ratio versus frequency plot.

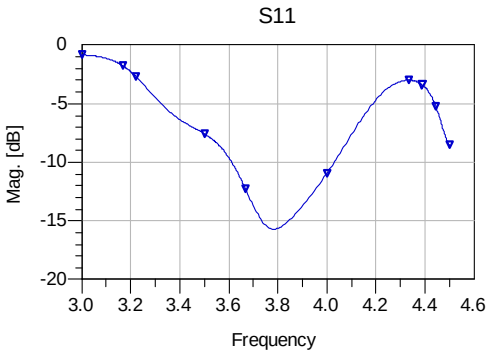

Figure 4.13 Return loss for EΦ polarization

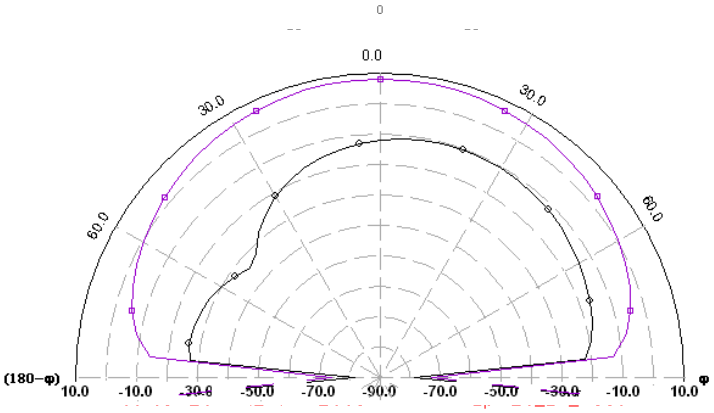

Figure 4.14 Polarization plot for EΦ
Violet --- EΦ Polarization
Black --- Eθ polarization

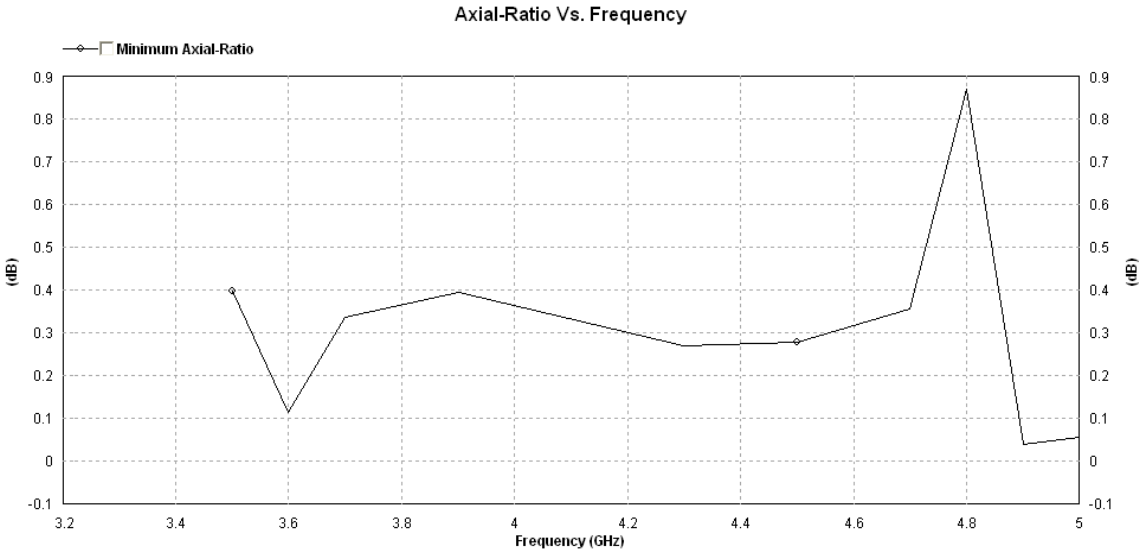

Figure 4.14(b) Axial ratio versus frequency

4.7.3 Left circular polarization

This polarization can be obtained by forward biasing the PIN diode at Plcp position and open-circuiting the remaining diodes. In this case, we get more bandwidth of the order of 700 GHz (3.6 GHz to 4.3 GHz). In the entire band, the difference between the left and right circular polarization is around 20 dB. The variation in return

loss (S_{11}) with respect to frequency and polarization plots are shown in figures 4.15 and 4.16(a) respectively. Figure 4.16(b) shows axial ratio versus frequency plot.

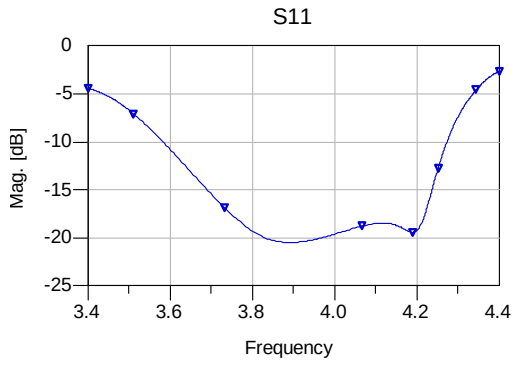

Figure 4.15 Return loss for lcp polarization

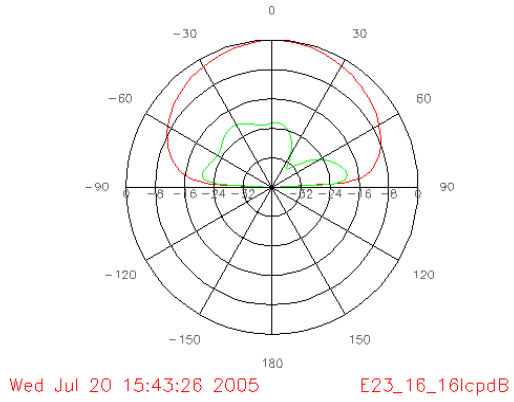

Figure 4.16(a) Polarization plot for lcp
Red --- lcp polarization
Green --- rcp Polarization

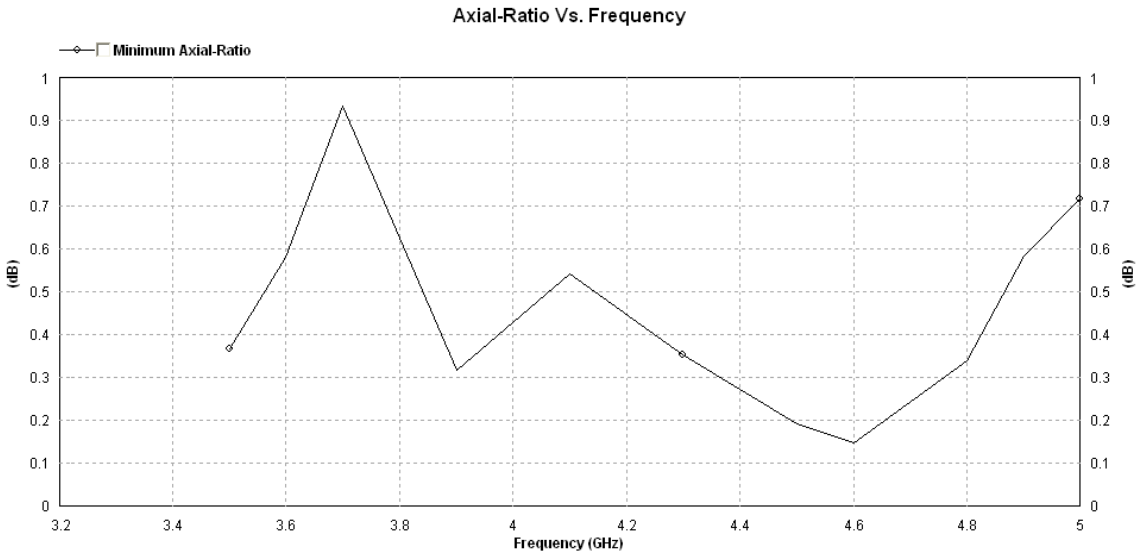

Figure 4.16(b) Axial ratio versus frequency

4.7.4 Right Circular Polarization

This polarization can be obtained by forward biasing the diode at Prcp position and open circuiting the remaining two diodes. In this case also, we get more bandwidth of the order of 700 MHz (3.6 GHz to 4.3 GHz). In the entire band, the difference between the right and left circular polarization is more than 18 dB. The variation in return loss (S11) with respect to frequency and polarization plots are shown in figures

4.17

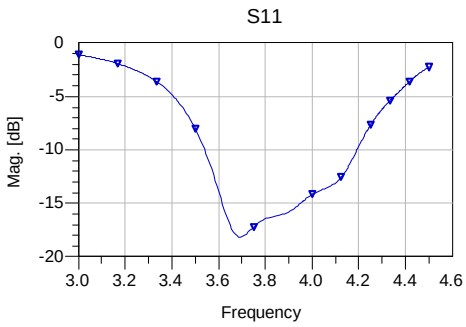

Figure 4.17 Return loss for rcp polarization

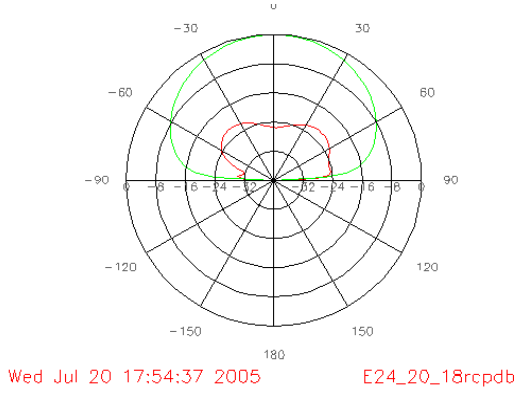

Figure 4.18(a) Polarization plot for rcp
Green --- rcp Polarization
Red --- lcp polarization

and 4.18(a) respectively. Figure 4.18(b) shows the axial ratio versus frequency plot.

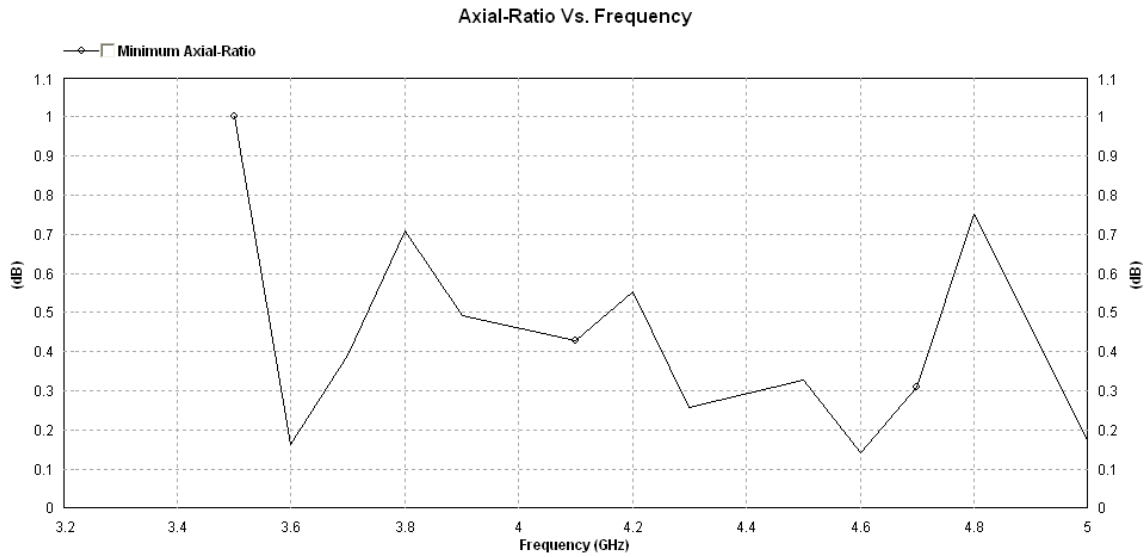

Figure 4.18(b) Axial ratio versus frequency

4.8 Design of Feed

The patch is fed with the help of microstrip line having characteristic impedance of 50 ohms. In order to obtain proper impedance matching between the feed line and the patch, the feed is placed at an offset. The exact position of the feed is shown in figure 4.10.

4.9 Design of Array

Using above patch, an array is designed. The separation between the two adjacent patches is kept as 30 mm. (approximately λ/2). At this separation, better bandwidth, polarization and low mutual coupling are obtained.

4.9.1 Design of Feed Network

Corporate feed is used to feed the patches in same phases. This is useful to obtain maximum directivity in the broadside direction. Most of the feed lines are having 50 ohm characteristic impedance. Metering is done at the bends or corners to improve the frequency response. Quarter wave transformers are used to match the impedances at the points where power is divided from one branch to two branches. A 100 ohm line is used at the port so that it will see 50 ohm impedance. The feed network feeds eight elements as shown in figure 4.19.

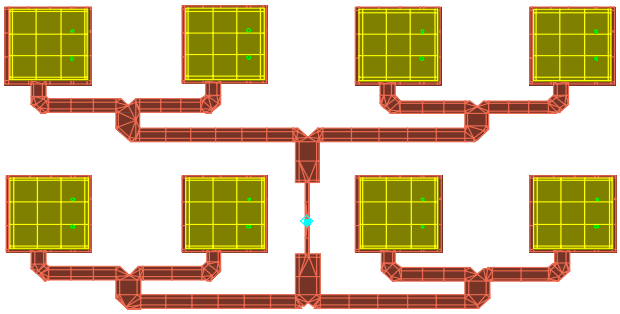

Figure 4.19 Array of eight elements array of eight elements (EΦ polarization)

4.10 Measurements

Figure 4.19 shows an array of 8 elements. It gives gain of 16.5 dB at 3.8 GHz and gain of 17.1 dB at 4.2 GHz. A single patch gives gain of 8.2 dB. Two patches gives gain

of 11.1 dB. Four patches give gain of 14 dB. If we double the number of patches, the gain also doubles or increases by 3 dB. In order to obtain gain of around 30 dB, it requires 256 patches.

Figure 4.20 shows the 3-dimensional radiation pattern. The variations in return loss (S11) with frequency are plotted in figure 4.21. The array gives bandwidth of 500 MHz approximately from 3.7 to 4.2 GHz.

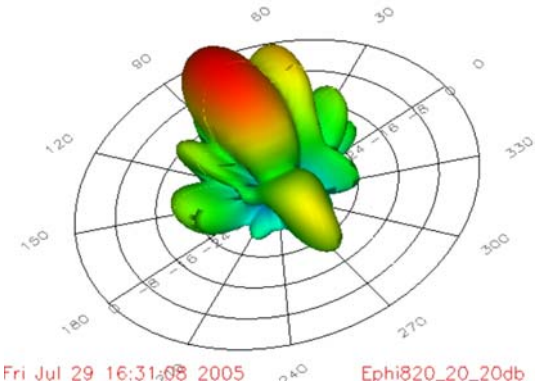

Figure 4.20 Three dimensional radiation pattern for array of eight elements (EΦ polarization)

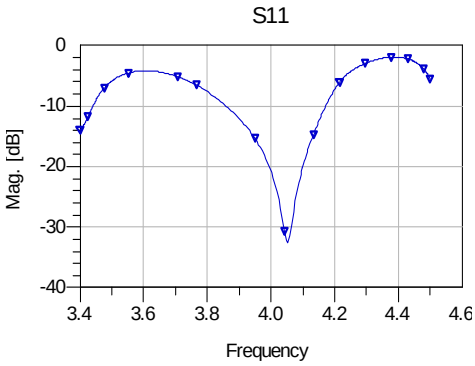

Figure 4.21 Return loss of array of eight elements (EΦ polarization)

Figure 4.22 shows the polarization levels. Red plot shows the levels of EΦ while green plot shows levels of Eθ. The difference between the EΦ and Eθ circular polarization is 20, 24 and 18 dB at start, middle and at end of the band respectively.

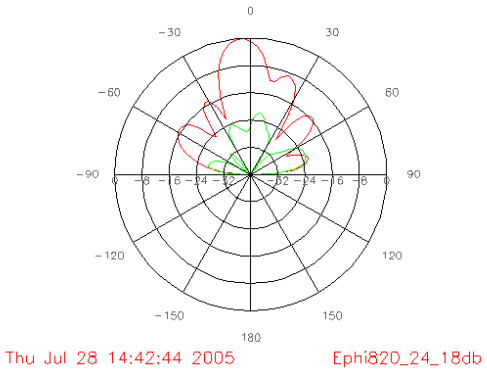

Figure 4.22 Polarization plot of array of eight elements (EΦ polarization)

Similar results can be obtained for other types of polarizations using 8 patches. Those results are not presented over here to avoid repeatability. When an array is formed, the positions of shorting pins need to be slightly adjusted to get more polarization purity. An array is designed for 256 patches, giving a gain of around 32 dB.

4.11 Conclusions

The electromagnetically coupled patch is compact and broadband. It can produce Eθ, EΦ and right as well as left circular polarizations. The array of 256 patches occupies just one square meter area. It gives gain of around 32 dB in the frequency range from 3.7 to 4.2 GHz. It is useful for C-band satellite TV reception.

5 Design of Feed and Feed Network for Microstrip Antennas

5.1 Introduction

The microstrip antenna can be excited either by a coaxial probe or by a microstrip line. It can also be excited indirectly using electromagnetic coupling or aperture coupling and a coplanar waveguide feed, in which case there is no direct metallic contact between the feed line and the patch [66-69]. Feeding technique influences the input impedance and characteristics of an antenna and is an important parameter.

5.1.1 The Coaxial or the Probe Feed

In the coaxial or the probe feed arrangement the centre conductor of the coaxial connector is soldered to the patch. Its main advantage is that it can be placed at any desired location inside the patch to match with its input impedance. The disadvantages are that the hole has to be drilled in the substrate and that the connector protrudes outside the bottom ground plane, so that it is not completely planar. Also, this feeding arrangement makes the configuration asymmetrical.

5.1.2 Microstrip Line Feed

A patch excited by microstrip line feed. This feed arrangement has the advantage that it can be etched on the same substrate, so the total structure remains planar. The drawback is the radiation from the feed line, which leads to an increase in the cross-polar level. Also in the millimeter-wave range, the size of the feed line is comparable to the patch size, leading to an increased undesired radiation.

5.1.3 Proximity Fed Microstrip Antenna

For thick substrates, which are generally employed to achieve broad bandwidth, both the above methods of feeding the microstrip antenna has problems. In the case of coaxial feed, increased probe length makes the input impedance more inductive, leading

to the matching problems. For the microstrip feed, an increase in the substrate thickness increases its width, which in turn increases the undesired feed radiation. The indirect feed discussed below, solves these problems. The electromagnetic coupling is known as proximity coupling [66, 69, 70]. The feed line is placed between the patch and the ground plane, which is separated by two dielectric media. The advantages of this feed configuration include the elimination of spurious feed-network radiation; the choice between two different dielectric media, one for the patch and other feed line to optimize the individual performances; and an increase in the bandwidth due to the increase in the overall substrate thickness of the microstrip antenna. The disadvantages are that the two layers need to be aligned properly and that the overall thickness of the antenna increases.

5.1.4 Aperture Coupled Microstrip Antenna

Another method for indirectly exciting a patch employ aperture coupling [71]. In the aperture-coupled microstrip antenna configuration, the field is coupled from the microstrip line feed to the radiating patch through an electrically small aperture or slot cut in the ground plane. The coupling aperture is usually centered under the patch, leading to lower cross-polarization due to symmetry of the configuration. The shape, size and location of the aperture decide the amount of coupling from the feed line to the patch [72-74]. The slot aperture can be either resonant or non-resonant [67, 68]. The resonant slot provides another resonance in addition to the patch resonance there by increasing the bandwidth at the expense of an increase in the back radiations. As a result, a non-resonant aperture is normally used. The performance is relatively insensitive to small errors in the alignment of the different layers. Similar to the electromagnetic coupling method, the substrate parameters of the two layers can be chosen separately for optimum antenna performance. This feeding method provides increased bandwidth.

5.1.5 Coplanar Waveguide Feed

The coplanar waveguide feed has also been used to excite the microstrip antenna [75-78]. In this method, the coplanar waveguide is etched on the ground plane of the microstrip antenna. The line is excited by a coaxial feed and is terminated by a slot,

whose length is chosen to be between 0.25 and 0.29 of the slot wave length. The main disadvantage of this method is the high radiation from the rather longer slot, leading to the poor front-to-back ratio. The front-to-back ratio is improved by reducing the slot dimension and modifying its shape in the form of a loop [79].

5.2 Corporate Feed

In the corporate feed configuration, the antenna elements are fed by 1:n power divider network with identical path lengths from the feed point to each element. The advantages of this topology include design simplicity, flexible choice of element spacing, and broader bandwidth, and they are amenable to integration with other devices such as amplifiers and phase shifters. The disadvantage of this type of array is that it requires more space for feed network. For large arrays, the length of feed lines running to all elements is prohibitively long, which results in high insertion loss. The insertion loss is even more pronounced at milimetre-wave frequencies, thereby adversely degrading gain of the array. At higher frequencies, the feed lines laid on the same plane as the patches will also radiate and interfere with the radiation from the patches.

Figure 5.1 shows the scheme of corporate feed. It consists of transmission lines, bends, power splitters or T junctions and quarter wave transformers.

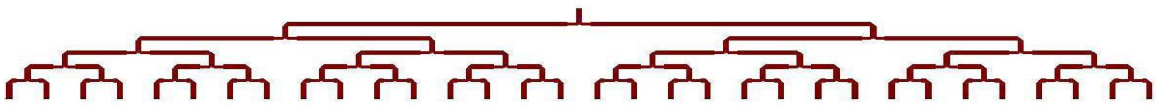

Figure 5.1 Corporate feed

5.3 Microstrip Transmission Line

Microstrip is a planar transmission line, similar to stripline and coplanar waveguide. Microstrip was developed by ITT laboratories as a competitor to stripline (first published by Grieg and Engelmann in the December 1952 IRE proceedings).

According to Pozar, early microstrip work used fat substrates, which allowed non-TEM waves to propagate which makes results unpredictable. In the 1960s, the thin version of microstrip became popular.

5.3.1 Overview of Microstrip

Microstrip transmission lines consist of a conductive strip of width "W" and thickness "T" and a wider ground plane, separated by a dielectric layer (the "substrate") of thickness "H" as shown in the figure below. Microstrip is by far the most popular microwave transmission line, especially for microwave integrated circuits and MMICs. The major advantage of microstrip over stripline is that all active components can be mounted on top of the board. The disadvantages are that when high isolation is required such as in a filter or switch, some external shielding may have to be considered. Given the chance, microstrip circuits can radiate, causing unintended circuit response. A minor issue with microstrip is that it is dispersive, meaning that signals of different frequencies travel at slightly different speeds. Variants of microstrip include embedded microstrip and coated microstrip, both of which add some dielectric above the microstrip conductor.

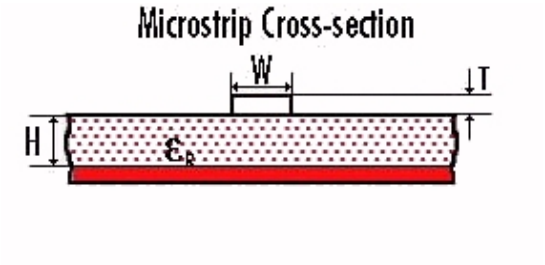

Figure 5.2 Microstrip line

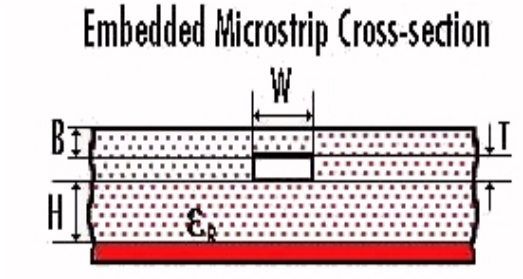

Figure 5.3 Stripline

5.3.2 Effective Dielectric Constant

Because part of the fields from the microstrip conductor exists in air, the effective dielectric constant is somewhat less than the substrate's dielectric constant (also known as the relative permittivity). According to Bahl and Trivedi [80], the effective dielectric constant ε_{eff} of microstrip is calculated by:

$$when \left(\frac{W}{H}\right) < 1$$

$$\varepsilon_e = \frac{\varepsilon_r + 1}{2} + \frac{\varepsilon_r - 1}{2}\left[\left(1 + 12\left(\frac{H}{W}\right)\right)^{-1/2} + 0.04\left(1 - \left(\frac{W}{H}\right)\right)^2\right]$$

$$when \left(\frac{W}{H}\right) \geq 1$$

$$\varepsilon_e = \frac{\varepsilon_r + 1}{2} + \frac{\varepsilon_r - 1}{2}\left(1 + 12\left(\frac{H}{W}\right)\right)^{-1/2}$$

The effective dielectric constant is a seen to be a function of the ratio of the width to the height of the microstrip line (W/H), as well as the dielectric constant of the substrate material. There are separate solutions for cases where W/H is less than 1, and when W/H is greater than or equal to 1. These equations provide a reasonable approximation for ε_{eff} (effective dielectric constant). This calculation ignores strip thickness and frequency dispersion, but their effects are usually small.

5.3.3 Wavelength

Wavelength for any transmission line can be calculated by dividing free space wavelength by the square root of the effective dielectric constant, which is explained above.

5.3.4 Characteristic Impedance

The characteristic impedance Z_0 is also a function of the ratio of the width to the height (W/H) of the transmission line, and also has separate solutions depending on the value of W/H. According to Bahl and Trivedi [80], the characteristic impedance Z_0 of microstrip is calculated by:

$$when \left(\frac{W}{H}\right) < 1$$

$$Z_0 = \frac{60}{\sqrt{\varepsilon_{eff}}} \ln\left(8\frac{H}{W} + 0.25\frac{W}{H}\right) \quad (ohms)$$

$$when \left(\frac{W}{H}\right) \geq 1$$

$$Z_0 = \frac{120\,\pi}{\sqrt{\varepsilon_{eff}} \times \left[\frac{W}{H} + 1.393 + \frac{2}{3}\ln\left(\frac{W}{H} + 1.444\right)\right]} \quad (ohms)$$

5.3.5 Effect of Metal Thickness

Having a finite thickness of metal for the conductor strips tends to increase the capacitance of the lines, which effects the ε_{eff} and Z_0. Following figure shows Electromagnetically coupled microstrip fed MSA. The substrate used for this microstrip antenna is having dielectric constant of 2.2 and thickness of 1.6 mm. In order to obtain characteristic impedance of this microstrip transmission line equal to 50 ohm, the width of the strip is kept 4.7mm. This calculation can be done using the above formulae.

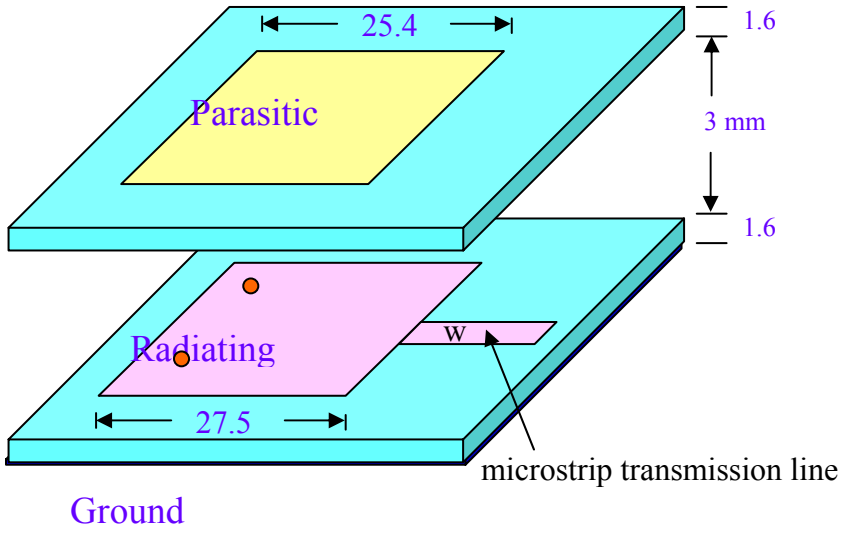

Figure 5.4 Electromagnetically coupled microstrip fed MSA

5.4 Bends in Transmission Lines

5.4.1 Overview

There is no best way to bend a microstrip or stripline transmission line. The first problem is that the discontinuity changes the line characteristic impedance; without compensation the bend adds shunt capacitance. But in reality the small capacitance that is usually a result doesn't change the circuit's performance very much. The other problem associated with bends is can cause far more damage to the intended performance of a highly tuned circuit: the effective length of the transmission line becomes shorter than the centerline length.

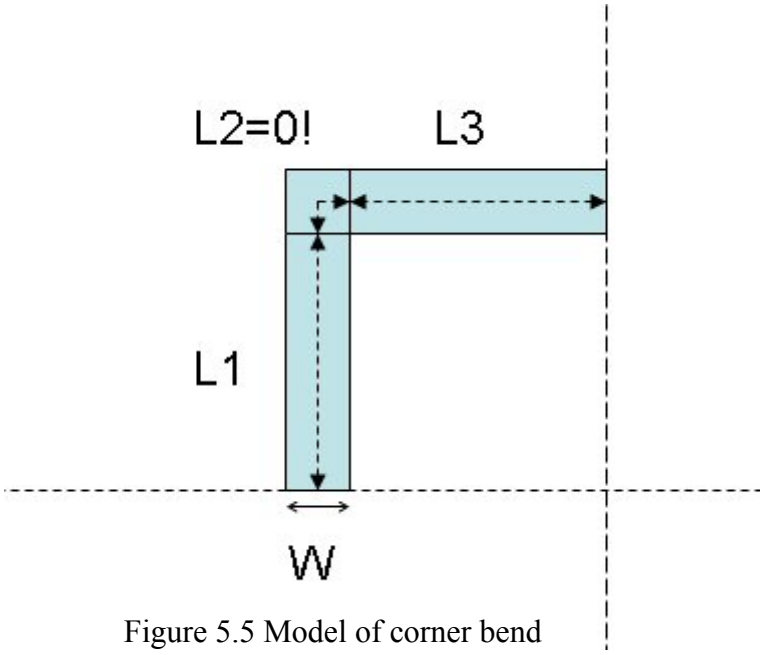

Figure 5.5 Model of corner bend

5.4.2 Mitered Bends

When a ninety degree bend is made in a transmission line, it adds a small amount of capacitance. "Mitering" the bend chops off some capacitance, restoring the line back to it's original characteristic impedance. The image below shows the important parameters of a mitered bend.

5.4.2.1 Microstrip Miter Compensation

The "optimum" mitered bend equations for microstrip were found empirically [81,82]. For a line of width W and height H,

D = W* SQRT(2) (the diagonal of a "square" miter)

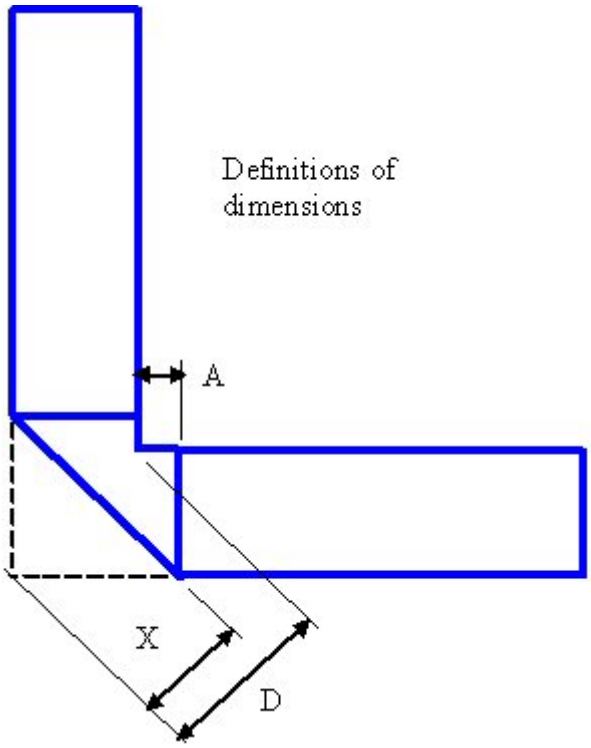

Figure 5.6 mitered bends

X= D* (0.52 + 0.65 e ^ (-1.35 * (W/H))

A = (X- D/2) * SQRT(2)

The miter is not a function of substrate dielectric constant. But the range that the accuracy of this calculation is valid is limited to:

$0.5 <= W/H <= 2.75$

$2.5 <= E_r <= 25$

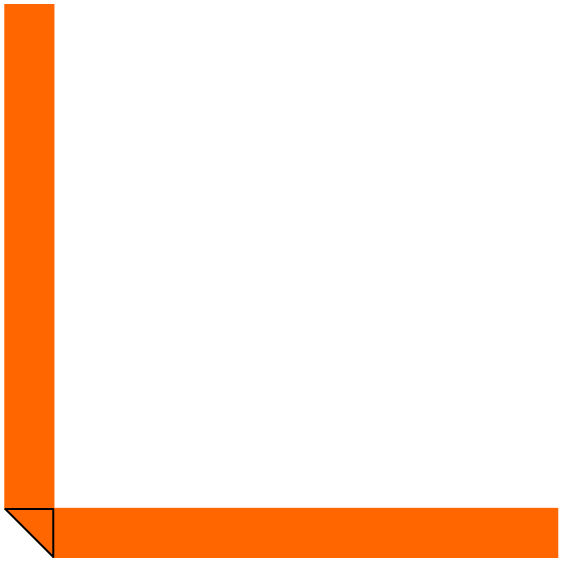

Figure 5.7 Metered bend used in the array

In the antenna array, design the bend used is as shown in the figure. Here X= D/2 and A=0. This bend gives good compensation for higher frequencies. If this kind of metering is not used then it affects higher frequencies in the band.

5.5 Junction

A junction between two dissimilar width sections also introduces a large discontinuity. A standard T-junction power divider is shown in figure 5.8.

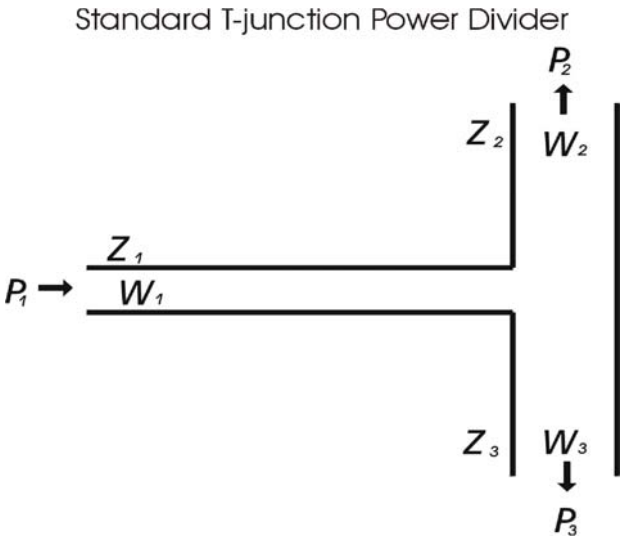

Figure 5.8 Standard T-junction power divider

In figure 5.8, the input power P_1 is delivered to the intersection on a microstrip of width W_1 and impedance Z_1. The line then branches into two arms with power, width and impedance given by Z_2, P_2, W_2 and P_3, W_3, Z_3 respectively. The design equations for this divider are

$$Z_1 = \frac{Z_2 \times Z_3}{Z_2 + Z_3}, \quad P_2 = \left(\frac{Z_1}{Z_2}\right) P_1, \quad P_3 = \left(\frac{Z_1}{Z_3}\right) P_1$$

This simplest type of matched T-junction is the lossless 3dB power divider. It can be seen from the equations above that if $Z_2 = Z_3 = 2Z_1$, the power will split evenly into the arms of the T with each arm having half the original power. The impedances of the two arms act just like resistors wired in parallel. To match the impedances of the arms of the T to the impedance of the base, the arms must have twice the impedance of the base.

The discontinuities are second order, become significant at frequencies above 3 GHz. Figure 5.10 shows the T used in the array design. In this array, as the frequency is above 1 GHz, it requires a V groove at the power divider. If this groove is not used some power is reflected back. The angle of groove $\theta=\arctan w_1/w$.

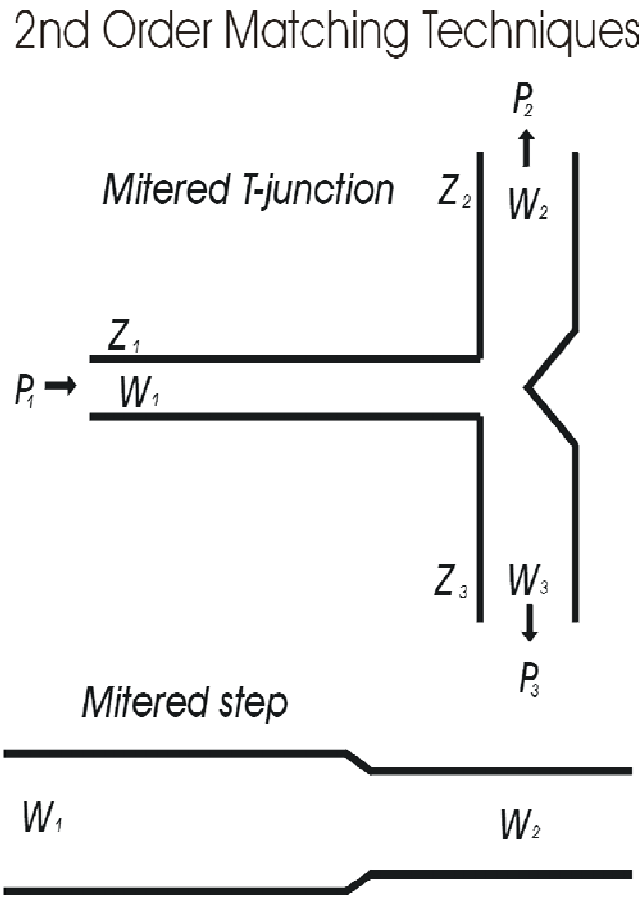

Figure 5.9 Second order discontinuities and their compensation techniques.

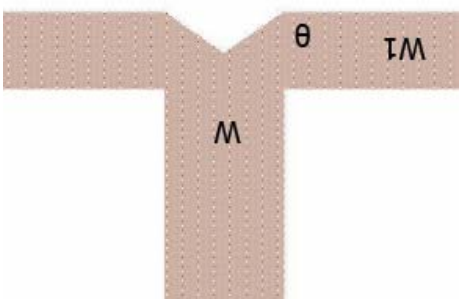

Figure 5.10 T-Junction with groove

5.6 Quarter-Wave Transformer

A general mismatch in impedance between two points on a transmission line can be compensated with a quarter-wave transformer [83-85]. The quarter-wave transformer is a very useful matching technique that also illustrates the properties of standing waves on a mismatched line. First, an impedance-based explanation of how a quarter-wave transformer works will be described; then a more intuitive explanation that is analogous to destructive interference in thin films will be discussed. A quarter wave transformer in microstrip is shown in figure 5.11.

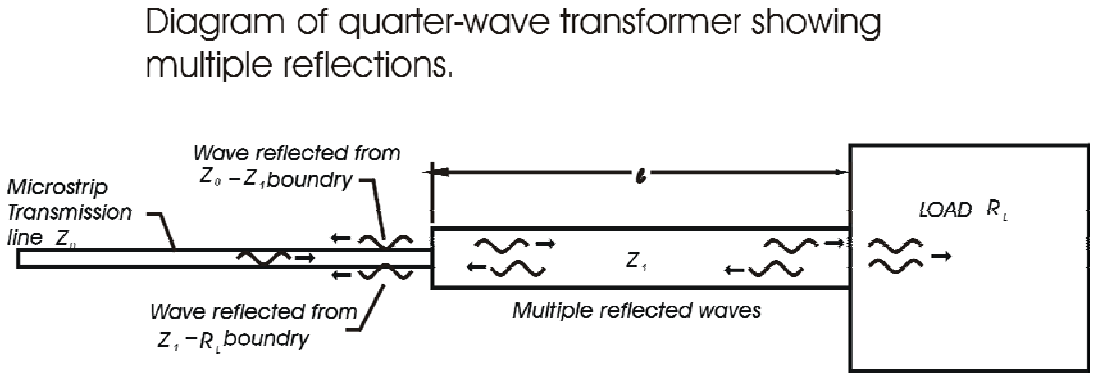

Figure 5.11 Quarter wave impedance transformer

In a quarter-wave transformer, a load resistance R_L need to be matched to the characteristic feedline impedance Z_0 through a short length of transmission line of unknown length l and impedance Z_1. The input impedance looking into the matching section of line is given by;

$$Z_{in} = Z_1 \frac{R_L + jZ_1 \tan \beta l}{Z_1 + jR_L \tan \beta l}$$

If we choose the length of the line = $\lambda/4$ then $\beta l = \left(2\pi/\lambda\right)\left(\lambda/4\right) = \pi/2$, divide through by $\tan\beta$ and take the limit as $\beta l \to \pi/2$ to achieve

$$Z_{in} = \frac{Z_1^2}{R_L}$$

For a perfect transition with no reflections at the interface between microstrip and load, $Z_{in} = Z_0$ and this gives us a characteristic impedance Z_1 as

$$Z_1 = \sqrt{Z_0 R_L}$$

which is the geometric mean of the load and source impedances. With this geometry, there will be no standing waves on the feedline although there will be standing waves on the $\lambda/4$ matching section. In fact, any odd multiple (2n + 1) of $l = \lambda/4$ will also work.

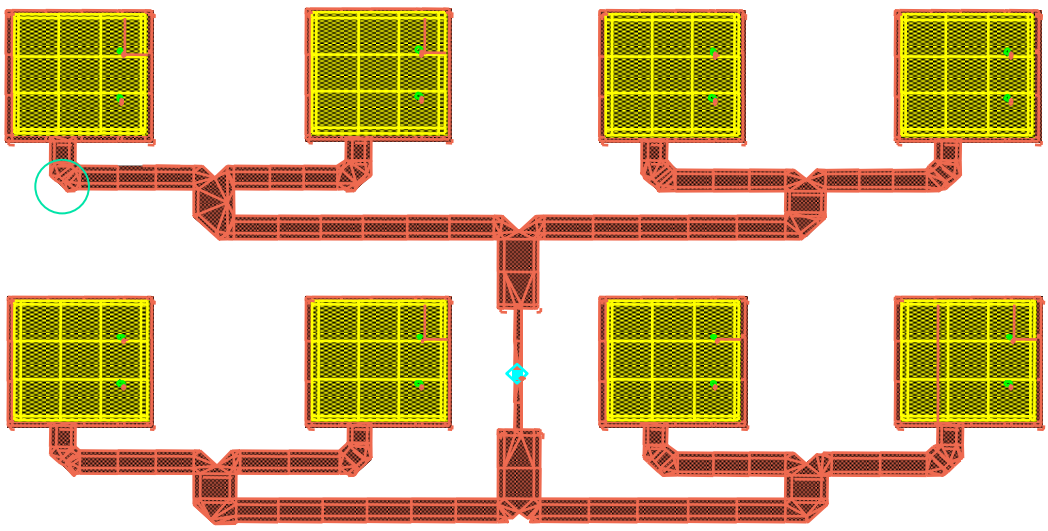

Figure 5.12 feed network for the array

When the line length is precisely $\lambda/4$ the reflected wave from the load destructively interferes with the wave reflected from the Z_0, Z_1 interface and they cancel each other out. It should be noted that this method can only match a real load. If the load has an appreciable imaginary component, it must be matched differently. It can be transformed into a purely real load, at a single frequency, by adding an appropriate length of feedline.

Figure 5.12 shows the complete feed network with the patches. There are many transmission lines, V grooves, power slitters, and quarter wave transformers.

5.7 Space Fed Microstrip Antennas

System studies and hardware investigations on high-speed wireless communications are being conducted at license free ISM (industrial, Scientific and Medical) band, millimeter-wave and quasi-millimeter-wave frequencies. These applications require compact, high-performance, and low-cost wireless equipment. A highly integrated RF module, the so-called system-on-package module, which employs a multilayer structure, is effective in achieving the above requirements. It is necessary to adopt active integrated antenna technology to achieve a module with antennas that are low-power consuming and have low-noise characteristics. Currently, there is considerable interest in incorporating active devices at the level of radiating elements of large phased arrays. However, use of phased array is often avoided because of its excessive cost, technological problems in heat dissipation, parasitic effects of bias networks, lack of available space etc. Moreover, microstrip technology allows monolithic implementation by fabricating both active devices and antennas on the same semiconductor substrate.

Microstrip-fed Microstrip Antenna (MSA) is designed to overcome the disadvantages of reflector antennas and line fed microstrip array or reflectarray antenna such as low efficiency, complicated design and aperture blockage. The resulting antenna is planar and since the feed is located behind the feed patch, there is no aperture blockage and the whole configuration can be mounted conformal to the host structure. In the

design of efficient and highly directive microstrip-fed microstrip antenna, physical dimension of parasitic antenna is increased. Higher order mode radiation is investigated while excitation of multimode is avoided by operating the feed patch in dominant mode and hence large phase array are avoided. Antenna performance of space fed microstrip antenna with parasitic patch dimensions ranging from λ/2 x λ/2 to 5λ/2 x 5λ/2 is investigated These antennas may find applications in mm range where fabrication is the major limitation.

Effect of shape of elements on directivity, bandwidth and side lobe level is investigated. Effect of superstrate height, substrate and superstrate dielectric and number of multilayer on directivity has also been incorporated.

5.8 Reported Work in Literature

Antennas are the fundamental component of any wireless communication system. The ubiquity of wireless and satellite communications has spurred the development of an extraordinary range of antenna shapes and sizes, each with its own advantages and limitations. There are many applications where space is at a premium, and where there is an urgent need for an antenna with the flexibility to efficiently combine the capabilities of multiple antennas. There are applications where omnidirectional antennas are required, however a highly directive and efficient antenna is a necessity in other applications.

System studies and hardware investigations on high-speed wireless communications are being conducted at license free ISM (industrial, Scientific and Medical) band, millimeter-wave and quasi-millimeter-wave frequencies [86-88].These applications require compact, high-performance, and low-cost wireless equipment. A highly integrated RF module, the so-called system-on-package module, which employs a multilayer structure, is effective in achieving the above requirements [89-92]. It is necessary to adopt active integrated antenna technology to achieve a module with antennas that are low-power consuming and have low-noise characteristics [93-95]. Several approaches to achieve an RF module that is integrated with antennas were

reported. One approach uses a semiconductor chip antenna such as a microstrip antenna (MSA) that is integrated with RF circuits on the same semiconductor substrate [89]. However, in this approach, it is difficult to establish a high-gain antenna that employs an array antenna configuration on a semiconductor substrate due to the substrate size. Therefore, high-gain compact antennas have not yet been integrated with monolithic microwave integrated circuits (MMICs). A multichip-module approach was also proposed to construct a module integrated with antennas [90-91]. In this module, antennas and MMICs are connected by wire bonding or a ribbon, which results in high-connection loss. This approach also requires a low-loss feeding circuit. The dielectric lens antenna was adopted to achieve a high-gain antenna [92]. However, the commonly used lens antenna is constructed using an expensive crystal material and it is difficult to mount it on the MMIC package. Additionally, a dielectric lens antenna constructed using resin was investigated as a low-cost alternative. There are problems, however, regarding mounting the antenna on the MMIC package and achieving high efficiency. Moreover, it is difficult to construct an array antenna substrate on a single layer due to the limitations in the manufacturing process for the millimeter-wave frequency band. The technique for improving the radiation efficiency by arranging parasitic elements above the feeding MSA elements is examined [96-101]. However, obtaining a sufficient absolute gain is difficult in this study [107–111]. This paper investigates the high-gain antenna using a low permittivity or the air layer [101]. However, only the directional gain is described and there is a problem in that it is difficult to support the parasitic element substrates. In particular, it is difficult to adopt this antenna in the system-on-package for the millimeter-wave frequency. To overcome the above problems, a multilayer parasitic microstrip antenna array (MPMAA) structure based on a parasitic antenna configuration [96] using a low-temperature co-fired ceramic substrate (LTCC) suited to packaging the MMIC chip [102]. However, since the LTCC substrate has a high electric constant, it is difficult to achieve wide-band and high-efficiency characteristics.

5.9 High Directive Antennas

High antenna directivity, required in space and mobile applications is usually achieved by using either parabolic reflector or line fed antenna array or by using reflectarray. In a great number of microwave applications, a highly directive antenna with a main beam scanned to a certain angle is required. To achieve this, a certain aperture illumination with progressive phasing is used. This can be primarily done by two ways viz. reflectors and arrays. The reflector uses its geometry to create the desired phase across the aperture while the array employs distinct elements fed with progressive phasing.

5.9.1 Parabolic Reflector Antenna

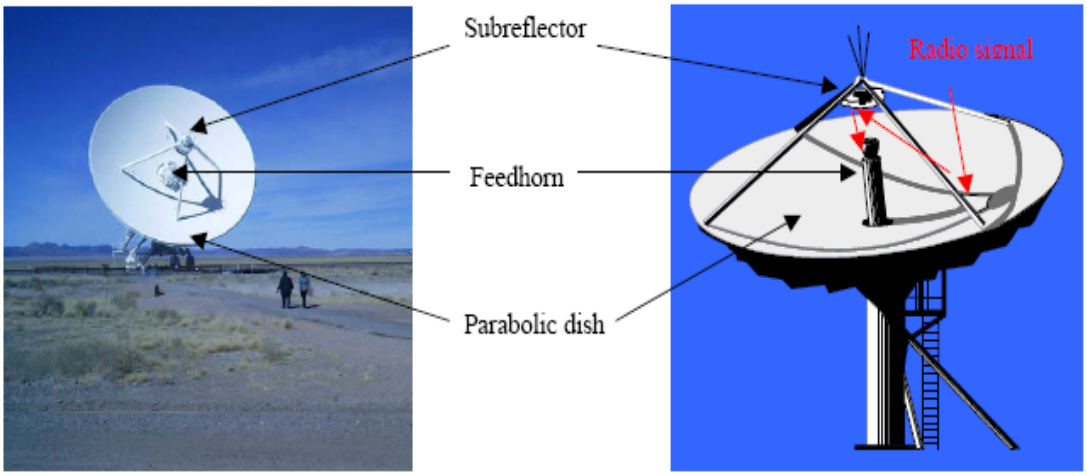

Figure 5.13 Parabolic reflector antennas

The parabolic reflector shown in figure 5.13 has the disadvantage due to its mechanical requirement and physical shape which comes as an obtrusion in space and mobile applications. However the parabolic reflector antenna operates over large bandwidth.

5.10 Antenna Array

High directive antennas can be accomplished by enlarging the electrical size of the antenna. A simple way to enlarge the dimensions of antenna without increasing the size of the individual element is to form an assembly of radiating elements in electrical and geometrical configurations. This new antenna, formed by multi-elements, is referred to as an array. The individual elements of an array may be of any form (wires, apertures etc).

The total field of the array is determined by the vector addition of the fields radiated by the individual elements. This assumes that the current in each element is the same as that of isolated element. But practically it depends on the separation between the elements. To provide highly directive patterns, it is necessary that the fields from the elements of the array interfere constructively in the desired directions and interfere destructively in the remaining space. In an array of identical elements there are five controls that can be used to shape the overall pattern of the antenna [93].
These are:

- The geometrical configuration of the overall array.
- The relative displacement between the elements.
- The excitation amplitude of the individual elements.
- The excitation phase of the individual elements.
- The relative pattern of the individual elements.

Multiple antennas can be interconnected by means of a feed network to form an array and made to work in concert to produce a more directional radiation pattern. Since the radiation pattern of an array is dependent on the summation of the far fields produced by the constituent elements, a high-gain antenna array can be designed by interconnecting a number of relatively low-gain antenna elements. It is important to distinguish between two types of arrays - those with similarly oriented, identical elements, and those with either dissimilar elements or elements with different orientations. The radiation pattern of an array of identical elements is the product of two parts- the pattern of each individual

element called the element pattern, and the array pattern that would result if the elements were isotropic radiators (also called the array factor):

$$F(\theta,\varphi) = ga(\theta,\varphi)\, f(\theta,\varphi)$$

In the above equation, $F(\theta,\varphi)$ is the overall normalized pattern of the array, $ga(\theta,\varphi)$ is the normalized element pattern, and $f(\theta,\varphi)$ is the normalized array factor.

The above principle, known as pattern multiplication, is fundamental to the operation of arrays. Pattern multiplication, however, is not applicable to arrays comprised of elements with dissimilar orientations, shapes or amplitude feed distribution since the factorization of the overall pattern into the element and array factors become complicated.

An arbitrarily configured two dimensional array comprised of similar elements, with the elements arranged in a rectangular grid is shown in figure 5.14.

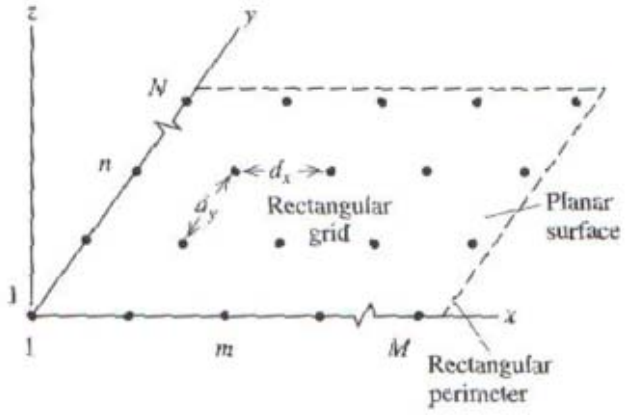

Figure 5.14 Planar array of elements

The elements are arranged in a rectangular grid, a particular element may be identified as, "mn", where m is the number of element along x axis and n is the number of elements along y axis. A vector that defines the position of each element in an arbitrary three dimensional array extends from the origin to the element with location "mn", and is given by:

$$r'_{mn} = x'_{mn}\, a_x + y'_{mn}\, a_y + z'_{mn}\, a_z$$

Thr array factor in three dimensional array is given by:

$$AF(\theta,\varphi) = \Sigma_{n=1 \text{ to } N} \Sigma_{m=1 \text{ to } M} I_{mn} e^{j(\beta \mathbf{a}_r \cdot \mathbf{r}'_{mn} + \alpha_{mn})}$$

where α_{mn} is the excitation current phase to the element "mn".

Antenna arrays are inherently more flexible than conventional antennas, and we can exercise far more control on the radiation pattern, whether in terms of beam scanning or for beam shaping purposes. A phase difference can be implemented in the currents feeding adjacent elements to steer the array main beam to any desired angle. Additionally, we can reduce side-lobe levels in the array pattern by implementing amplitude tapering in the currents. The radiation pattern of an array is thus determined by the number and type of constituent antenna elements, their spatial locations and orientations, and the amplitudes and phases of the currents feeding them.

5.11 Line Fed Microstrip Antenna Arrays

Line fed microstrip antenna array, shown in figure 5.15, has been developed to increase the directivity of antenna. However the microstrip array have the disadvantage of low efficiency due to line losses and high cross polar radiation by the feed line network. Beside this feed line network employed between the microstrips patches also increase the overall size of the line fed microstrip arrays. Sophisticated fabrication techniques are required to meet the matching constraints of the feeding network. Hence continuous research is on to meet the demand of efficient, high gain planar antennas.

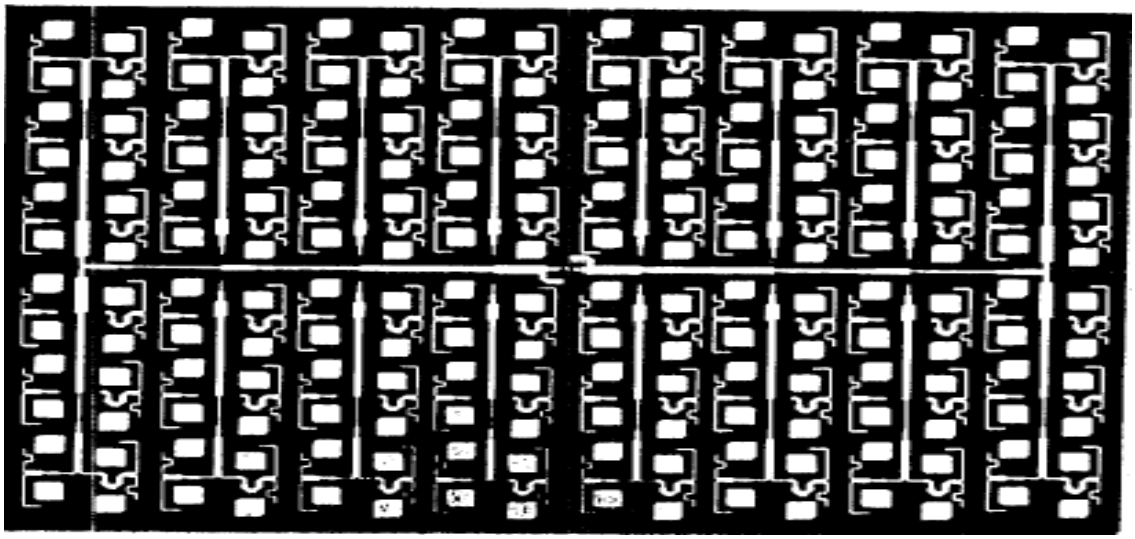

Figure. 5.15 Line fed microstrip antenna array

A reflectarray combines the features of both a reflector and an array and was first introduced in 1963 by Berry *et al.*[86]. A reflectarray is an array of antennas which are illuminated by a primary feed horn instead of conventional transmission line feeds. The elements of the reflectarray receive and then reradiate the incident energy of the feed horn with a given phase determined by the phase-shifting device attached to the element.

The concept of a reflectarray is shown in figure 5.16. There are several advantages of this type of antenna versus a phased array or a conventional reflector. First, there is no complex feed network which could introduce a high loss or phase shift of the transmitted or received signal. Second, for the most part, the reflectarray is a two-dimensional structure and can be conformed to a given surface shape, reducing the bulk and mechanical complexity of the antenna. Reflectarrays in the past [86] have used waveguides as the array elements. Waveguides or other conventional antennas, however, are relatively bulky and expensive to manufacture. An appealing option is to use a microstrip antenna, such as a dipole or patch antenna, as the array elements due to its compactness, simple packaging requirements, conformal abilities, and low manufacturing cost. The microstrip reflectarrays can be easily mounted on roofs and walls for wireless communications and broadcasting. However reflectarray also suffer from the disadvantage of low efficiency due to dielectric loss and complicated design.

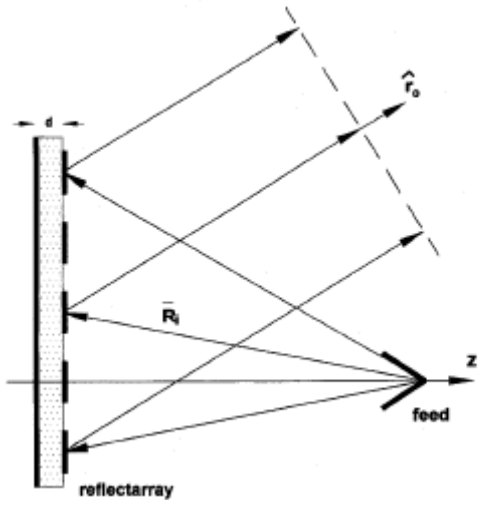

Figure 5.16 Reflectarray

The main disadvantage of reflector is geometrical constraint it imposes on the design. Basically, both these antennas have distinct advantages – reflector antennas are simple, while arrays yield more precise control and versatility at the expense of simplicity. In order to overcome the disadvantages of reflector antennas such as low efficiency, complicated design and aperture blockage, microstrip-fed Microstrip Antenna (MSA) Array is proposed [91-92].

Space fed microstrip antenna array shown in figure 5.17 is a planar array in which the location of the feed antenna is behind the radiating elements eliminating any aperture blockage and the whole configuration can be mounted conformal to the host structure. Since the feed-line network is completely avoided, there are lesser requirement on fabrication tolerance and no loss in the feeding network. The elements are fed from the radiation of a microstrip antenna.

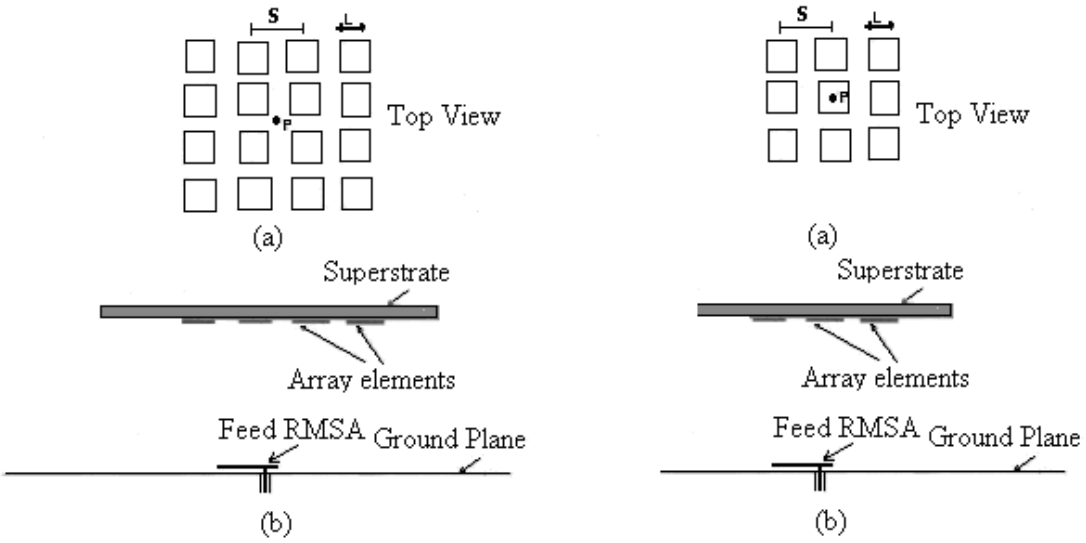

Figure 5.17 Geometry of even (4x4) and odd (3x3) space fed micro strip array Antenna (a) top view (b) side view

Space Fed Microstrip Array Antenna is planar and flexible than a conventional parabolic reflector; the whole configuration can be mounted conformal to the host structure. Since the feed is located behind the array, there is no aperture blockage. Space Fed Microstrip Array Antenna also has the advantages of high directivity, high efficiency, low side- lobe level (SLL) and low cross polarization.

In the design of an efficient, low SLL, planar, space-fed microstrip antenna array, the array theory has been applied to obtain the necessary phasing between adjacent array elements. This phasing has been done in an innovative and easy- to-design formulation. However Space Fed Microstrip Array Antenna also requires sophisticated fabrication techniques at millimeter or sub millimeter range.

Currently, there is considerable interest in incorporating active devices at the level of radiating elements of large phased arrays. This is due to the fact that the feed line loss increases with the array size and can become excessive for microstrip arrays. The proximity of the amplifiers to the radiating elements reduces the feed network loss and thus improves the array performance. Also, it enables simple control of the radiation

pattern and beam scanning. These become feasible since the gain of the active devices can be used to control the array element excitation, in both amplitude and phase, to compensate for the losses and achieve proper aperture distributions. Moreover, microstrip technology allows monolithic implementation by fabricating both active devices and antennas on the same semiconductor substrate. However, the use of an active device for each radiating element of the array is often avoided because of its excessive cost, technological problems in heat dissipation, parasitic effects of bias networks, lack of available space etc. A good solution to all these problems is, therefore, to dedicate active devices to a group of elements in the form of contiguous sub arrays. A convenient choice is the four-element sub array, which leads to a symmetrical arrangement in both directions, the elements of which can be fed by a simple feed network. The effect of partitioning an array into sub arrays on the radiation characteristics usually introduces grating lobes [86]. However, the effect can be controlled by tapering the sub array excitation [87]. Also, the sub array architecture can be used to eliminate scan blindness [88]. In using sub arrays, a further benefit can be gained by eliminating the feed lines to subarray elements. This is achieved here by electromagnetically coupling four radiating elements to a driven patch etched on a lower substrate.

Analysis and design of microstrip fed microstrip antenna requires an understanding of microstrip antenna, which is discussed in the following chapter along with the approach and the design formulation of microstrip fed microstrip array antenna.

5.12 Analysis of Space Fed Microstrip Antenna

The radiation pattern of microstrip antenna has large beam width and the patch provides 6 – 8 dB directivity. Microstrip antennas also suffer from low efficiency and low gain. In many applications, it is necessary to design antennas with very high directive characteristics to meet the demand of long distance communication. This can be accomplished by enlarging the size of the antenna. But increasing the size of antenna will result in excitation of higher order modes or multimode. In space fed microstrip antenna the length of the fed patch element is kept $\lambda_o /3$ L < $\lambda_o /2$, while dimensions of parasitic

patch are increased beyond λ_o /2 to study higher order mode radiation. An attempt is made to observe its effects on antenna performance. A detailed investigation is required to understand the higher order mode radiation in space fed microstrip antenna.

The parasitic patch is fed from the radiating field of a microstrip antenna. The geometry of space fed microstrip antenna is shown in figure 5.18 The feed patch is a metallic patch of thickness 0.7 mm at a height of 2.0 mm from an infinite ground plane. The parasitic patch is located at a height 'hs' from the feed patch and fabricated on the bottom side of FR4 superstrate. This superstrate also acts as a radome to the antenna. Air is used as a dielectric medium between feed patch and ground plane and also between superstrate and feed patch to achieve high efficiency. Feed patch is fed through a coaxial probe of 50 Ω. The space fed single patch antenna is designed to operate in 5.725 – 5.875 GHz ISM band.

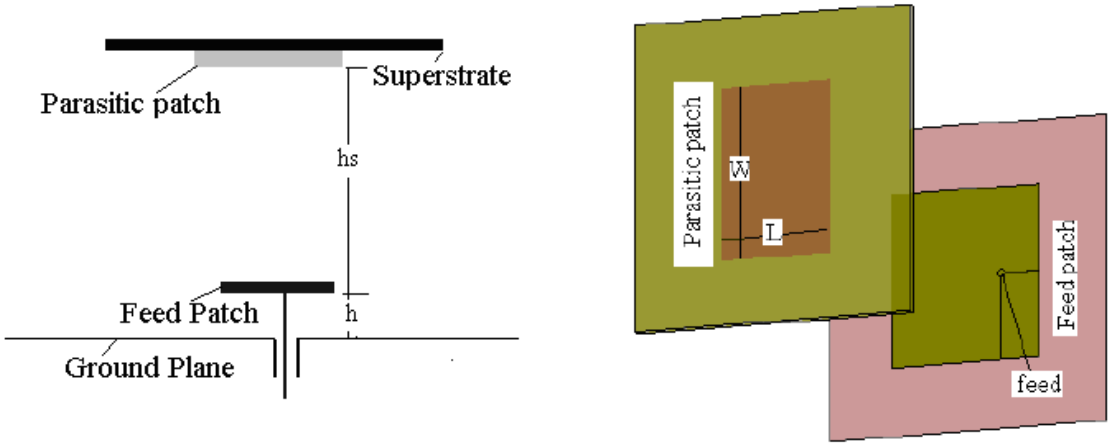

(a) (b)

Figure 5.18 Geometry of space fed microstrip antenna (a) side view (b) top view

5.13 Parametric Study

Initially a single parasitic patch (PP) is placed at hs1 = 0.5 λ_o above the microstrip feed patch and the dimensions of microstrip antenna and parasitic patch are optimized to operate at 5.725 – 5.875 GHz ISM band. The optimized structure has feed and parasitic

patch dimensions of 21.9 mm x 25.4 mm and 14.0 mm x 25.4 mm respectively. This structure is also a reference structure. The resonant conditions can be shifted by changing the dimensions of feed and parasitic patch. It also depends on the relative height between parasitic and feed patch. The feed patch and parasitic patch resonate separately depending on their dimensions and the whole structure resonates when both patches resonate at same frequency. The structural resonance depends on the relative position and dimensions of patches. Since at resonance, the reflection coefficient is + 1 the parasitic patch is placed at $\lambda_o/2$ and at integral multiple of $\lambda_o/2$ in a structure with multiple parasitic patches.

5.13.1 Effect of Length of Parasitic Patch

The increase in parasitic patch length results in decrease in resonance frequency for a fixed feed patch dimensions which indicates that the parasitic patch resonates at different frequency. The structure resistance increases and becomes more capacitive. The impedance variation vs. parasitic patch length is shown in figure 5.19 Change in length of parasitic patch with respect to reference antenna will cause the two patches to resonate separately and hence gain decreases with increase or decrease in length of parasitic patch.

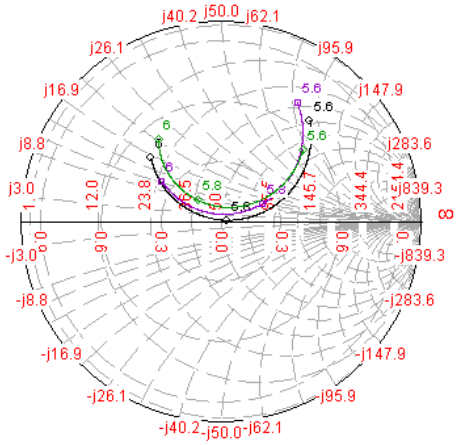

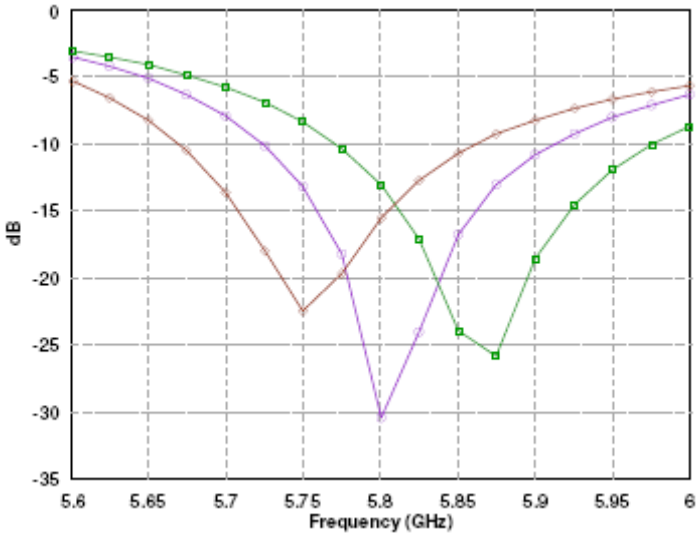

Figure 5.19 Impedance variations vs. length of parasitic patch
(10 mm 14 mm 18 mm)

5.13.2 Effect of Width of Parasitic Patch

There is little effect on resonance frequency with change in width of parasitic patch. Directivity, gain, efficiency and impedance bandwidth increase with width of parasitic patch but Side lobe level also increases with width, however cross polarization decreases marginally. Beamwidth in E– plane decreases while there is no effect on beamwidth in H plane.

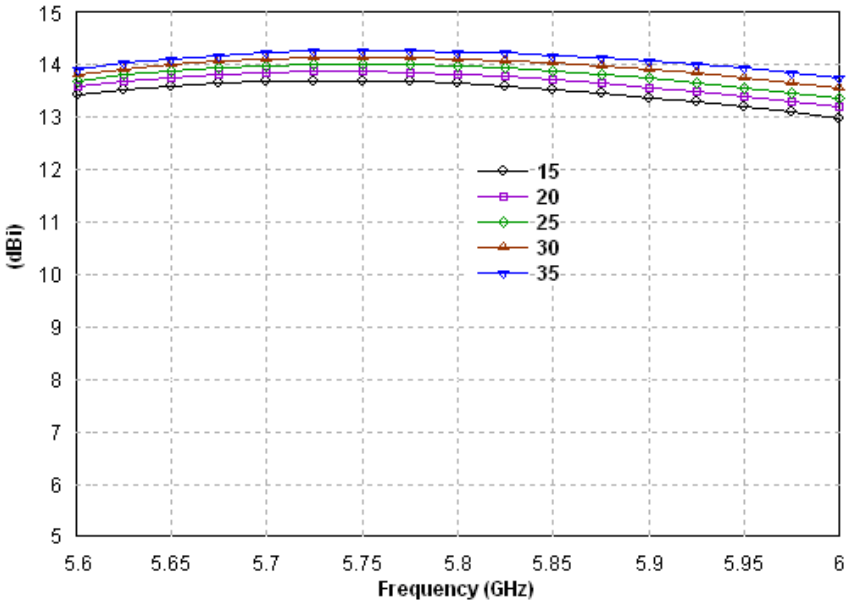

Figure 5.20 Directivity variations vs. width (mm) of parasitic patch

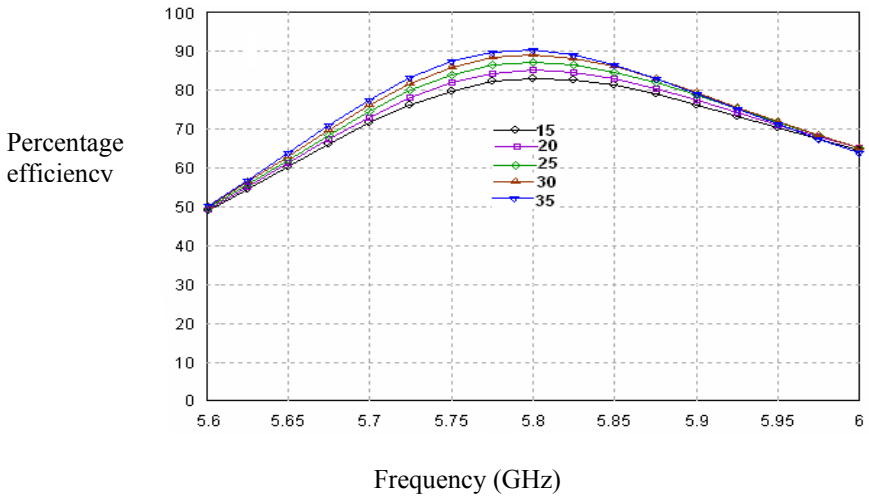

Figure 5.21 Efficiency vs. frequency for various widths (mm) of parasitic patch

5.13.3 Effect of Superstrate or Parasitic Patch Height

Change in the height of superstrate results in decrease in gain and impedance bandwidth. Since the reflection coefficient is +1, the structure resonates at $\lambda_o/2$.The impedance variation vs. superstrate height is shown in figure 5.22 With increase in parasitic height, the impedance becomes inductive and coupling between the parasitic and feed patch decreases resulting in smaller loop area of impedance variation on the smith chart.

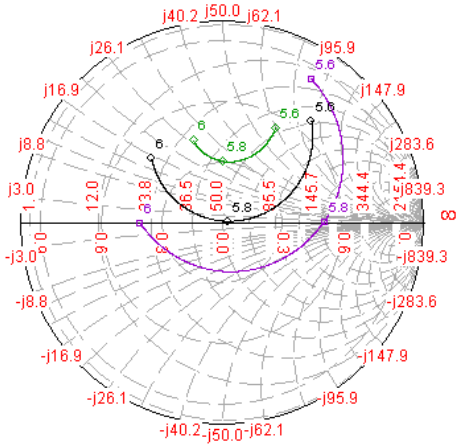

Figure 5.22 Impedance variations vs. superstrate height
(0.45 λo 0.5 λo 0.55 λo)

5.13.4 Effect of Feed Patch Height

Increase in feed patch height has little effect on the directivity. The resonance frequency changes with change in height of feed patch but it can be restored by changing the dimensions of feed patch. Bandwidth increases with height of feed patch but cross polarization and SLL increases. Impedance variation with feed patch height is shown in figure 5.25.

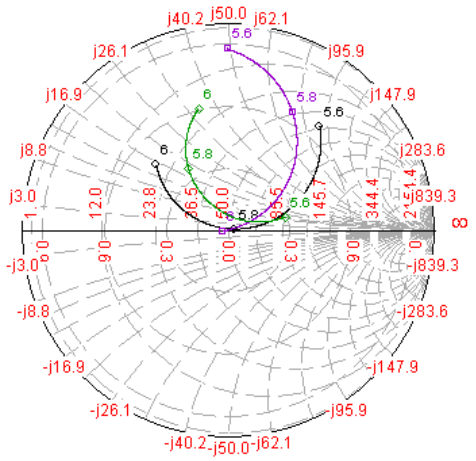

Figure 5.23 Impedance variations vs. feed patch height
(1.5 mm 2.0 mm 2.5 mm)

5.13.5 Effect of Feed Patch Length

The increase in feed patch length results in decrease in resonance frequency for a fixed parasitic patch dimensions which indicates that the parasitic and feed patch resonates at different frequency. The structure resistance increases and becomes more capacitive. The impedance variation vs. feed patch length is shown in figure 5.24. Change in length of feed patch with respect to reference antenna will cause the two patches to resonate separately and hence gain decreases with increase or decrease in length of parasitic patch.

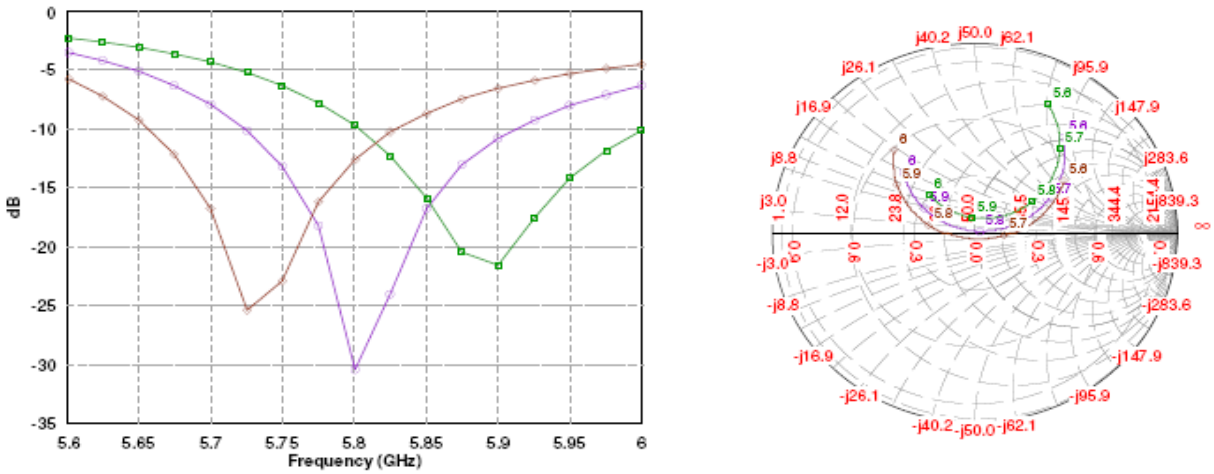

Figure 5.24 Impedance variations vs. feed patch length
(21.9 mm 22.3 mm 21.5 mm)

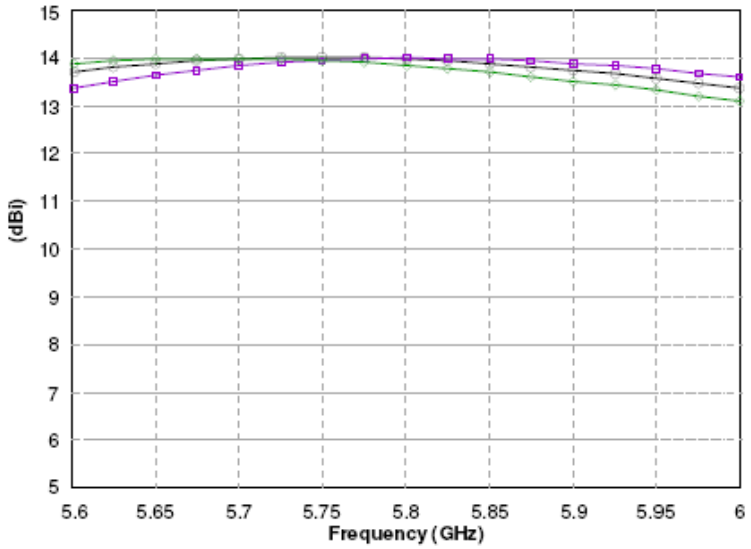

Figure 5.25 Directivity variations vs. feed patch length
(21.5 mm 21.9 mm 22.3 mm)

5.13.6 Effect of Feed Patch Width

There is little effect on resonance frequency with change in width of parasitic patch. Directivity, Gain, efficiency and impedance bandwidth increase with width of parasitic patch but Side lobe level also increases with width, however cross polarization decreases marginally. Beamwidth in E– plane decreases while there is no effect on beamwidth in H plane.

5.14 Parasitic Patches at Multiple of $\lambda_o / 2$

Structures are also designed and optimized for maximum gain with single parasitic patch at superstrate height of 1.0 λ_o and 1.5 λ_o, an integral multiple of $\lambda_o / 2$. Gain is observed to same at superstrate height of 0.5 λ_o, 1.0 λ_o and 1.5 λ_o, which can be explained on the basis of resonance of two patches viz. feed and parasitic patch. The maximum gain is obtained when the whole structure resonates in unison at same frequency and it does not depend on parasitic patch height. Parasitic patch intercepts the field radiated by feed patch, reconfigures it and reradiate it. Radiations from feed patch which is not intercepted by parasitic patch contribute to side lobe level. A larger effective overlap by parasitic patch decreases SLL. As overlap or field intercepted by parasitic patch decreases with parasitic height, SLL and cross polarization increases with superstrate height. The optimized structure has parasitic patch dimensions of 15.0 mm x 25.4 and 16.0 mm x 25.4 mm at superstrate height of 1.0 λ_o and 1.5 λ_o respectively, while the feed patch dimensions are 22.7 mm x 25.4 mm in both cases. Impedance variation, current distribution and radiation pattern at 0.5 λ_o, 1.0 λ_o and 1.5 λ_o superstrate height is shown in figure 5.26 (a). Antenna performance of optimized structures at 0.5 λ_o, 1.0 λ_o and 1.5 λ_o superstrate height is tabulated in Table 5.1.

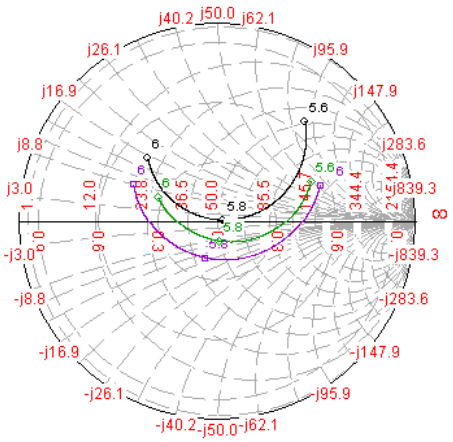

Figure 5.26 (a) Impedance variations vs. Superstrate height

(0.5 λo 1.0 λo 1.5 λo)

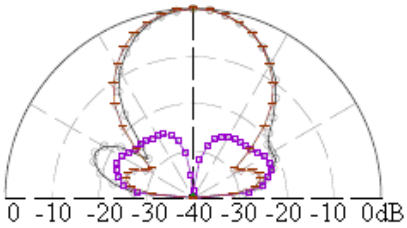

(i) 0.5 λo

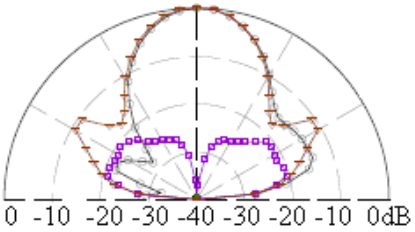

(ii) 1.0 λo

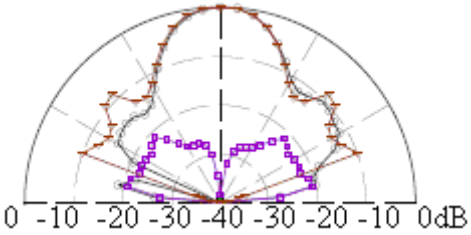

(iii) 1.5 λo

Figure 5.26(b) Radiation patterns

(Eθ EΦ at Φ = 0° and Eθ EΦ at Φ = 90°)

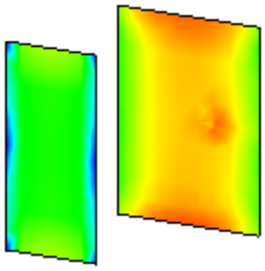

(i) 0.5 λo

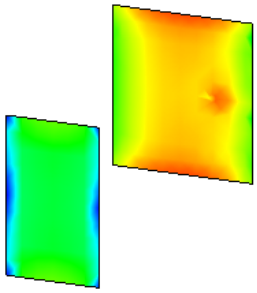

(ii) 1.0 λo

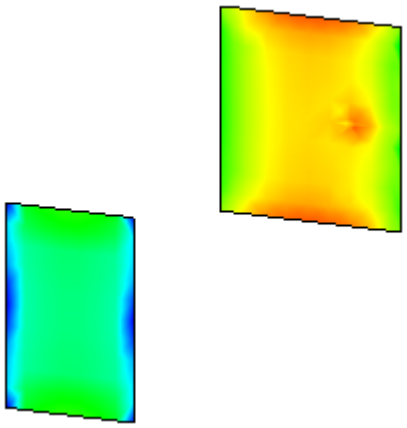

(iii) 1.5 λo_o

Figure 5.26 (c) Current distributions

Parasitic patch height	Direct-ivity (dB)	Gain (dB)	SLL (dB)	Beam-width E / H plane (degrees)	Cross-Pol level (dB)
0.5 λ_o	14.0	13.4	-17.1	37.5/39.3	-22.3
1.0 λ_o	14.4	13.3	-11	31.1/31.9	-20.7
1.5 λ_o	13.9	13.4	-8.6	29.4/30.7	-20.7

Table 5.1 Antenna performance at 0.5 λ_o, 1.0 λ_o and 1.5 λo superstrate height

5.15 Effect of Superstrate Height at Multiple of $\lambda_o / 2$

Because of fringing effects, electrically the length of the microstrip antenna is greater than the physical dimensions. The fringing field effect had been studied for microstrip antenna for h<< λ. Here an attempt is made to investigate fringing field effect on a parasitic patch positioned at a height comparable to λ.

Directivity vs. length (L < 0.5λ) for constant width of a parasitic patch at superstrate height of λ/2, λ and 3λ/2 is studied and tabulated in table 5.2. The feed patch obstructs the electric field lines to the ground and the field lines flare more resulting in decrease in physical dimension of the patch. It is observed that the physical dimensions for maximum directivity decreases with superstrate height. Directivity of 14.15 dB, 14.37 dB and 13.92 dB are obtained by parasitic patch length of 0.29 λ, 0.31 λ and 0.33 λ at superstrate height of λ/2, λ and 1.5 λ respectively. Current distribution, impedance variation and radiation pattern these antennas are shown in Figure 5.26.

S.No	Patch length (mm)	Directivity (dB) at superstrate height		
		0.5 λ	1.0 λ	1.5 λ
1	13	13.96	13.72	13.53
2	15	14.15	14.2	13.80
3	16	14.12	14.37	13.84
4	17	14.01	14.34	13.92
5	19	13.68	14.3	13.85
6	21	13.27	14.22	13.73
7	23	12.87	14.10	13.59
8	25	12.54	13.9	13.2

Table 5.2 Directivity vs. length of parasitic patch at hs = 0.5 λ, 1.0 λ and 1.5 λ

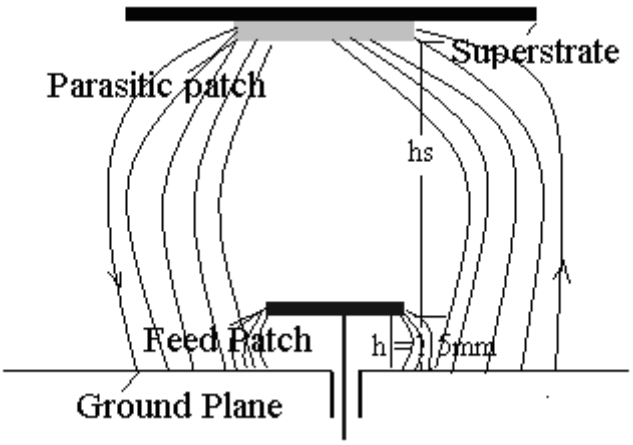

Figure 5.27 Fringing effect at superstrate height comparable to wavelength

The Electric field lines will terminate Fringing effect increases the physical size of the element and reduction in physical size will be useful in employing large size array in an area. At lower height of the substrate the effective obstruction of the feed patch is more pronounced and hence smaller physical length of parasitic patch is expected. As the superstrate height increases fringing effect will decrease as effective obstruction of patch decreases and hence physical size increases. As the dimension of parasitic patch is increased, the physical length increases due to lesser obstruction or fringing effect

5.16 Effect of Shape of Parasitic Patch

Antenna performance is also studied for different shapes of parasitic patch at superstrate height of λ/2, λ and 3λ/2 and tabulated in table 5.3. SLL is observed to degrade with increase in superstrate height. Elliptical parasitic patch is observed to have better SLL at different superstrate heights while square patch has the maximum impedance bandwidth. Rectangular patch is observed to have maximum directivity. Antenna performance vs. parasitic patch of different shape at superstrate height of λ/2, λ and 3/2λ are tabulated in tables 5.3, 5.4 and 5.5 respectively, while current distribution, impedance variation and radiation pattern are shown in Figure 5.28 (a), 5.28 (b) and 5.28 (c) respectively. Directivity and gain variation vs. frequency at superstrate height of λ/2, λ and 3/2λ is shown in figure 5.31, 5.32 and 5.33 respectively.

Parasitic patch	Parasitic patch dimensions	Area (sq. mm)	Dir (dB)	Gain (dB)	η (%)	SLL (dB)
Rectangle	14 x 25.4	355.6	14.2	13.3	83	-17
Ellipse	14x25.4	279.3	14.1	13.2	83	-18
Square	14x14	196	13.6	12.4	75	-16
Circle	Radius 7	153.9	13.8	12.7	79	-18

Table 5.3 Antenna performance vs. shapes of parasitic patch at hs = 0.5 λ

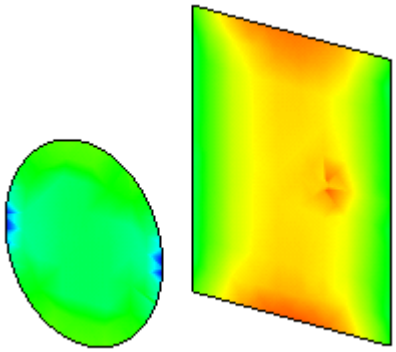

(Circular parasitic patch)

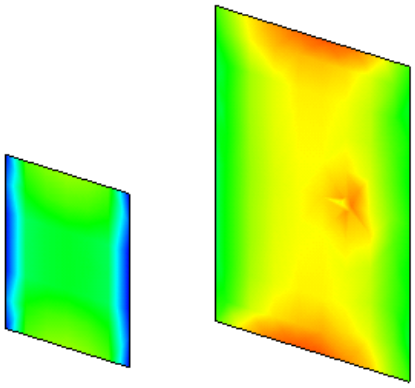

(Square parasitic patch)

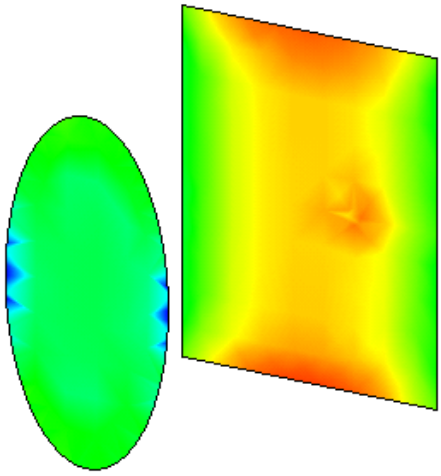

(Ellipse parasitic patch)

(a)

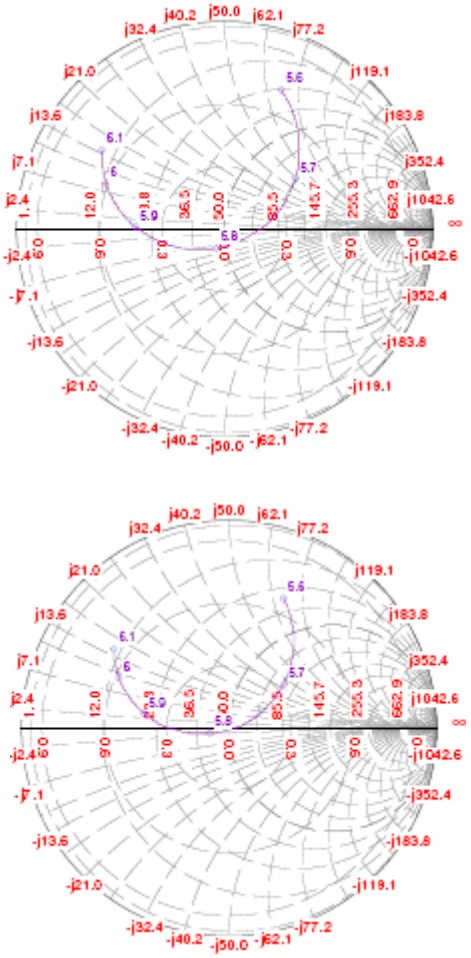

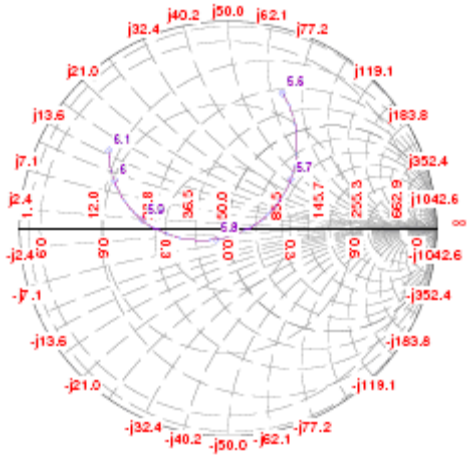

(b)

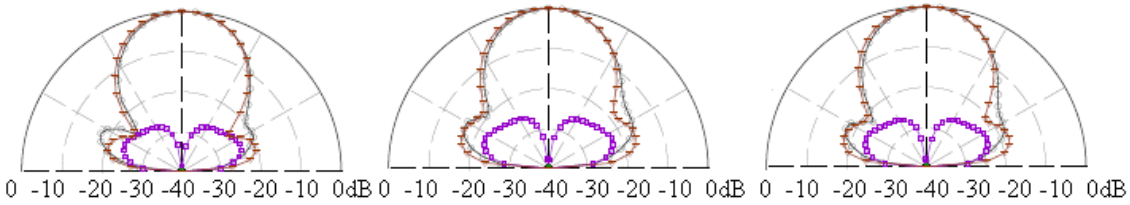

(c)

(i) Elliptical patch (ii) Square patch (iii) Circular patch

Figure 5.28 (a) Current distribution (b) impedance variation and (c) radiation pattern at hs = 0.5 λ (—○— Eθ —○— EΦ at Φ = 0° and —□— Eθ —□— EΦ at Φ = 90°)

Table 5.4 shows the directivity, gain, efficiency and side lobe level in dB for various shapes of parasitic patches at a spacing of λ.

Parasitic patch	Parasitic patch dimensions	Dir (dB)	Gain (dB)	η (%)	SLL (dB)
Rectangle	16x25.4	14.37	13.31	78	-10.3
Ellipse	19x25.4	14.26	13.2	78	-10.5
Square	16x16	13.95	12.8	77.3	-9.95
Circle	Radius 10	14.07	12.9	76	-10.4

Table 5.4 Antenna performance vs. shape of parasitic patch at hs = 1.0 λ

Figure 5.29 shows impedance variation and radiation pattern at hs = 1.0 λ for Elliptical, square and circular patch.

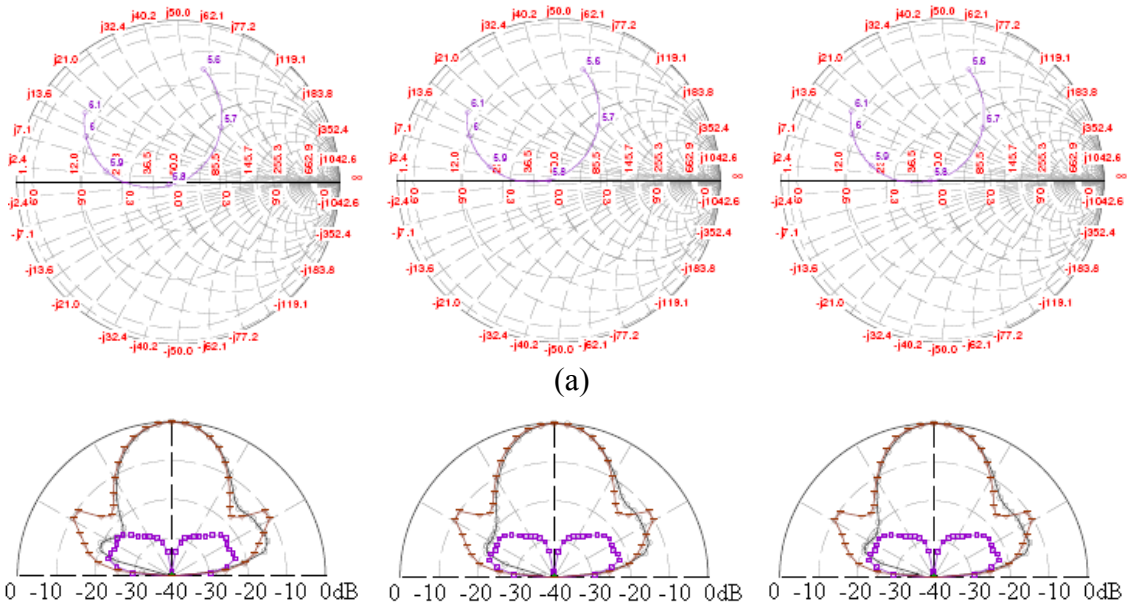

(a)

(b)

(i) Elliptical patch (ii) Square patch (iii) Circular patch

Figure 5.29 (a) Impedance variation and (b) radiation pattern at hs = 1.0 λ
(—— Eθ —— EΦ at Φ = 0° and —— Eθ —— EΦ at Φ = 90°)

Table 5.5 shows the directivity, gain, efficiency and side lobe level in dB for various shapes of parasitic patches at a spacing of 1.5λ.

Parasitic patch	Parasitic patch dimensions	Dir dB	Gain dB	η %	SLL dB
rectangle	17x25.4	13.92	13.25	83.8	- 8.8
Ellipse	20.0x 25.4	13.8	13.03	84	-8.6
Square	22.0x22.0	13.4	12.6	83.8	-7.5
Circle	Radius 11	13.6	12.8	83.9	-8.0

Table 5.5 Antenna performance vs. shape of parasitic patch at hs = 1.5 λ

Figure 5.29 shows impedance variation and radiation pattern at hs = 1.5 λ for elliptical, square and circular patch.

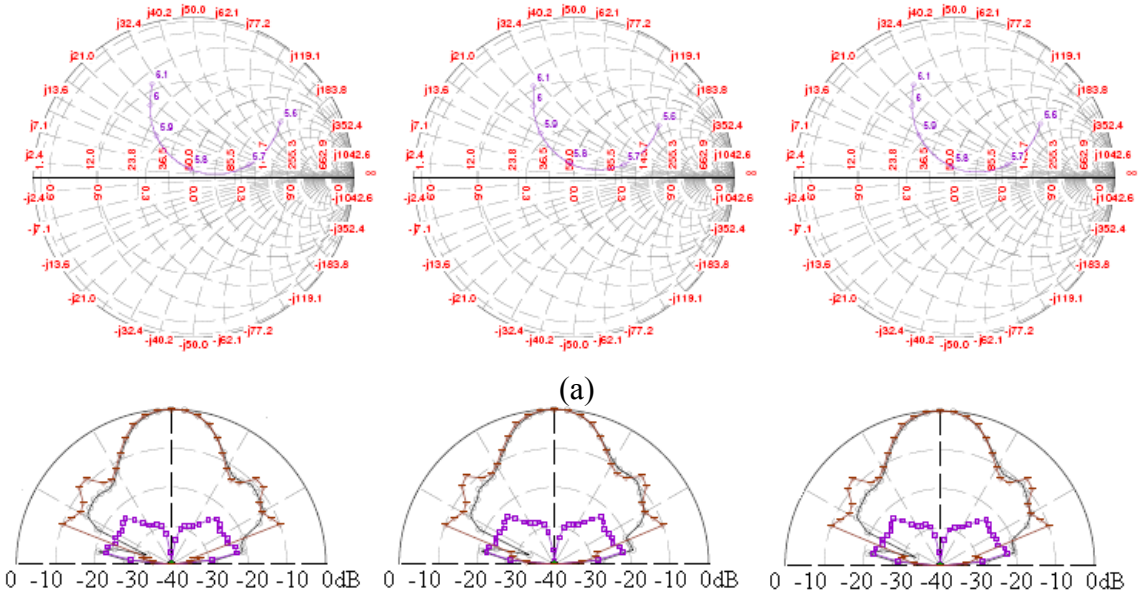

Figure 5.30 (a) Impedance variation and (b) radiation pattern at hs = 1.5 λ
(Eθ EΦ at Φ = 0° and Eθ EΦ at Φ = 90°)

Directivity and gain variation vs. frequency at superstrate height of λ/2, λ and 3/2λ are shown in figures 5.36, 5.37 and 5.38 respectively.

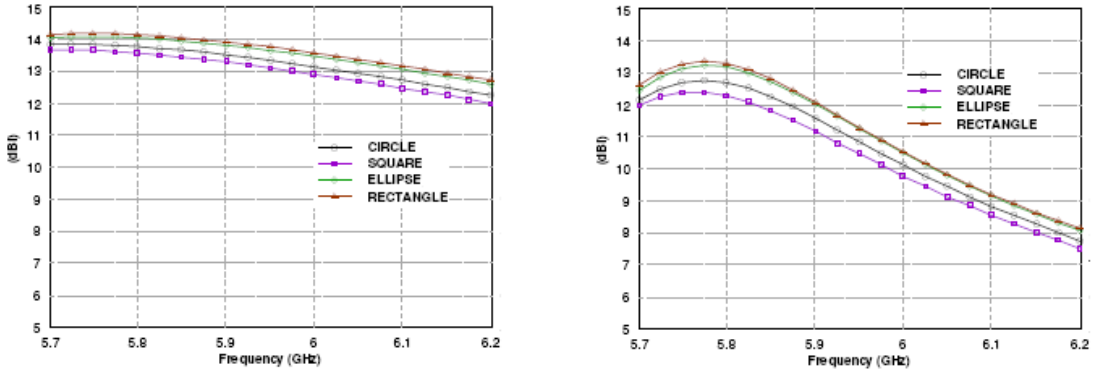

Figure 5.31 (a) Directivity (b) Gain vs. frequency at hs = 0.5 λ

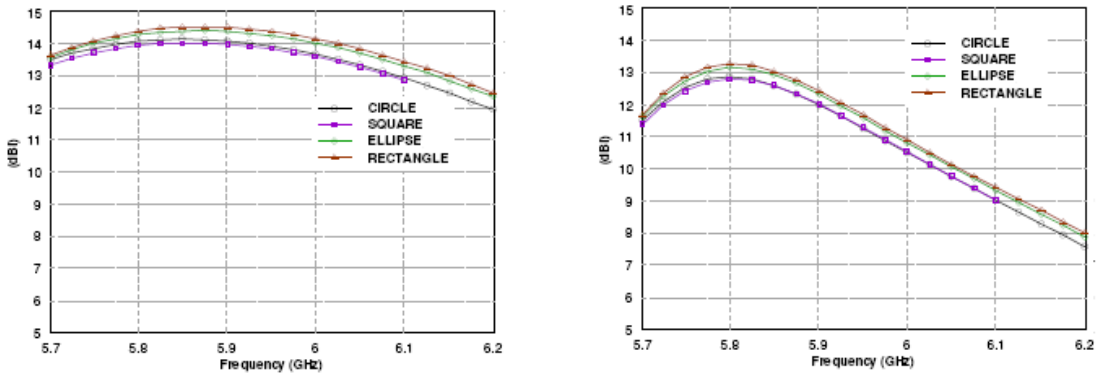

Figure 5.32 (a) Directivity (b) Gain vs. frequency at hs = 1.0 λ

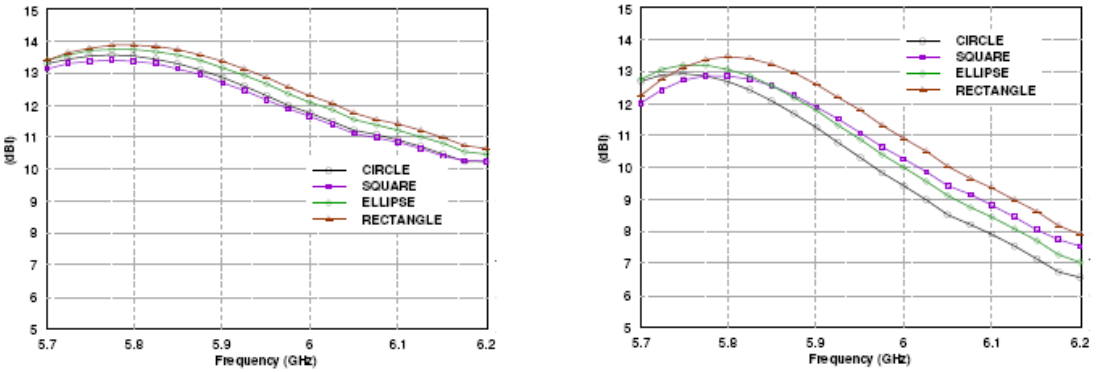

Figure 5.33 (a) Directivity (b) Gain vs. frequency at hs = 1.5 λ

From the above tables, it is clear that as the spacing between radiating patch and the parasitic patch increases, the directivity and gain decreases little bit while the side lobe level increases.

5.17 Multiple Parasitic Patches

Effect of superstrate height on antenna performance for constant width parasitic patch of L_{eff} = 0.5 λ (L < 0.5λ) is also studied about superstrate height of λ/2, λ and 3/2λ and tabulated in table 5.6. It is observed that:

- Impedance bandwidth increases
- SLL degrades with increase in substrate height.

Parasitic patch height	Bandwidth (MHz)	Dir (dB)	Gain (dB)	η (%)	SLL (dB)
0.54 λ	170	13.58	12.78	83	-15.3
0.5 λ	145	14.15	13.32	82.8	-16.8
0.46 λ	124	14.07	13.12	81	-17.3

Parasitic patch height	Bandwidth (MHz)	Dir (dB)	Gain (dB)	η (%)	SLL (dB)
1.04 λ	167	14.17	13.11	76	-9.3
1.0 λ	141	14.37	13.31	78	-10.3
0.96 λ	123	13.2	11.9	74	-6.3

Parasitic patch height	Bandwidth (MHz)	Dir (dB)	Gain (dB)	η (%)	SLL (dB)
1.54 λ	191	13.92	13.25	83.8	- 8.8
1.5 λ	166	13.26	12.68	88	-5.8
1.46 λ	148	11.62	11.1	88	-3.2

Table 5.6 Antenna performance vs. height of parasitic patch

Higher directivity is also explained using resonance of structure in unison. The resonance gain method has been studied using moment method [92]. This resonance gain method involves a limited structural geometry, resonant frequency drift, narrow impedance bandwidth. The resonant condition can always be satisfied by adjusting the superstrate position and the value of the resonant gain is a function of the thickness of the superstrate [93-94]. However, it is also reported that all high-gain conditions obtained by geometrical optimization are not the result of the structural resonance. A multilayer effect on microstrip antennas away from the structural resonance is reported and discussed [99]. The technique for improving the radiation efficiency by arranging parasitic elements above the feeding MSA elements is investigated [101-102]. A multilayer parasitic microstrip antenna array structure using a low-temperature co-fired ceramic substrate (LTCC) suited to packaging the MMIC chip is proposed. However, since the LTCC

substrate has a high electric constant, it is difficult to achieve wide-band and high-efficiency characteristics [102]. A highly efficient multilayer parasitic microstrip antenna array structure constructed on a Teflon substrate for a system-on-package is reported at millimeter-wave frequency bands. Another antenna structure is reported at 60 GHz with high radiation efficiency of greater than 91% associated with high gain that is greater than 11.1 dBi [103].

Structures are designed and optimized for maximum gain with multiple patches. Structures with two parasitic patches (PP1 and PP2) at superstrate height of 0.5 λ_o and 1.0 λ_o, 0.5 λ_o and 1.5 λ_o, and 1.0 λ_o and 1.5 λ_o are optimized. A structure with three parasitic patches (PP1, PP2 and PP3) at 0.5 λ_o, 1.0 λ_o and 1.5 λ_o (an integral multiple of $\lambda_o / 2$) above the feed patch is also optimized. Width of Feed patch (FP) and parasitic patches (PPs) is kept 25.4 mm in all cases. Optimized dimensions are tabulated in table 5.7.

Height of parasitic patches (PPs)	FP length	PP1 Length	PP2 length	PP3 length
0.5 λ_o and 1.0 λ_o	21.5	14	14	-----
0.5 λ_o and 1.5 λ_o	22.2	14.5	15.4	-----
1.0 λ_o and 1.5 λ_o	22.7	15	14	-----
0.5 λ_o, 1.0 λ_o and 1.5 λ_o	21.6	14.5	14.5	14.1

Table 5.7 Optimized dimensions of feed and parasitic patches

An increase in gain and comparatively higher SLL is observed with multiple patches. Maximum gain is obtained when the whole structure resonate at one frequency while the SLL depends on the effective overlap of feed patch by parasitic patch and radiations from multiple patches as parasitic patch intercepts the field radiated by feed patch, reconfigures it and reradiate it. Antenna performance of optimized structures is tabulated in table 5.8. whereas impedance variation, current distribution and radiation pattern of structures with multiple parasitic patches are shown in figures 5.39 to 5.41.

PPs height (λ_o)	Dir (dB)	Gain (dB)	SLL (dB)	beamwidth E / H plane	Cross Pol (dB)
0.5 – 1.0	15.8	15.4	-14.4	26.2 / 27.0	-23
0.5-1.5	16.8	15.8	-16.8	25.9 / 26.7	-24.3
1.0-1.5	16	15.2	-11.9	24.2 / 24.9	-21.0
0.5-1.0-1.5	17.1	16.4	-13.1	22.2 / 22.6	-24.3

Table 5.8 Antenna performance of structures with multiple parasitic patches

Figure 5.34 shows Impedance variations of multiple parasitic patches with frequency on the Smith chart.

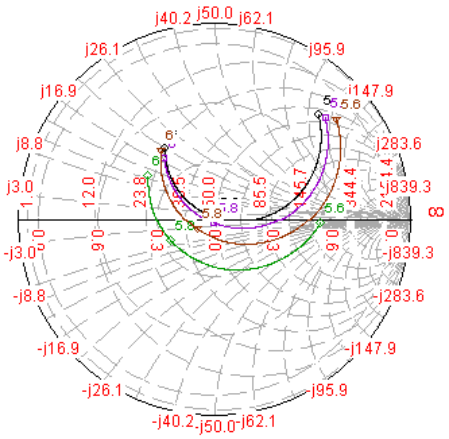

Figure 5.34 (a) Impedance variations of multiple parasitic patches
(—◊— 0.5 and 1.0 λo —▫— 0.5 and 1.5 λo
—◊— 1.0 and 1.5 λo —▽— 0.5, 1.0 and 1.5 λo)

Figure 5.36 shows current distribution of multiple parasitic patches.

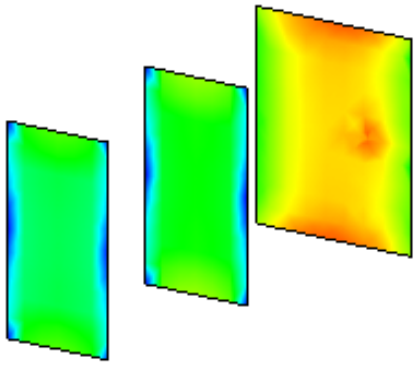

(i) 0.5 λ_o and 1.0 λo

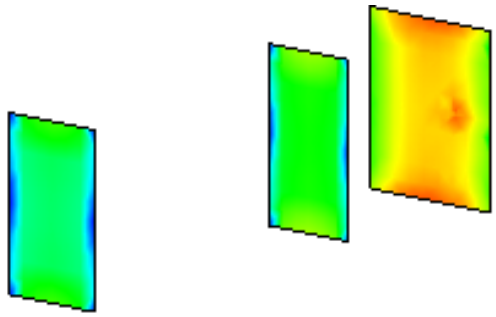

(ii) 0.5 λ_o and 1.5 λo

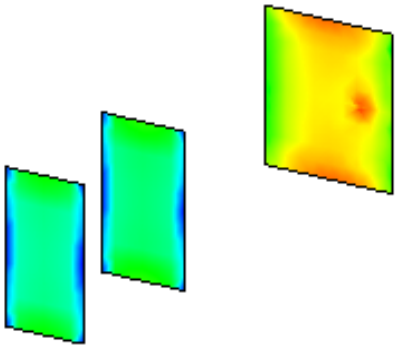

(iii) 1.0 a λ_o nd 1.5 λo

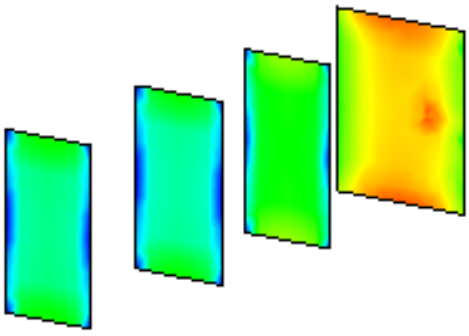

(iv) 0.5 λ_o, 1.0 λ_o and 1.5 λo

Figure 5.35 Current distributions

Figure 5.37 shows radiation pattern for multiple parasitic patches.

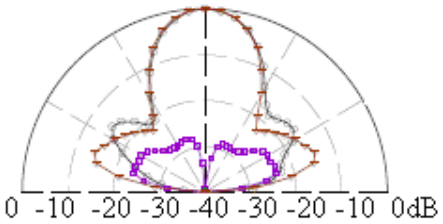

(i) 0.5 λ_o and 1.0 λo

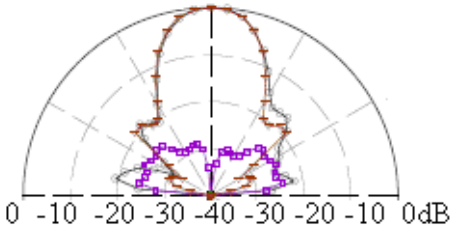

(ii) 0.5 λ_o and 1.5 λo

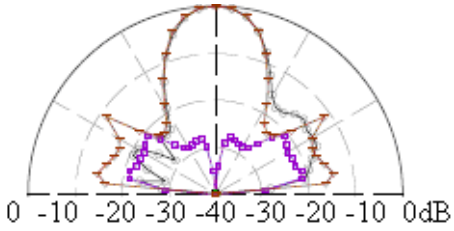

(iii) 1.0 λ_o and1.5 λo

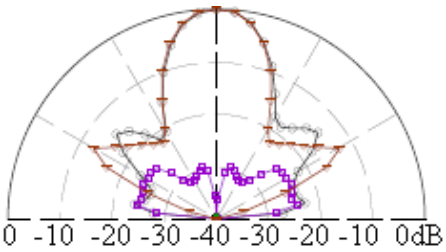

(iv) 0.5 λ_o, 1.0 λ_o and 1.5 λo

Figure 5.36 Radiation pattern

Thus it can be concluded that using multiple parasitic patches, all most all the parameters such as directivity, gain, side lobe level and cross polarization can be improved simultaneously to some extent.

5.18 Microstrip Fed Parasitic Patch - Higher Order Mode Radiations

5.18.1 Effect of Parasitic Patch Dimensions at Superstrate Height of 0.5 λ

The directivity of microstrip antenna increases with increase in the width and therefore the width of parasitic patch is increased from 0.5 λ to 1.5 λ while electrical length of the patch is kept 0.5 λ. It is observed that as the width increases, the physical length of the patch increases for maximum directivity. This may be attributed to the decrease in effective obstruction and thus less flaring of field lines with increase in the width of the patch. However, in case of parasitic patch of length 1.0 λ, electrical length is observed to be same as the physical length.

Since the parasitic patch is fed from the radiation of feed patch and therefore it should be within the half power beamwidth of radiation of feed patch and this is the reason for decrease in directivity with increase in parasitic patch length beyond λ. It is observed that bandwidth depends on the dimensions of parasitic patch. Antenna performance vs. patch dimension at superstrate height 0.5 λ is tabulated in table 5.9.

Parasitic patch	parasitic patch Dimensions (mm)	Dir (dB)	Gain (dB)	η (%)	SLL (dB)
0.5 λ X 0.5λ	15.1 x 25.4	14.15	13.32	82.8	-16.8
0.5 λ X 1.0λ	16.1 x 51.8	14.55	13.6	80.5	-11.7
0.5 λ X 1.5 λ	17.0 x 77.6	14.65	14.07	88	-11.3
1.0 λ X 0.5 λ	51.8 x 25.4	12.14	10.22	65	-8.4
1.0 λ X 1.0λ	51.8 x 51.8	13.57	12.3	78	-8.6

Table 5.9 Antenna performance vs. patch dimension at hs = 0.5 λ

5.18.2 Effect of Parasitic Patch Dimensions at Superstrate Height of 1.0 λ

Similar effects on antenna performance are observed at superstrate height of 1.0 λ as observed at superstrate height of 0.5 λ It is observed that as the width increases, the physical length of the patch increases for maximum directivity. Directivity decreases as the parasitic patch dimensions are increased beyond 1.5 λ x 1.5 λ. and bandwidth depends on the dimensions of parasitic patch. Antenna performance vs. patch dimension at superstrate height 1.0 λ is tabulated in table 5.10.

Single patch	parasitic patch dimensions (mm)	Dir (dB)	Gain (dB)	η (%)	SLL (dB)
0.5λ X 0.5λ	16.0 x 25.4	14.37	13.31	78	-10.3
0.5λ X 1.0λ	20.0 x51.8	15.08	13.73	73	-7.8
1.0λ X 0.5λ	51.8 x25.9	13.8	12.4	72	-9.3
1.0λ X 1.0λ	51.8 x51.8	15.71	14.2	71	-10.3
1.0λ X 1.5λ	51.8 x77.6	15.95	15.06	81	-7.1
1.5λ X 0.5λ	56.6 x25.4	13.94	12.46	72	-9.3
1.5λ X 1.0λ	59.6 x51.8	16.2	14.52	68	-11.4

Table 5.10 Antenna performance vs. patch dimension at hs = 1.0 λ

5.18.3 Effect of height of feed patch at superstrate height of 1.5 λ

Effect of height of feed patch on antenna performance is also studied at superstrate height of 1.5 λ. Bandwidth increase with increase in height of feed patch. The antenna performance vs. height of feed patch is tabulated in table 5.11.

Feed patch height	Parasitic patch dimensions (mm)	Band-width (MHz)	Dir (dB)	Gain (dB)	η (%)	3 dB Beamwidth H / E Plane	SLL (dB)
1.4	17x25.4	162	13.75	13.21	88.4	30.6°/29.6°	- 8.7
1.5	17x25.4	166	13.92	13.25	83.8	30.3°/29.4°	- 8.8
1.6	17x25.4	231	13.97	13.50	89.3	30.3°/29.1°	- 8.7

Table 5.11 Antenna performance vs. height of feed patch

5.18.4 Effect of Parasitic Patch Dimensions at Superstrate Height of 1.5 λ

Effect of parasitic patch dimensions on antenna performance is also studied at superstrate height of 1.5 λ. The width of parasitic patch is increased from 0.5 λ to 2.5 λ while electrical length of the patch is kept 0.5 λ. It is observed that directivity decreases for W>2.0 λ. Antenna performance vs. patch dimension at superstrate height 1.5 λ is tabulated in table 3.7.1. Directivity of 15.4 dB and Side lobe level of more than 9.0 dB is obtained for 0.5 λ X 1.5 λ patch. The efficiency of more than 88% is obtained. Current distribution, impedance variation, radiation pattern, directivity and gain variation vs. frequency of 0.5 λ X 1.5 λ patch are shown in Figure 5.37.

Single patch	Parasitic patch dimensions (mm)	Band-width (MHz)	Dir (dB)	Gain (dB)	η (%)	3 dB Beamwidth H / E Plane	SLL (dB)
0.5 λ X 0.5 λ	17.0 x 25.4	166	13.92	13.25	83.8	30.3°/29.3°	- 8.8
0.5 λ X 1.0 λ	17.0 x 51.7	184	14.87	14.34	88.5	26.9°/26.3°/	-8.3
0.5 λ X 1.5 λ	21.0 x 77.6	198	15.38	14.83	88.2	24.4°/24.1°	-9.1
0.5 λ X 2.0 λ	24.0 x 103.4	204	15.57	15.07	88.9	23.4°/23.1°/	-8.4
0.5 λ X 2.5 λ	24.0 x 129.3	213	15.52	15.2	92.5	23.0°/22.8°/	-7.2

Table 5.12 Antenna performance vs. width of parasitic patch (L_{eff} = 0.5 λ)

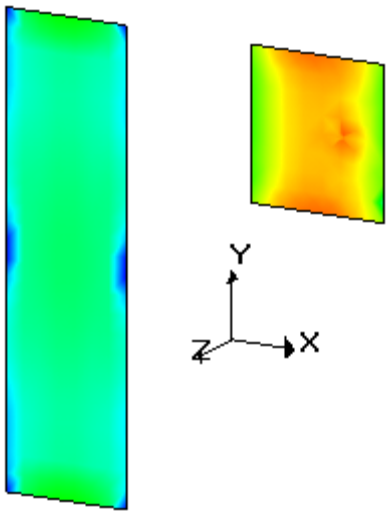
Y
Z
X

(a)

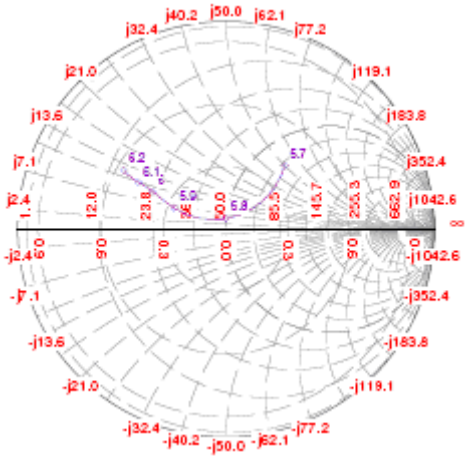
j40.2
j50.0
j62.1
j32.4
j77.2
j21.0
j119.1
j13.6
j183.8
j7.1
j352.4
j2.4
j1042.6
-j2.4
-j1042.6
-j7.1
-j352.4
-j13.6
-j183.8
-j21.0
-j119.1
-j32.4
-j77.2
-j40.2
-j50.0
-j62.1

(b)

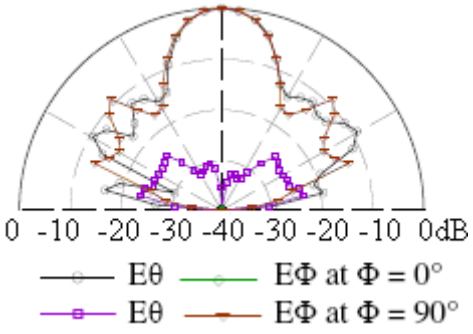
0 -10 -20 -30 -40 -30 -20 -10 0dB
Eθ
EΦ at Φ = 0°
Eθ
EΦ at Φ = 90°

(c)

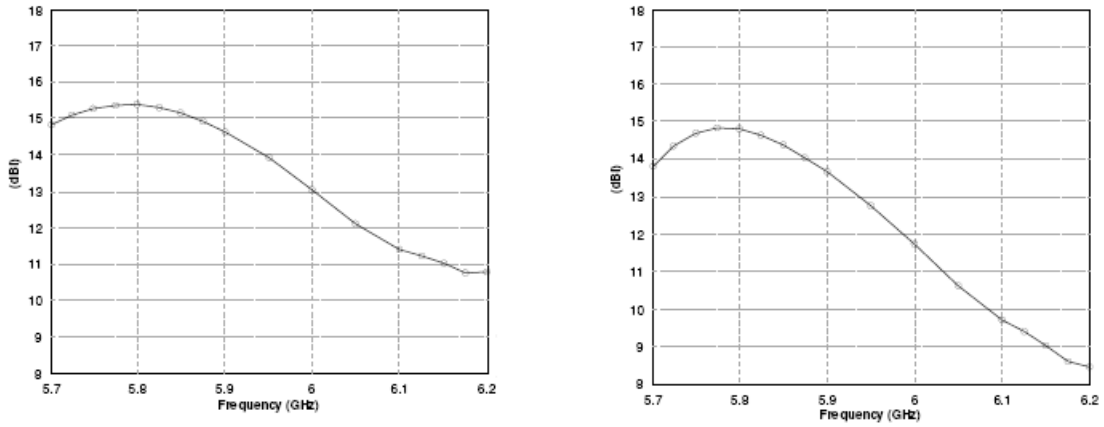

(d) (e)

Figure 5.37 (a) Current distribution (b) impedance variation and (c) radiation pattern (d) directivity and (e) gain vs. frequency of 0.5 λ X 1.5 λ patch

Since parasitic patch is fed from the radiation of MSA designed for 5.725 – 5.875 GHz band, length of parasitic patch can be increased to improve directivity and to investigate higher order mode radiation. Directivity of 15.4 dB and side lobe level of -9.4 dB are obtained in case of λ X λ parasitic patch. Directivity decreases if width of the patch is increased more than 2 λ. Antenna performance of parasitic patch of L_{eff} = λ and 0.5 λ < W < 2.5 λ is tabulated in table 5.13. Current distribution, impedance variation and radiation pattern, directivity and gain vs. frequency of 1.0 λ X 1.0 λ patch are shown in Figure 5.38.

Single patch	parasitic patch dimensions	Band-width (MHz)	Dir (dB)	Gain (dB)	η (%)	3 dB Beamwidth H / E Plane	SLL (dB)
1.0λ X 0.5λ	51.8 x 25.4	302	13.84	13.04	84	29.0°/27.3°	-8.5
1.0λ X 1.0λ	51.8 x 51.8	392	15.41	14.6	88	23.4°/22.4°	-9.4
1.0λ X 1.5λ	51.8 x 77.6	470	16.25	15.6	86.9	21.0°/20.7°	-7.6
1.0λ X 2.0λ	51.8 x 103.4	500	16.28	15.84	90.5	19.8°/20.2°	-5.7
1.0λ X 2.5λ	51.8 x 129.3	471	16.14	15.87	94	18.0°/18.7°	-4.3

Table 5.13 Antenna performance. Vs. width of parasitic patch (L_{eff} = 1.0 λ)

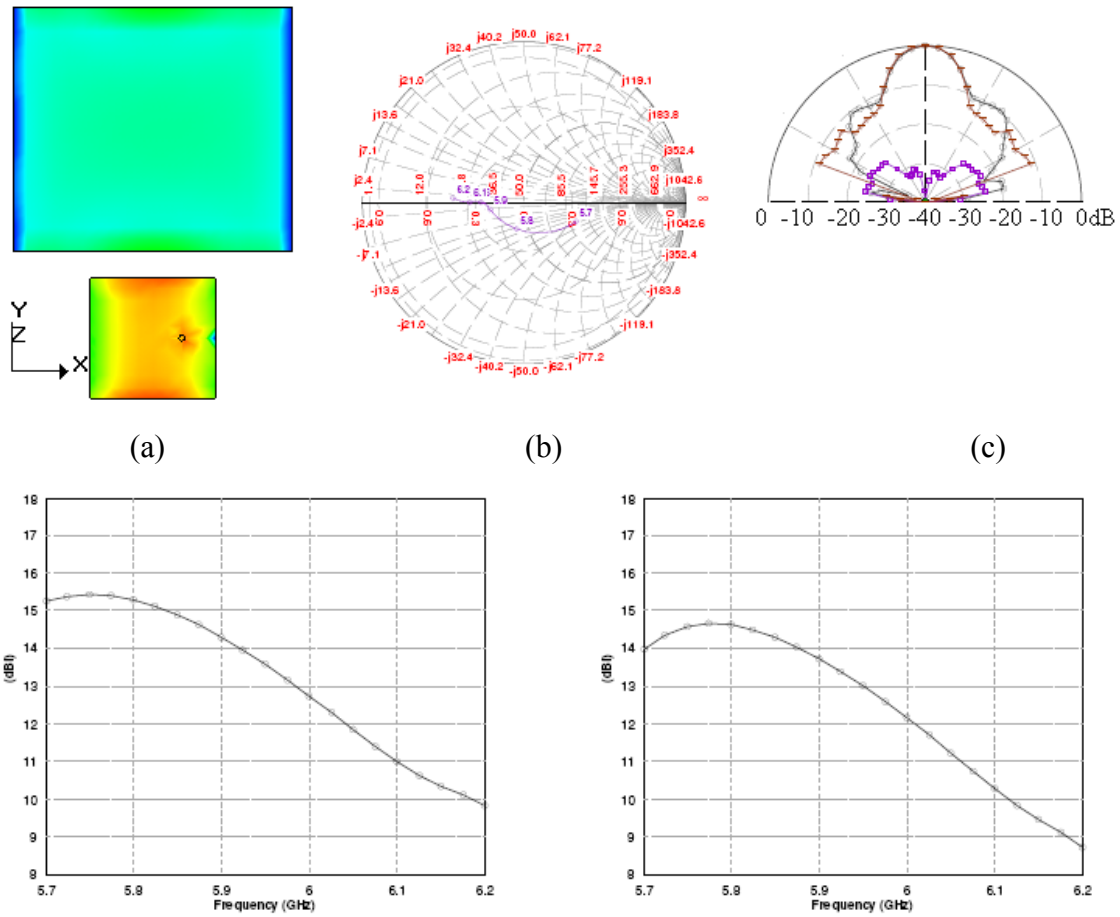

Figure 5.38 (a) Current distribution (b) impedance variation and (c) radiation pattern (d) directivity and (e) gain Vs. frequency of 1.0 λ X 1.0 λ patch

Performance of the antenna is also analyzed for L_{eff} =1.5 λ and 0.5 λ<W<2.5 λ and tabulated in table 5.14. It is observed that fringing effect is more prominent in 1.5 λ x 0.5 λ and its physical length is 1.13 λ for maximum directivity. Directivity of 16.0 dB and 17.2 dB and side lobe level of -11.7 dB and -10.5 dB are obtained in case of 1.5λ X 1.0λ and 1.5λ X 1.5λ parasitic patch respectively. Current distribution, impedance variation and radiation pattern, directivity and gain variation vs. frequency of 1.5λ X 1.0λ and 1.5λ X 1.5λ patch are shown in figures 5.39 and 5.40 respectively.

Single patch	Parasitic patch dimension	Band-width (MHz)	Dir (dB)	Gain (dB)	η (%)	3 dB Beamwidth H / E Plane	SLL (dB)
1.5λ X 0.5λ	58.6 x 25.9	339	14.1	13.31	85.1	27.2°/25.7°	-8.4
1.5λ X 1.0λ	61.6 x 51.8	458	16.0	15.2	83.4	21.3°/20.9°	-11.7
1.5λ X 1.5λ	66.6 x 77.6	500	17.2	16.3	83	18.7°/17.8°	-10.5
1.5λ X 2.0λ	74.6 x 103.4	402	17.65	16.93	84.5	15.2°/15.1°	-8.7
1.5λ X 2.5λ	74.6 x 129.3	280	18.0	17.55	90.1	13.5°/14.0°	-7.3

Table 5.14 Antenna performance vs. width of parasitic patch (L_{eff} = 1.5 λ)

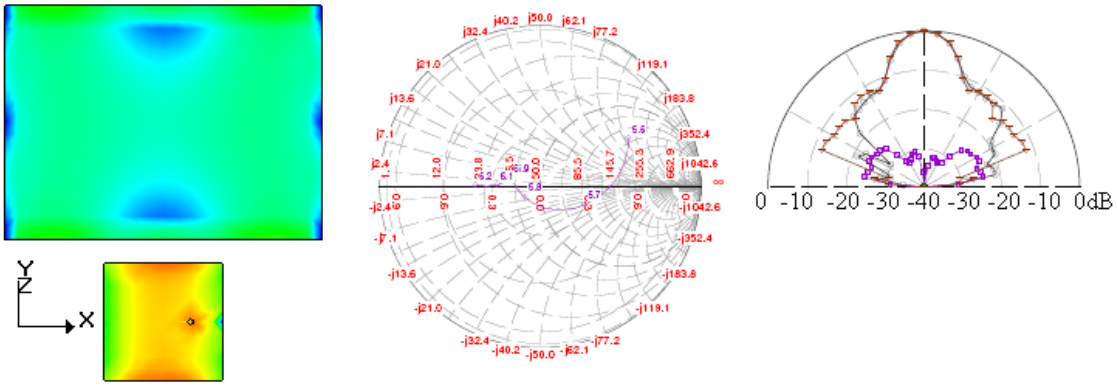

(a) (b) (c)

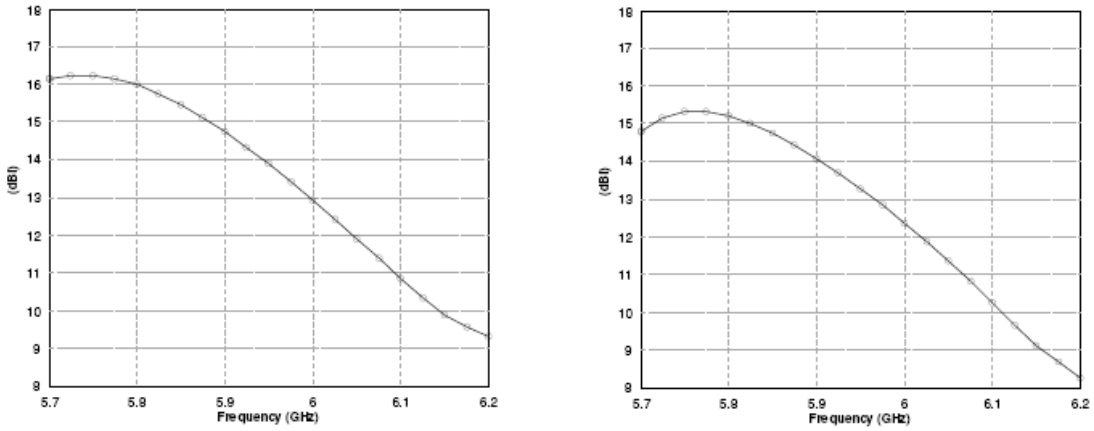

(d) (e)

Figure 5.39 (a) Current distribution (b) impedance variation and (c) radiation pattern (d) directivity and (e) gain Vs. frequency of 1.5λ X 1.0λ

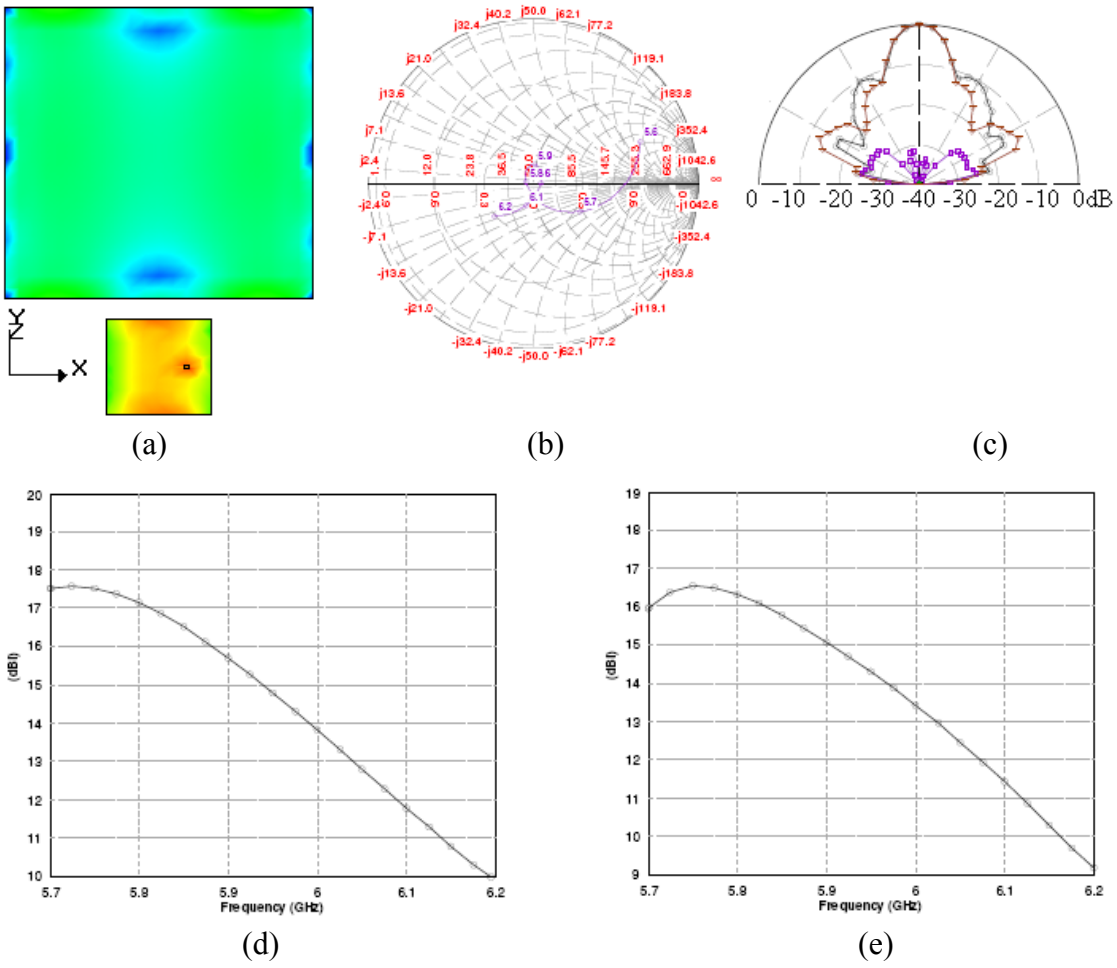

(a) (b) (c)

(d) (e)

Figure 5.40 (a) Current distribution (b) impedance variation and (c) radiation pattern (d) directivity and (e) gain Vs. frequency of 1.5λ X 1.5λ parasitic patch

Performance of the antenna is also analyzed for L_{eff} = 2.0 λ and 0.5 λ<W<2.5 λ and tabulated in table 5.15. It is observed that the directivity improvement is not in proportion with the dimensions of the parasitic patch. This may be attributed to feed distribution of parasitic patch as the patch is fed from the radiation of MSA. Directivity of 17.65 dB and side lobe level of -9.5 dB is obtained in case of 2.0λ X 2.0λ parasitic patch. Current distribution, impedance variation, radiation pattern, directivity and gain variation of 2.0λ X 2.0λ patch are shown in Figure 5.46.

Single patch	Parasitic patch dimensions	Band-width (MHz)	Dir (dB)	Gain (dB)	η (%)	3 dB Beamwidth H / E Plane	SLL (dB)
2.0λ X 0.5λ	97.4 x 25.9	389	13.4	12.5	83.7	27.7°/26.3°	-4.1
2.0λ X 1.0λ	101.6 x 51.8	460	15.35	14.65	85	20.4°/17.9°	-5.9
2.0λ X 1.5λ	101.6 x 77.6	355	16.95	16.15	83.3	15.8°/14.3°	-7.9
2.0λ X 2.0λ	103.4 x 103.4	233	17. 5	16.9	86	13.2°/12.6°	-9.5
2.0λ X 2.5λ	103.4 x 129.3	200	18.1	17.36	86.2	11.8°/11.9°	-8.2

Table 5.15 Antenna performance vs. width of parasitic patch (L_{eff} = 2.0 λ)

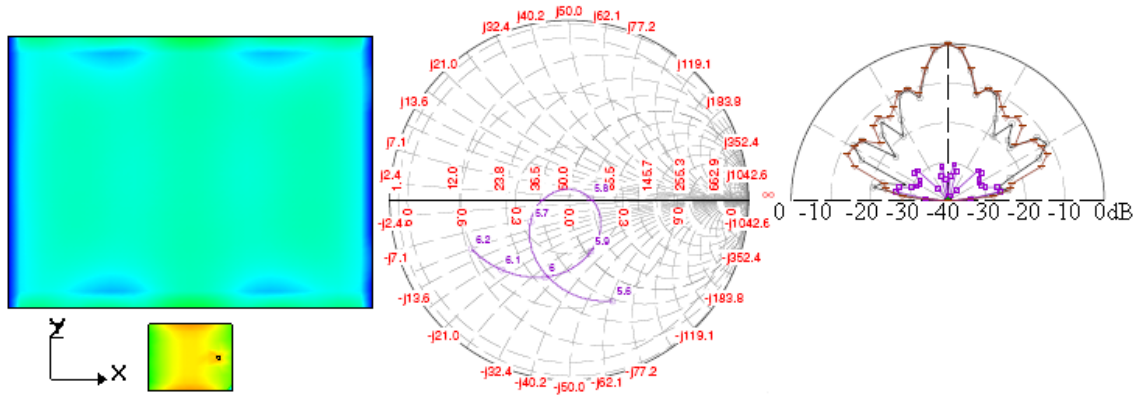

(a) (b) (c)

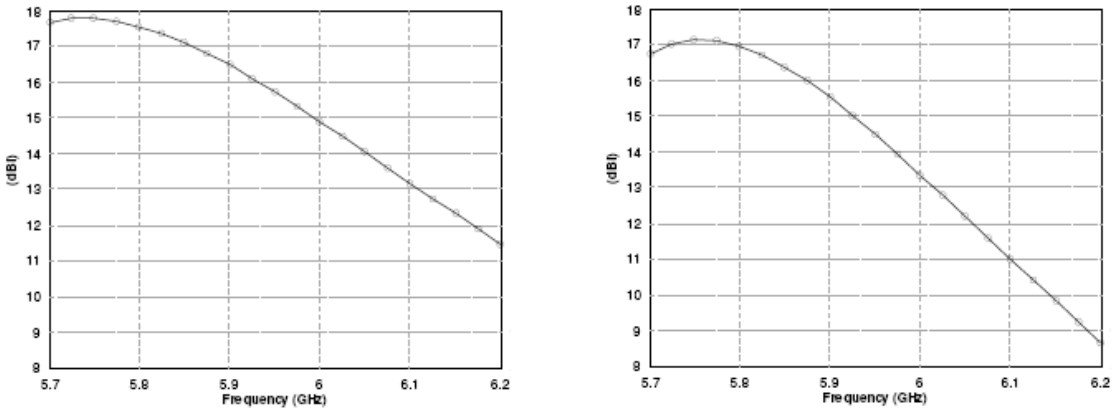

(d) (e)

Figure 5.41 (a) Current distribution (b) impedance variation and (c) radiation pattern (d) directivity and (e) gain vs. frequency of 2.0λ X 2.0λ parasitic patch

Performance of the antenna is also analyzed for L_{eff} = 2.5 λ and 0.5 λ<W<2.5 λ and tabulated in table 5.16. Directivity of 17.65 dB and side lobe level of -9.5 dB is obtained in case of 2.5λ X 2.5λ parasitic patch. Current distribution, impedance variation and radiation pattern, directivity and gain vs. frequency of 2.5λ X 2.5λ patch are shown in Figure 5.42.

Single patch	Parasitic patch dimensions	Band-width (MHz)	Dir (dB)	Gain (dB)	η (%)	3 dB Beamwidth H / E Plane	SLL (dB)
2.5λ X 0.5λ	123.5 x 25.9	234	12.8	11.5	76	30.9°/30.3°	-3.4
2.5λ X 1.0λ	123.5 x 51.8	332	14.9	14.1	83	20.2°/17.8°	-3.9
2.5λ X 1.5λ	123.5 x 77.6	238	16.9	16.0	81	14.9°/13.0°	-6.0
2.5λ X 2.0λ	125.5 x 103.4	200	18.0	17.2	83	12.5°/11.3°	-7.8
2.5λ X 2.5λ	127.5 x 127.5	165	18.6	17.7	83	11.1°/10.7°	-8.6

Table 5.16 Antenna performance Vs. width of parasitic patch (L_{eff} = 2.5 λ).

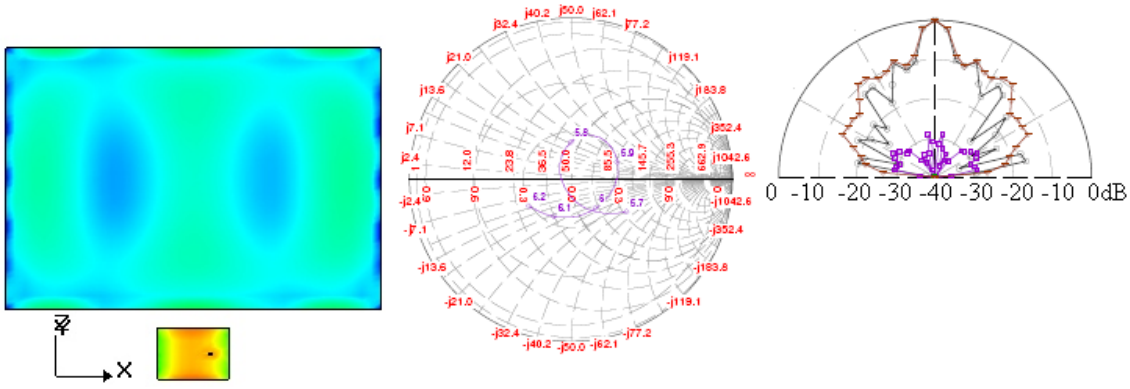

(a) (b) (c)

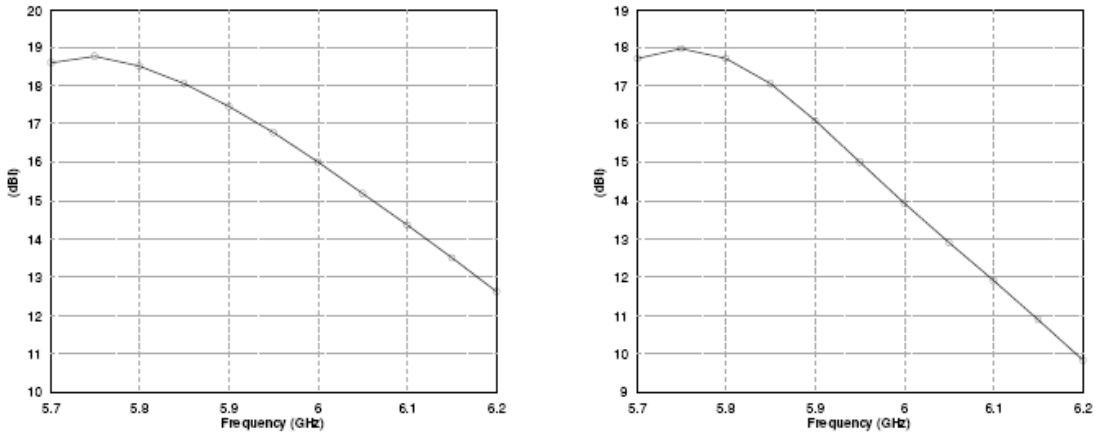

(d) (e)

Figure 5.42 (a) Current distribution (b) impedance variation and (c) radiation pattern (d) directivity and (e) gain vs. frequency of 2.5λ X 2.5λ parasitic patch

5.19 Microstrip Fed Parasitic Patch with Finite Ground Plane

5.19.1 Antenna on Finite Ground – Design and Results

Structures with single, two and three parasitic patches are designed and optimized on finite ground dimensions. Single parasitic patch with ground plane dimensions of 100 mm x 100 mm and two parasitic patches at 0.5 λo and 1.0 λo and three patches at 0.5 λo and 1.0 λo and 1.5 λo with ground plane dimensions of 200 mm x 200 mm provide front-to-back ratio of more than 20 dB. Multiple parasitic patches structures are simulated with less number of cells due to computational limitations. Width of Feed patch (FP) and parasitic patches (PPs) is kept 25.4 mm in all cases. Optimized dimensions are tabulated in table 5.17 and performance of optimized structures is tabulated in table 5.18. The antennas with one, two and three parasitic patches are analysed. The measured results are in close agreement with simulated results. The radiation patterns are shown in figure 5.43. The gain and directivity variation over the frequency range 5.725 – 5.875 GHz is found to be less than 1 dB. The measured and simulated S^{11} versus frequency plots of single and multiple parasitic patches are shown in figures 5.44 and 5.45 respectively.

Height of parasitic patches (PPs)	Size of ground plane at Z=0	Size of feed patch at z=2mm (air dielectric)	Size of first parasitic patch at 0.5λo=25.8 mm	Size of second parasitic patch at 1.0λo =51.7 mm	Size of third parasitic patch at 1.5λo =77.6 mm
0.5 λo=25.8mm	100mmx100 mm	25.4mm x21.5mm	25.4x14	-----	-----
0.5 λo=25.8mm and 1.0λo =51.7 mm	100mmx100 mm	25.4mm x21.9mm	25.4x14.5	25.4x14.4	-----
0.5 λo=25.8mm, 1.0λo =51.7 mm and 1.5λo =77.6 mm	200mmx200mm	25.4mm x21.6mm	25.4x14.5	25.4x14.5	25.4x14.1

Table 5.17 Optimized dimensions of antenna structures with finite ground

The important simulated results of above three antennas are tabulated in the following table 5.18.

PPs height (λ_o)	Dir dB	Gain dB	SLL dB	beamwidth E / H plane	Cross Pol dB
0.5	13.7	13.3	-19.5	38.5/40.1	-21.2
0.5-1.0	15.4	14.6	-18.6	25.0/25.6	-24.2
0.5-1.0-1.5	16.9	16.4	-16.7	22.8/22.0	-25.5

Table 5.18 Antenna performance of structures with finite ground

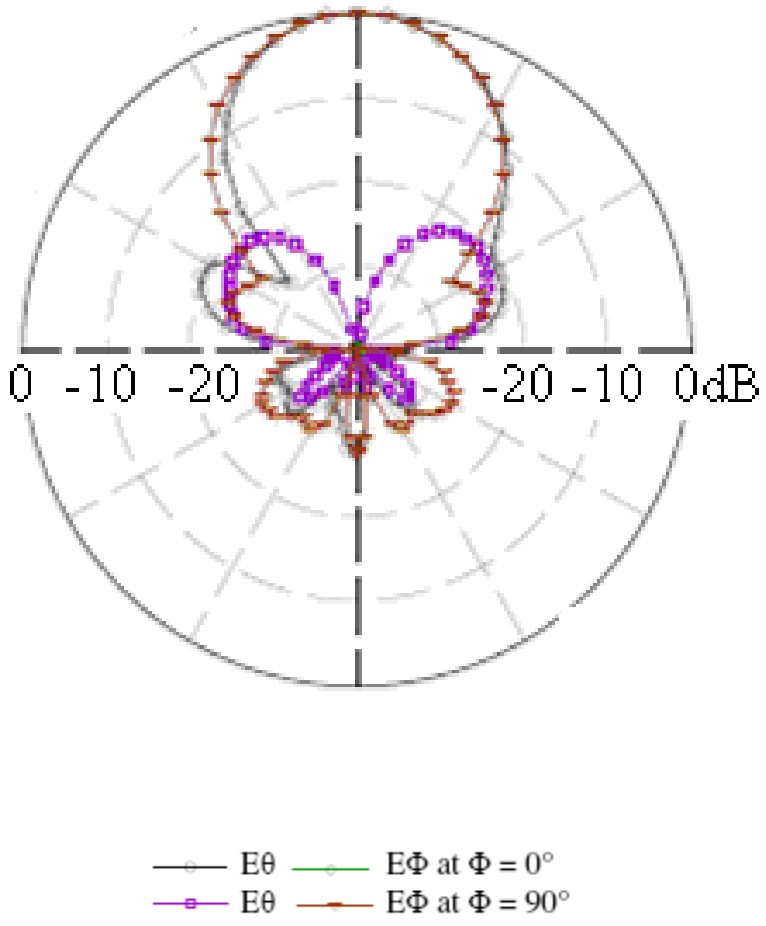

(i)Radiation pattern with only one parasitic patch at 0.5 λo

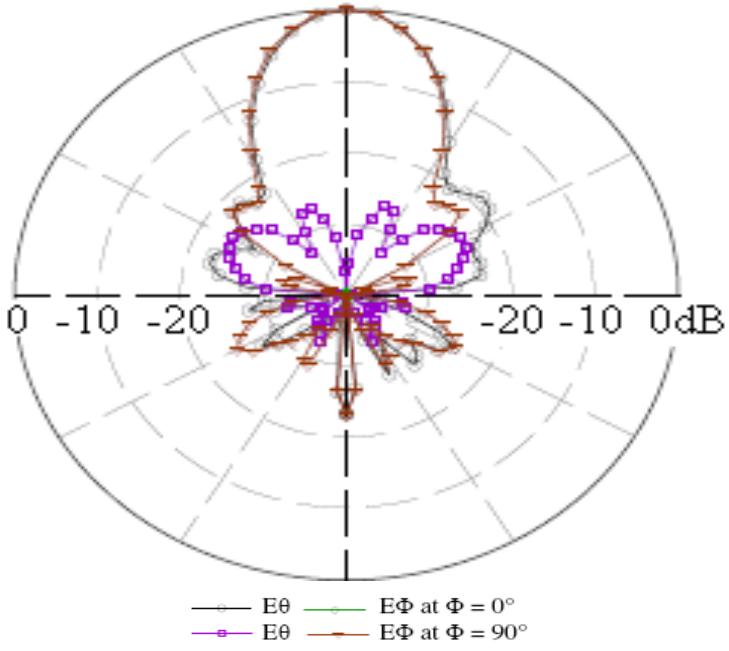

(ii) Radiation pattern with two parasitic patch at 0.5 λo and 1

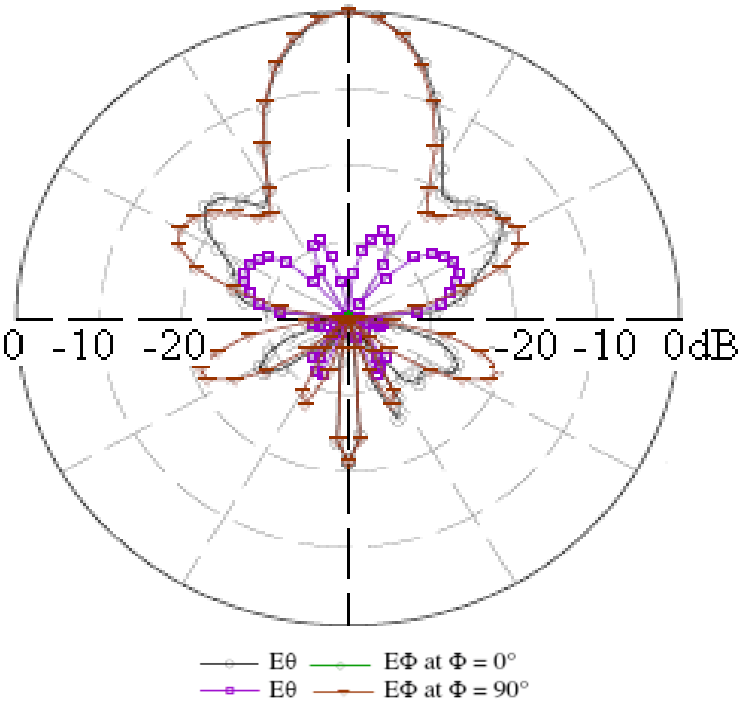

(iii) Radiation pattern with three parasitic patch at 0.5 λo , 1 λo and 1.5 λo

Figure 5.43 Radiation pattern

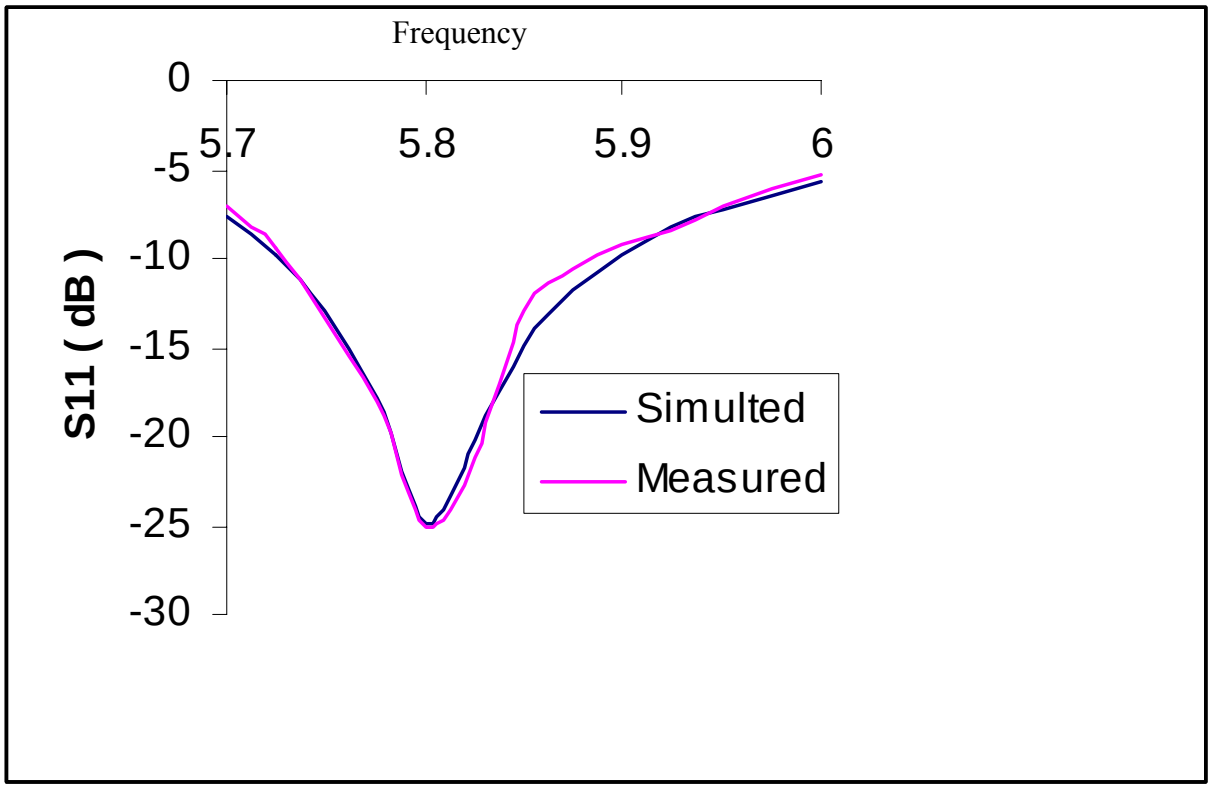

Figure 5.44 Measured and simulated S11 versus frequency plot of single parasitic patch

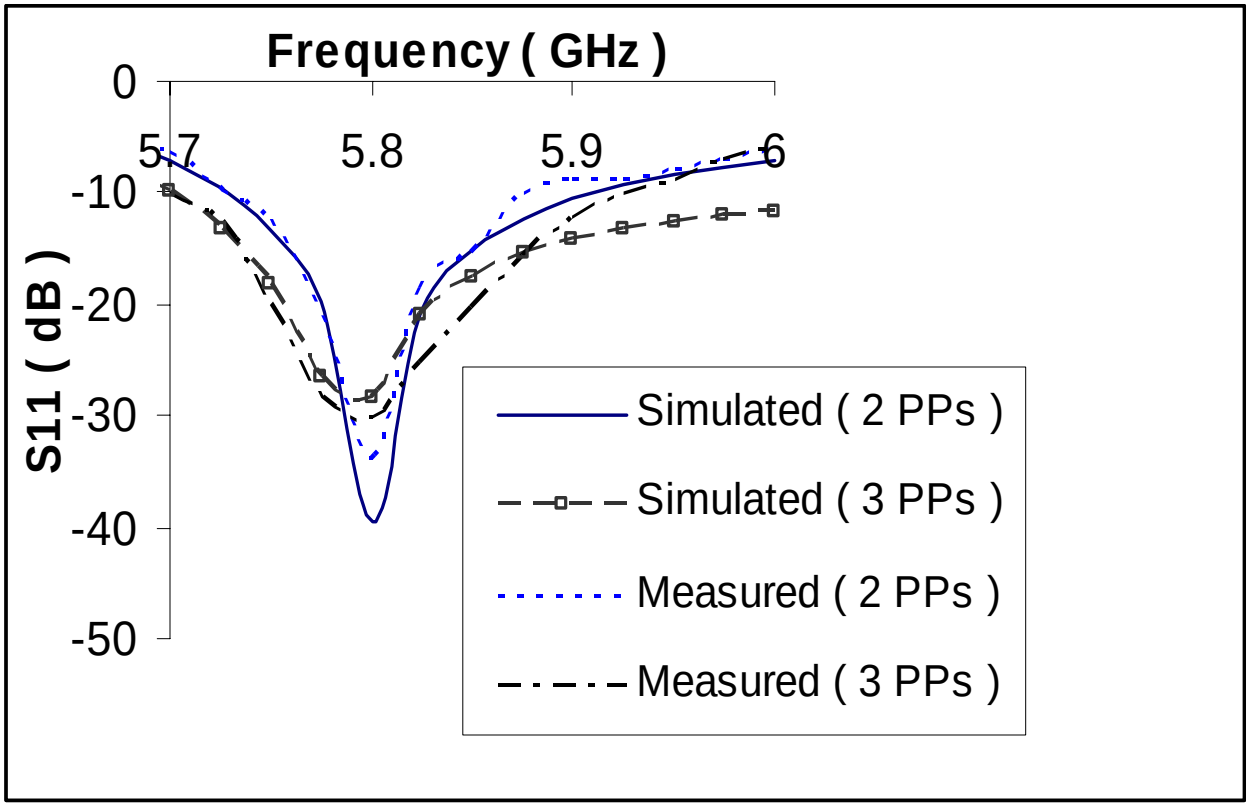

Figure 5.45 Measured and simulated S11 versus frequency plot of multiple parasitic patches

5.19.2 Conclusion

A novel efficient high gain multilayered antenna is proposed. Gain improvement in multi-layered antennas suggests that gain is a function of volume. The proposed antenna is designed on low cost easily available FR4 superstrate. Impedance and radiation pattern bandwidth characteristics are observed which cover 5.725 – 5.875 ISM bands. The results obtained clearly indicate that the proposed antenna is capable of generating efficient directive radiation pattern in the desired frequency bands.

6 Fractal Antennas

6.1 Introduction

Fractals - this word came to stand for a way of describing, calculating and thinking about shapes that are irregular and fragmented, jagged and broken up shapes. From the crystal lines of snowflakes to the discontinuous lines of dust of galaxies all are measured by fractal. 'Fractals' were first brought to light by Benoit Mandelbrot in 1975 as a way to mathematically define structures whose dimensions cannot be limited to whole numbers[103]. He coined Fractal from Latin adjective Fractus means irregular to name his shapes, his dimension and his geometry. Mandelbrot realized that it is very often impossible to describe nature using only Euclidean geometry, that is in terms of straight lines, circles, cubes and such like. Euclidean measurements represent object in terms of 0, 1, 2 or 3 dimension that unable to relate it with the geometry of irregular objects. The kind of irregularity, the complexities that are occurring in nature are not just random. Mandelbrot's work made a claim about the world and the claim was that such odd shapes and randomness carry meaning and he had even bewildered many scientists by claiming that clouds are not spheres, mountains are not cones, coastlines are not circles, and bark is not smooth, nor does lightning travel in a straight line.

One classical conundrum depicting the need for fractal geometry is the attempt to measure the boundary, like the boundary of India shown in figure 6.1. As in this thought experiment, say a surveyor were to use a ruler that is 1 kilometer long to measure the length by counting the number of ruler, lines up end to end, that fit around the boundary. By multiplying the number of rulers by 1 kilometer, has an approximate measure of length. However if he repeats the experiment with a ruler that is only 1 meter in length, the result will be different. The 1-meter ruler will measure inside coves and lagoons that the 1 Km. ruler smoothed over. Continuing in the same fashion, a 1 cm ruler will measure around rocks that the 1meter ruler missed. This can continue down to the atomic scale, with the measured length of the coast increasing every time. This way while the coast of India will fit in a finite volume on earth's surface, it is possible to take this thought experiment to limit and suggest that with a ruler small enough; the surveyor will measure the length to be infinite!!

Figure 6.1 Coastline of India

Mandelbrot's studies of irregular patterns in nature and his explorations of infinitely complex shapes evolved an idea of self-similarity. Fractals are way of seeing in infinity and it possess unique space-filling property that it can have an infinite length while fitting in a finite volume. Other than this it also possess the property of self-similarity. Self-similarity is symmetry across scale and it implies recursion, pattern inside of pattern. The self-similarity is built in to technique of constructing the curve-the same transformation is repeated at smaller and smaller scales [107]. Fractals are structures of infinite complexity with self-similar nature. What this mean, is that as the structure is zoomed in upon, the structure repeats. There never is a point where the fundamental building blocks are found. This is because the building blocks themselves have the same form as the original object with infinite complexity in each one. An example of this in nature can be seen in a fern. The entire frond has the same structure as each branch. If the individual branches were zoomed in upon, it is quite conceivable to imagine this as a completely separate frond with branches of its own [108].

Figure 6.2 Frond

The Euclidean geometry failed to explain such possibilities and thus cannot handle such situations. Therefore a better geometry was needed to handle such cases. We live in a 3dimensional world, that implies we need 3 numbers to specify appoint, for example longitude, latitude and altitude. The 3 dimensions are imagined as directions at right angles to each other. This is still the legacy of Euclidean geometry, where space has 3 dimensions, a plane has 2 and a line has one and a point has 0.

Thus Euclidean geometry was failed to capture the essence of irregular shapes that are occurring in nature and that boosted Mandelbrot to move beyond the dimension 0,1,2,3 to a seeming impossibility: fractional dimension that includes special characteristics to measure degree of roughness, randomness in nature [109]. Fractal dimension proved to be precisely the right yardstick and as a measure of how much space the fractal occupies. To define the fractional dimension of self-similar fractal geometrical structures, Mandelbrot incorporated the dimension that was formulated by Hausdorff in 1919 and put in final form by Besicovitch and called it as Fractal dimension. Thus we can find the fractal dimension using Hausdorff-Besicovitch dimensionality [103][107] that is equal to D=log (N)/log (.) where N= no. of scaled down pieces and .=scaling factor. One example of fractals that represent fractal geometry and possess fractional dimension is described in next section.

6.2 Koch Curve

Here is one classic example of Koch curve discovered by Helge Von Koch [107]. It is made up from one dimension line that explains the elegance of fractal geometry. To construct a Koch curve take a line of one unit length. Remove the middle third and replace it with two lines the same length as the one you removed. These two lines and the segment removed should make up an equilateral triangle. Repeating this with the four lines; continue repeating this with all the lines.

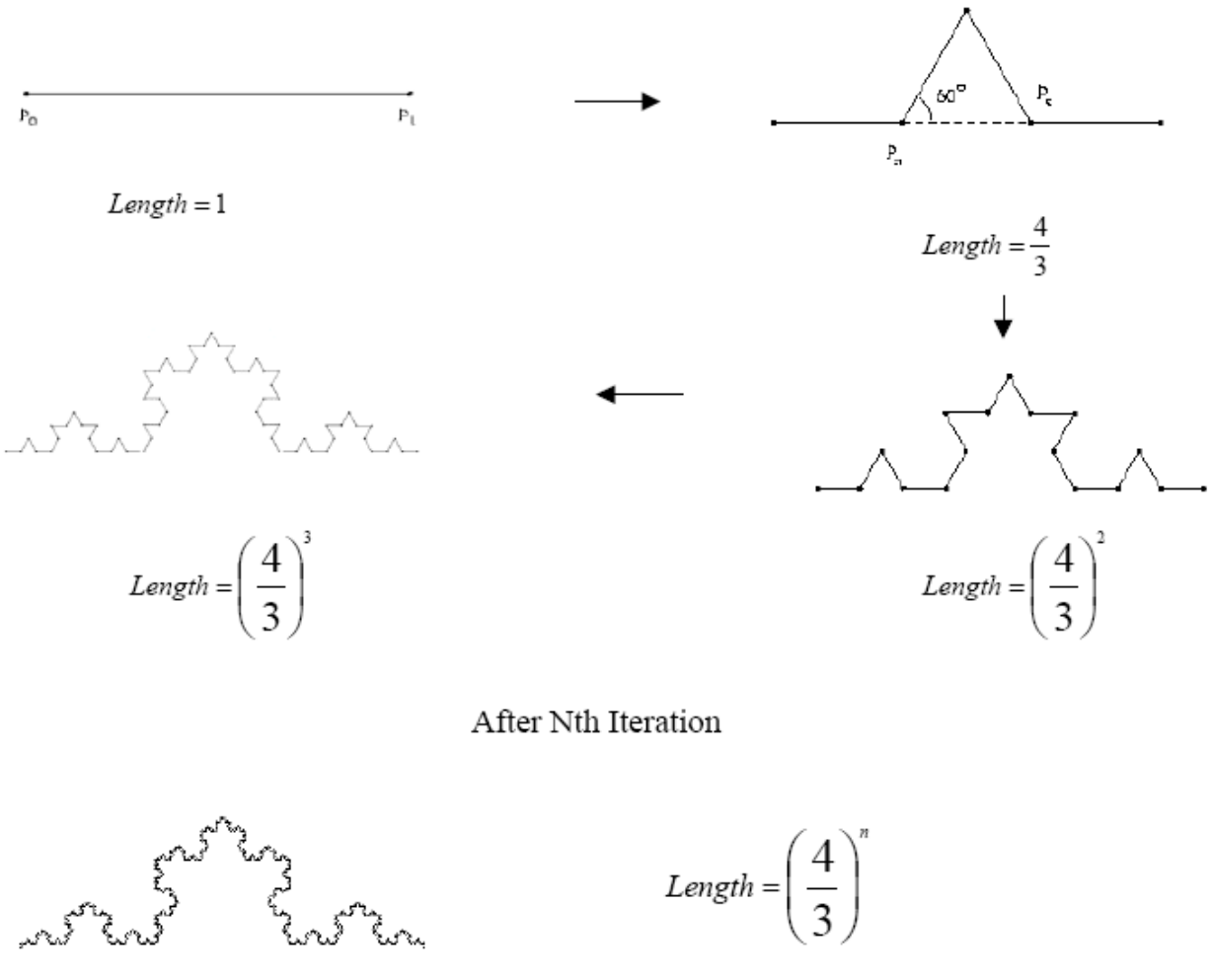

Figure 6.3 Koch Curves

The Koch Curve is a fractal object possessing a fractal dimension. Each smaller segment of the Koch Curve is an exact replica of the whole curve. As we can see from figure 6.3, at each scale there are four scaled down pieces and each one is one-third reduction of the original curve. Thus N=4, .=3 and fractal dimension will be D=log (4)/log (3)=1.2618, [110]. Thus fractal geometries possesses two important property of space-filling and self-similarity and has non-integer dimensions i.e. fractional dimensions and thus they are used to describe the structure of universe, the branching of tree leaves and plants, the sparse filling of water vapor that forms clouds, the random erosion that carves mountain faces, the jaggedness of coastline and bark and many more examples in nature.

Just as nature is not confined to Euclidean geometries, antenna designs should not be confined as well. Looking at geometries whose dimensions are not limited to integers may lead to the discovery of antennas with improved characteristics over that which exists today. This geometry was made use to design better antennas than the one with Euclidean geometry can provide. Fractal antennas have shown the possibility to miniaturize antennas and to improve input matching. Mathematicians usually refer to fractals as having n-iterations where n is taken to infinity. In fact, no graphic or physical representation of a fractal is capable of meeting this criterion. Physicists, computer scientists, and engineers have adopted the less constraining and realistic description of fractals as having a finite number of iterations. Certainly one needs at least two to claim the self-similar aspect of fractals. We in our project have moved onto 3 iterations.

6.3 Other Fractal Antennas

An FEA (Fractal Element Antenna) is an antenna that has been shaped in a fractal fashion. This can either be through bending or shaping a volume or introducing holes. Fractal elements have been around for a very long time—but were not discussed as such. The log periodic array element of Isbell and DuHamel is clearly a fractal. Log periodic have been an important antenna design class for 50 years. The home TV antenna is a variation of this idea. Twenty years ago, Landstorfer and Sacher, using optimization

approaches, came up with randomly bent antenna designs, which are clearly random fractals—but again not discussed as such [112].

In 1988, Dr. Nathan Cohen built the first bona fide FEA [112]. In October 1994, Cohen first publicly reported his results, defining FEA and elaborating on their characteristics, such as multi-band and broadband capabilities; shrinking of size; and so on. In August 1995 Cohen published the very first FEA article. This included modeling and measurement data on multi-band and broadband capabilities; shrinkage; and so on. An independent corroboration of some FEA properties by a university group in Spain was submitted only two months later and published in January 1996. The science of FEA is now well established in the mainstream of electromagnetics and engineering. All this happened in less than a decade from first discussion to recognition and acceptance and it started with the humble bending of a piece of wire. FEA are self-loading so no antenna parts, such as coils and capacitors, are needed to make them resonant. In addition they often do not require any matching circuitry for their multiband or broadband capabilities. In effect the fractal design 'does the work', thus lowering the cost and increasing the reliability compared to other options. Multiband behavior is manifest at non-harmonic frequencies, while some bands are broadened. At the higher frequencies the FEA is extremely and naturally broadband.

6.4 Sierpinski Carpet

The Sierpinski Carpet is named after the Polish mathematician Waclaw Sierpinski 1882- 1916 who described some of the main properties of this fractal shape in 1969. To construct Sierpinski Carpet a square was taken as shown in figure 6.4(a). It was then virtually divided into 9 smaller congruent squares, each of which is one-third of the original square and the center square was removed to get the first iteration shown in figure 6.4(b). Similarly subdividing each of the eight remaining solid squares into 9 congruent squares and removing the center square we get the figure 6.4(c), the second iteration. Continuing in the same fashion we obtain further iterations of the Carpet. For ideal fractal this process goes on for infinite number of times [113].

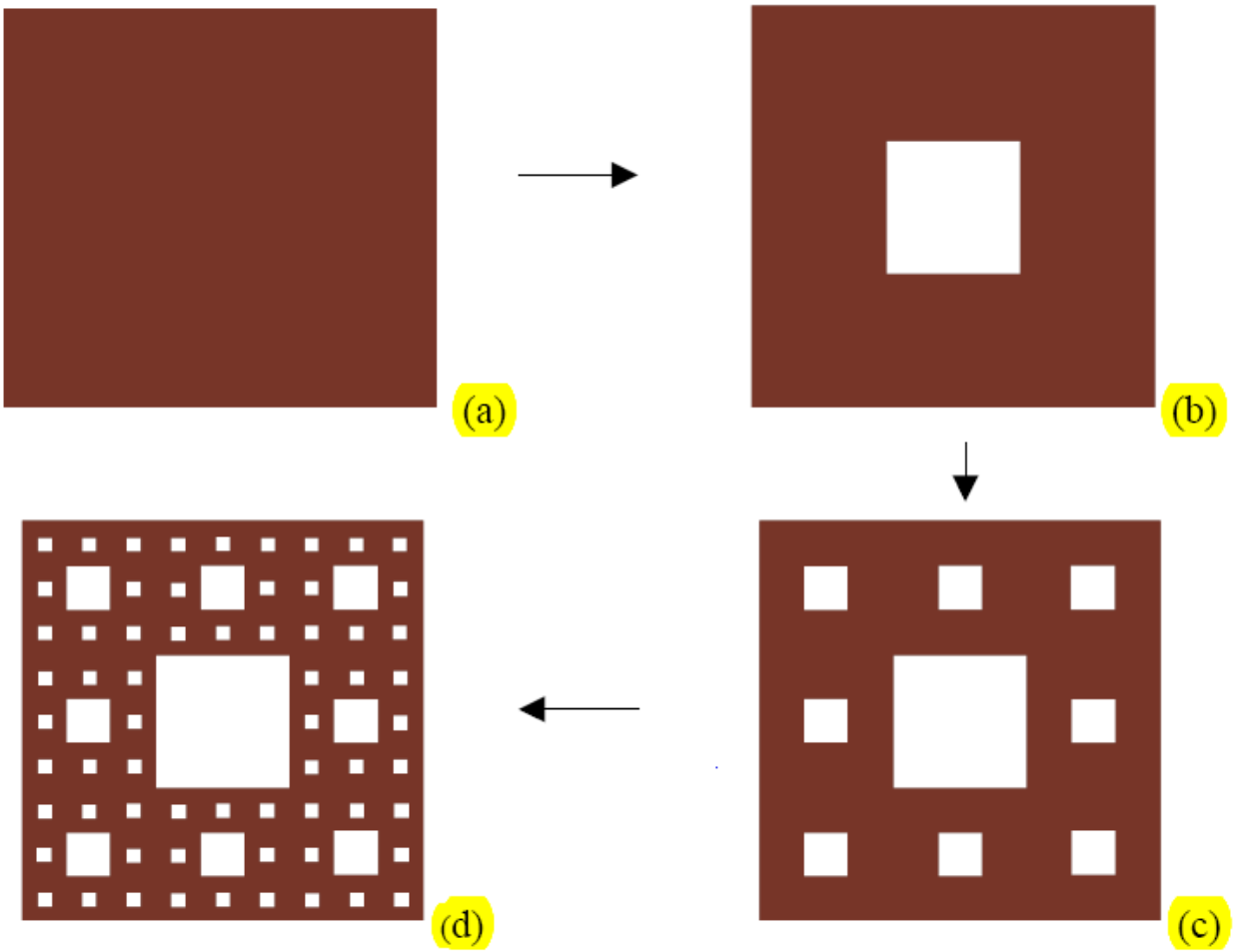

Figure 6.4 Sierpinski carpet antnnas

The fractal dimension is found using the Hausdorff-Besicovitch dimensionality, which comes out to be D=log 8 / log 3 = 1.89. After every iteration, we leave 8/9 of the area of the figure. To find the area of the figure after some number of iterations, we have to raise 8/9 to the power of that number. Although it doesn't seem so, after an infinite number of iterations, the area will become 0. In ideal case it is repeated for infinite number of times but we have shown the finite number to describe its multi-band characteristics. Here we have compared the scaled down version of patch that results due to self-similar pattern and how it incorporated the multi-band characteristics.

6.5 Fractal Antenna Analysis

The Sierpinski Carpet Antenna (SCA) was designed using the Microstrip Patch of length of 54.0 mm. The RT-Duroid 5880 substrate layer was used with dielectric constant Єr =2.2 and thickness h=1.6mm. The S_{11} parameter (return loss) was measured for each case. The antenna was analyzed using the moment method and resonant frequency was observed using the S_{11} plot. The Sierpinski Carpet Antennas are of 54.0 mm X 54.0 mm and are fed with co-axial feed.

From the S_{11} plots of sierpinski carpet (figure 6.5) it is observed that SCA is resonating around 1.8 GHz, 2.7 GHz, 3.6 GHz and 5.8 GHz.

First Iteration: The 54.0 mm X 54.0 mm patch is divided into nine equal squares and the middle square is removed. This operation generates the geometry as shown in figure 6.7. The feed is placed at (-10-10). The analysis is done over the frequency range from 1 GHz. to 7 GHz. The S_{11} plot of this patch is shown in figure 6.8. The patch resonates at 1.6 GHz, 4.0 GHz, 5.6 GHz and 6.0 GHz etc.

Second Iteration: In the first iteration, the 54.0 mm X 54.0 mm patch was divided into nine equal squares and the middle square was removed. In the second iteration, all the remaining eight squares are again divided into nine squares and the middle square is removed. This operation generates the geometry as shown in figure 6.9. The feed is placed at (-18-9). The analysis is done over the frequency range from 1 GHz to 7 GHz. with a mesh frequency of 7 GHz. The S_{11} plot of this patch is shown in figure 6.10. The patch resonates at 2.4 GHz, 4GHz, 5.6 GHz and 6 GHz etc.

Third Iteration: After doing the third iteration on the geometry as shown in figure 6.9, generates the geometry as shown in figure 6.11. The feed is placed along the left lower diagonal. The simulation is done over the frequency range upto 10 GHz. with a

mesh frequency of 7 GHz. The S_{11} plot of this patch is shown in figure 6.12. The patch resonates at 1.7 GHz, 2.4GHz, 5.0 GHz and 9.5 GHz.

6.6 Results

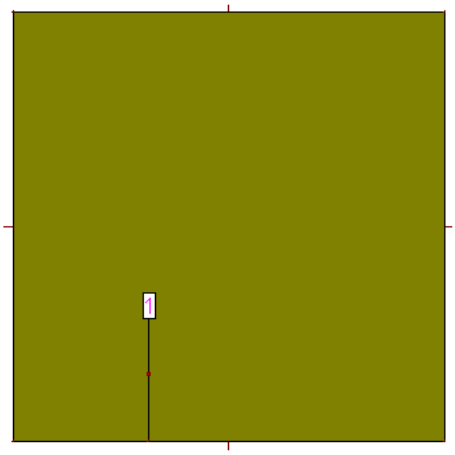

Figure 6.5 Sierpinski carpet

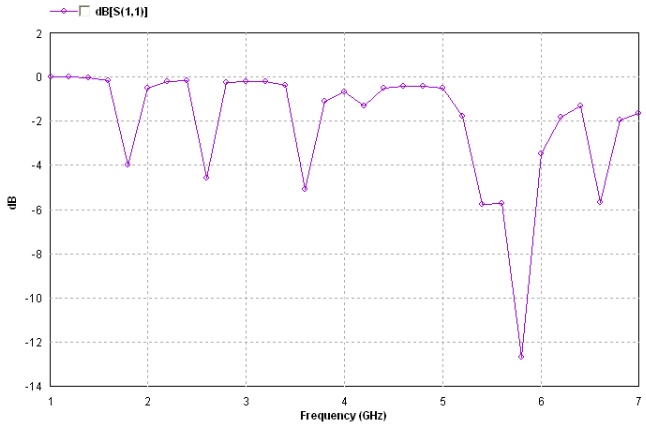

Figure 6.6 S_{11} plot for Sierpinski carpet

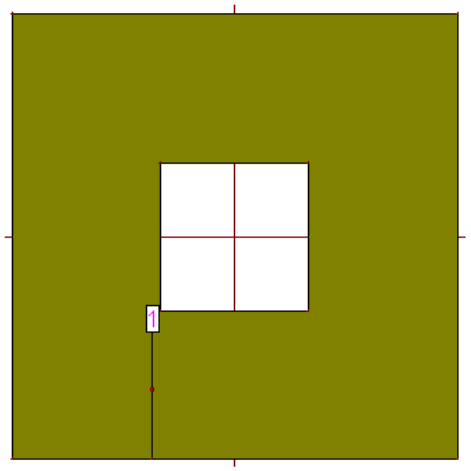

Figure 6.7 Sierpinski carpet - Ist Iteration

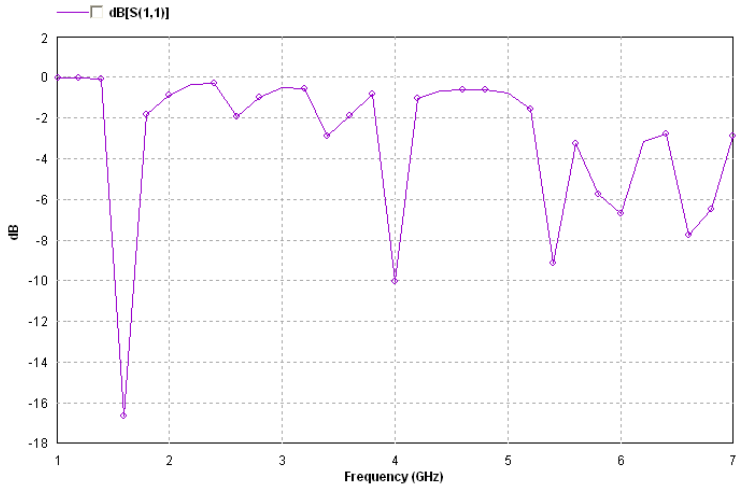

Figure 6.8 S_{11} plot for Sierpinski carpet - Ist Iteration

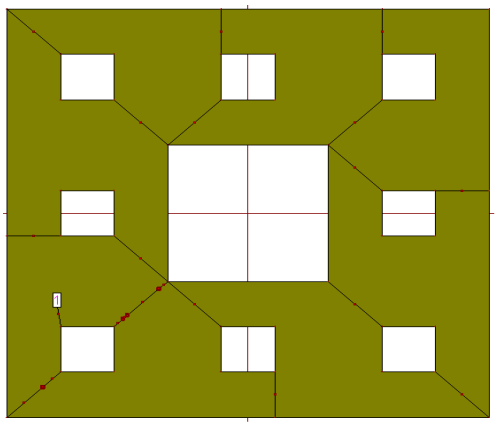

Figure 6.9 Sierpinski carpet - IInd Iteration

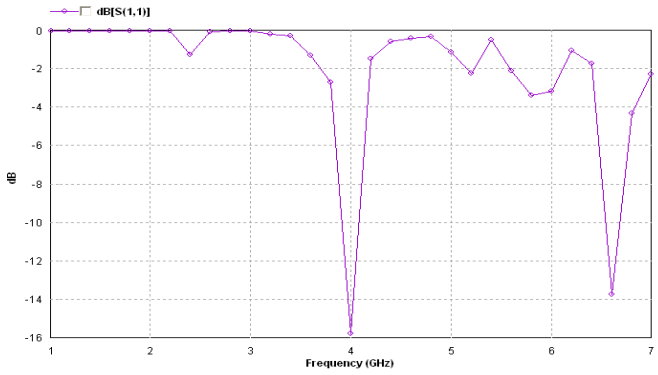

Figure 6.10 S_{11} plot for Sierpinski carpet - IInd

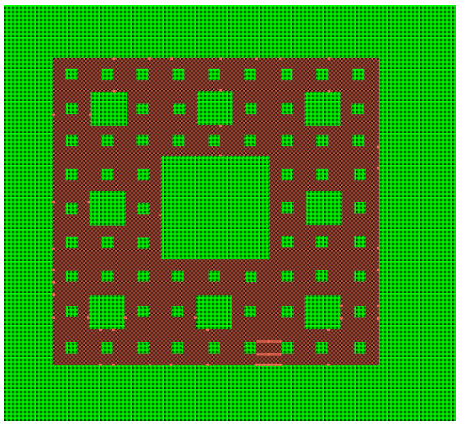

Figure 6.11 Sierpinski carpet - IIIrd Iteration

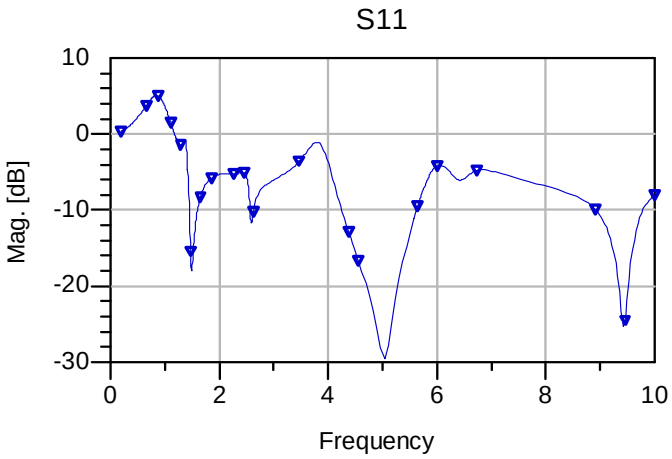

Figure 6.12 S_{11} plot for Sierpinski carpet - IIIrd Iteration

6.7 Application of Fractal Element Antennas

While much of the current research and development work has centered on the 900 MHz, PCS and S-band applications, fractal antenna design techniques can be applied to any frequency and any type of antenna, such as dipoles, monopoles, and helices. FEA's proven products and embedded components power some of today's most innovative applications—from RFID, to telematics, to electronic warfare and signal

intelligence. Fractal antennas have superior multi-band performance. The main motives for considering fractal antennas for such applications are:

• Design multi-band antennas: -Antennas are usually designed to operate over a small frequency band. In order to achieve a completely frequency-independent antenna it must be designed to not have any characteristic size, or the structure must at least include many characteristic sizes in order to be able to operate over many different frequency bands. Fractals do not have any characteristic size. Fractal structures with a self-similar geometric shape consisting of multiple copies of themselves on many different scales have therefore the potential to be frequency-independent or at least multi-frequency antennas.

• Design effective antennas: - Fractal antennas are of uneven shapes and sharp edges, corners, and discontinuities tend to enhance radiation of electromagnetic energy from electric systems. Fractal antennas have therefore the potential to be efficient. This is particularly interesting when small antennas are to be designed, since small antennas are not generally good at radiating electromagnetic energy. For example, it has been found that a monopole based on the Koch fractal curve is more efficient than an ordinary monopole of same size.

Furthermore fractal antennas can also enrich applications that include multi-band transmissions. This area has many possibilities ranging from dual-mode phones to devices integrating communication and location services such as GPS, the global positioning satellites. Fractal antennas also decrease the area of a resonant antenna, which could lower the radar cross-section (RCS). This benefit can be exploited in military applications where the RCS of the antenna is a very crucial parameter [108].

6.8 Conclusion

The object of the above work presented in this chapter was to study the fractals, their geometry and applying that geometry in design of an antenna. The self-similar property of fractals and how that property can be utilized in multi-band antenna construction are studied and implanted here. Fractals have self-similarity in their geometry, which is a feature where a section of fractals appears the same regardless of how many times the section is zoomed in upon. Self similarity is the geometry creates effective antennas of different scales. This can lead to multi-band characteristics in antennas, which is displayed when an antenna operates with a similar performance at various frequencies. The Sierpinski Carpet fractal is chosen as the geometry to test this feature due to its astounding similarities in performance as an antenna at various frequencies. The self-similar nature of Sierpinski Carpet was analysed using the Agilent's Advanced Design System (ADS) Momentum Electromagnetic Magnetic (EM) Simulator [106]. The results presented here establish a link between the self-similarity of Sierpinski Carpet Antenna and its frequency response. It has been shown that the Sierpinski Carpet Antenna is an efficient radiating element, which exhibits multi-band characteristic.

In future, fractal antennas can be studied in several ways. They can be implemented into current developing technologies in wireless market. For specific application changes have to be subsequently made into the antenna before fabrication. There are many applications that can be benefit from fractal antennas. Examples of these types of applications include personal hand-held wireless devices such as cell phones and other wireless mobile devices such as laptops on wireless LANs and PDAs. Thus, a possible avenue for future work is to investigate other types of fractals for antenna applications. A novel and intriguing development is the use of fractal patterns for antenna arrays.

6.9 Discussion

6.9.1 Method to Increase Horizontal Component

Let the patch is placed in horizontal plane. The radiations are produced due to the field between the ground plane and the radiating patch. The electric field lines directed towards or away (receding / going away) the radiating patch are terminated at the ground patch. The size of the radiating patch decides the resonance frequency. The intensity of horizontal component does not increase much more if the size of the ground plane is equal or more or even infinite as compared to the size of the radiating patch. Because in all these cases the field generated at the edges of the radiating patch get terminated immediately in the near by ground patch.

On the other hand if the size of the ground patch or ground plane is smaller than the radiating patch, the field generated along the edges of the radiating patch have to travel more distance in horizontal direction to get terminated in the ground patch. This increases the horizontal component of the field and hence increases the radiating field and the bandwidth also.

6.9.2 Bandwidth Improvement

The above paragraph explains that the horizontal component increases the far field radiations. It does not explain how the bandwidth increases due to increase in the horizontal components. Following section explains how the horizontal components increase the bandwidth.

6.9.2.1 Fields in an ordinary MSA (Microstrip Antenna)

When a wave is launched on the patch at the feed point, it travels in both the directions (right & left). Most of the power is radiated from the edges due to the horizontal component of the fields. The horizontal components start exactly at the edge

and have equal lengths. In actual sense, few lines originate little bit inside the edge also; this field is responsible for radiating high frequencies of the band. The field produced exactly at the edge and the fringing field are responsible for producing low frequencies of the band. This is shown clearly in the figure 6.13.

6.9.2.2 Fields in a MSA (Ground Patch Size Less Than Radiating Patch)

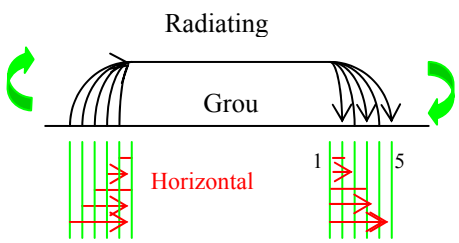

Figure 6.13 Electric fields in a patch (radiating patch smaller than ground patch)

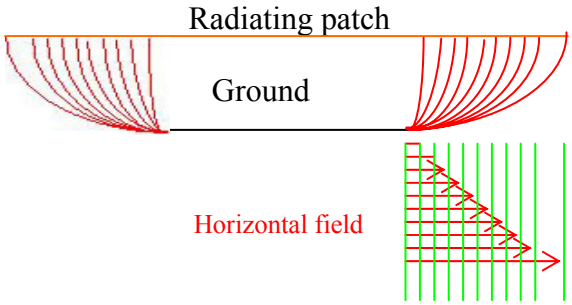

Figure 6.14 Electric fields in a patch (ground patch smaller than radiating patch).

In the above figure 6.13, the size of the radiating patch is less than the ground. If we take a patch in which the size of the radiating patch is more than ground then obviously the horizontal component will increase as discussed above. The field pattern between the radiating patch and the ground will be as shown in Figure 6.14. In this case, as shown in figure 6.14, the horizontal field increases a lot. The length of the H field is many times larger than the field produced in case of the ordinary patch in which the radiating patch is smaller than ground. The inner side field produces high frequencies and the outer side field must be producing lower frequencies. As the difference between the H component of the inner field and the H component of the outer field is more we get very wide bandwidth. The bandwidth depends on the absolute as well as the relative sizes of the two patches. It also depends on the relative positions of the two patches.

6.10 Sierpinski Gasket Microstrip Antenna

Figure 6.15 shows the sierpinski gasket antenna. The area of the ground plane is around twice the sierpinski gasket radiating patch. The thickness of the substrate is 1.6 mm and the dielectric constant is 2.2. The dimensions of the sierpinski are 54.0 mm X 54.0 mm. The feed is placed along diagonal at the lower left corner. The bandwidth obtained in this case is shown in Figure 6.16.

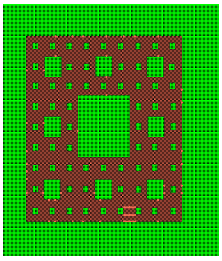

Figure 6.15 Sierpinski gasket

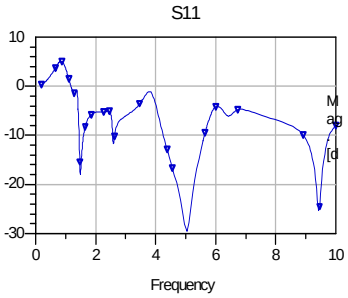

Figure 6.16 Plot for bandwidth

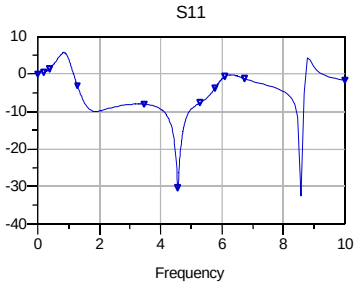

Figure 6.17Plot of bandwidth (for slotted multi point)

The ground and the patch are interchanging (the ground is connected to the sierpinski patch and the port is connected to the green bigger patch) and in order to improve the frequency response or the bandwidth the slotted patch is grounded at various points. The improved frequency response is shown in figure 6.17. Here we get wide bandwidth from approximately 1.98 GHz to 5.00 GHz. Between 2.0 to 4.0 GHz, the S_{11} curve comes little bit above the –10 dB, this also can be improved by proper grounding.

6.11 Conclusions

This is a totally new technique to improve the bandwidth. It gives deeper understanding for improving bandwidth of microstrip antenna. The bandwidth of sierpinski antenna can be increased using this method. This method may be used to improve bandwidth of other types of microstrip antennas.

7 Conclusions and Future Work

The impedance bandwidth of the microstrip antenna (MSA) is around 1% only for thin substrates. The bandwidth of the MSA can be increased by increasing thickness of the substrate. If the thickness is increased, it creates problems for impedance matching, produces radiations from the feed and distortions in the radiation patterns due to higher order modes. Therefore to avoid these problems, thicker substrate is not used. The common techniques to improve the bandwidth are Planar multi-resonator configurations, Electromagnetically coupled MSAs; Aperture coupled MSAs, Impedance matching networks for broadband MSAs & Log periodic MSA configurations. It is advantageous to use Electromagnetically coupled MSA because of its small size and no back radiations. Therefore, Electromagnetically coupled MSA is used to design the antenna.

Antenna polarization is a very important consideration when choosing and designing an antenna. Most communications systems use either vertical, horizontal or circular polarization. Knowing the difference between polarizations and how to maximize their benefit is very important to the antenna user. A linear polarized antenna produces linearly polarized wave, a circular polarized antenna produces circularly polarized wave. Here, the microstrip antenna with switchable polarization [30-37] are designed which are useful for some specific applications in wireless communication, such as multi-system operation, frequency reuse and reducing multipath fading.

Modern communication systems, such as those for satellite links (GPS, vehicular-Jar, etc.), for mobile communication, and for emerging applications, such as Wireless local-area networks (WLANs), often require compact antennas at low cost [12-16] Further, due 1:0 their lightness, micros trip antennas are well suited for Airborne applications, such as synthetic aperture radar (SAR) systems and scatterometers. In addition to compactness the antenna may be required to provide circular polarization as in satellite links. In some applications, operation at two or more discrete bands and an arbitrary separation of bands is desired. Further, all bands may be required to have the same polarization, radiation Pattern, and input impedance characteristics.

Microstrip patch antennas are very narrow band antennas. There are various methods to improve the bandwidths of such types of antennas, for example using parasitic elements, impedance matching networks and stacked multiresonators [17] etc. But the design of such antennas become complex and can yield maximum 30% bandwidth. In this report an easy method is described to obtain large (up to 95%) bandwidth. A single layer C shape micro strip patch suspended (5 mm) above ground plane gives the large bandwidth. It is compact and radiates in a wide band.

In case of microstrip antenna the most important factors are wide bandwidth, polarization purity, high gain and high power handling capability. These demands can be fulfilled using an array of wideband antennas. Apart from these factors some times various types of polarizations schemes are important to handle the problems of fading, co-channel interference etc. In this chapter, design and simulated results of a compact broadband microstrip fed antenna are presented. This antenna gives wide bandwidth and all types of polarizations such as linear, left and right circular polarizations.

The microstrip antenna can be excited either by a coaxial probe or by a microstrip line. It can also be excited indirectly using electromagnetic coupling or aperture coupling and a coplanar waveguide feed, in which case there is no direct metallic contact between the feed line and the patch [66-69]. Feeding technique influences the input impedance and characteristics of an antenna and is an important parameter.

System studies and hardware investigations on high-speed wireless communications are being conducted at license free ISM (industrial, Scientific and Medical) band, millimeter-wave and quasi-millimeter-wave frequencies. These applications require compact, high-performance, and low-cost wireless equipment. A highly integrated RF module, the so-called system-on-package module, which employs a multilayer structure, is effective in achieving the above requirements. It is necessary to adopt active integrated antenna technology to achieve a module with antennas that are low-power consuming and have low-noise characteristics. Currently, there is considerable interest in incorporating

active devices at the level of radiating elements of large phased arrays. However, use of phased array is often avoided because of its excessive cost, technological problems in heat dissipation, parasitic effects of bias networks, lack of available space etc. Moreover, microstrip technology allows monolithic implementation by fabricating both active devices and antennas on the same semiconductor substrate.

Fractal geometries are usually used to characterize unique occurrences in nature that were difficult to define with Euclidean geometries, including the length of coastline, density of clouds, the branching of trees etc. Here antennas using fractal patters are realized in order to obtain desired performance properties such as compact size and multi-band behavior.

One of the prevailing trends in modern wireless mobile devices is a continuing decrease in physical size. In addition, as integration of multiple wireless technologies becomes possible, the wireless device will operate at multiple frequency bands. A reduction in physical size and multiband capability are thus important design requirements for antennas in future wireless devices. The use of fractal patterns in antenna design provides a simple and efficient method for obtaining the desired compactness and multi-band properties. There are many advantages of using fractals in the design of an antenna but in the present work the self-similar nature was exploited for operating fractal antenna at various frequencies and finally the fractal multi-band antenna was designed and analysed on Sierpinski Carpet Pattern. This report looks into the multi-band characteristics of Fractal Element Antennas especially, Sierpinski Carpet Antenna (SCA). Sierpinski Carpet Antenna is an approach to antenna miniaturization and exhibit multi-band characteristics due to its self-similar nature.

7.1 Discussion of Results

The impedance bandwidth of MSA is around 1% only for thin substrates. There are many techniques to increase bandwidth. It is advantageous to use Electromagnetically coupled MSA because of its small size and no back radiations. With this configuration,

10% to 30% bandwidth can be achieved. The increase in the bandwidth is obtained due to increase in the overall height of the antenna, a decrease in the effective dielectric constant ϵ_e and the multiresonator effect [17].

Polarization diversity [25] of reception is important to counter the effect of fading in communications, especially in mobile communications. The polarization of a microstrip antenna can be selected by making a proper choice for the feed location. It is also possible to obtain four different polarizations - horizontal, vertical, right-hand circular, and left-hand circular-with a single feed. Methods of obtaining circular polarization using diagonal feed, modified edge, Square microstrip antenna with modified corners, square microstrip antenna with a rectangular diagonal slot are discussed.

A C shape patch is discussed in chapter 3. It is designed and simulated to obtain wide bandwidth. If a simple rectangular patch is used, the continuous wide band from 3.7 GHz to 5.3 GHz is not achieved. In this antenna, rectangular slot is used as resonating structure, due to which this patch is converted in to C shape. In this antenna, the slot size is chosen sufficiently large so that it will resonate from 3.7 GHz to 5.3 GHz. It also radiates at ISM (2.45 GHz.) band. It gives a bandwidth of 40 MHz at ISM band. In these bands the S_{11} is less than –10 dB or the VSWR is less than 2.

Compact broadband microstrip fed electromagnetically coupled MSA is designed and analysed. In this antenna, the –10 dB bandwidth for which VSWR is less than 2 ranges from 3.7 GHz to 4.44 GHz (a bandwidth of 744 MHz). In this antenna, two types of circular polarizations (right cp & left cp) are obtained. In both the polarizations, the cross-polar level is 16 dB lower than the co-polar level.

In certain cases, an antenna which can give all types of polarizations such as E_θ, E_Φ as well as right and left circular polarizations with acceptable polarization levels, are required. High gain is obtained by forming an array. The array gives gain of 17 dB in the frequency band of 3.7 to 4.2 GHz.

In microstrip antennas, various types of feed networks are used. These have certain advantages and drawbacks. Particular type of feed is used for a particular application or antenna. All types of feeds and their advantages and drawbacks are discussed. To design an array, microstrip line, bends, corners, power splitters, power combiners and quarter wave transformers are used. All these and their design procedure are also discussed. Finally, an antenna array is designed.

Space fed microstrip antennas results shows that the side lobe level improves if the electrical length of parasitic patch is comparable to the width. Fringing effect at superstrate height comparable to λ and higher order mode radiation has been studied A detailed investigation is required to understand the higher order mode radiation in space fed microstrip antenna. These antennas may find application in mm range.

Mutual coupling effect has been studied in arrays .The results show that space fed non uniform antenna array is a promising antenna as it has the advantage of small size improved directivity and gain but also provide increased impedance bandwidth. Impedance bandwidth increases with superstrate height, feed patch height, and array size. The shape of the element and position of elements also affect antenna performance.

Other broadband antenna configurations are described in chapter 6. Here, fractal antennas are designed and analyseded. There are various types of fractal antennas like Koch curves, sierpinski antennas, etc. Koch curves and the sierpinski carpet antennas are designed and analysed. To design a sierpinski carpet antenna, a square patch is taken, port is connected to it and simulated. This is first iteration. Then for second iteration, the antenna is divided into nine parts and middle one is removed. In the second iteration the each of the remaining eight squares are again divided into nine parts and middle one is removed. Similarly third iteration results are obtained. From the results obtained here, it is clear that for the first iteration, proper bandwidth is not obtained. As one goes for higher iterations, the antenna resonates properly at various multibands giving multiband response. Again to get more bandwidth than this ground and ports are interchanged.

7.2 Proposed Further Work

Microstrip antennas should provide wide bandwidth , desired polarization and high gain. These goals are almost achieved in this work. In addition to this, some more work can be done in following areas.

- Reducing the size of microstrip element
- Improving cross-polar to co-polar levels.
- Designing the feed network which avoids unwanted radiations.
- Designing the feed network which will not affect the polarization of the antenna even if it is used in an array.
- Designing the feed network having minimum losses.

The following work can be done in case of space-fed microstrip antennas.

- Effect of shape of parasitic patch can be further investigated.
- Effect of orientation of elements in an array can be investigated
- Design and analysis of uniform spaced and non uniform 7x7 to 12x12 arrays of elements of different shapes.
- Design and analysis of stacked arrays.
- Design and analysis of circularly polarized and dual band planar arrays.

In future, fractal antennas can be studied in several ways. These can be implemented into current developing technologies. For specific applications, changes have to be subsequently made into the antenna before fabrication. There are many applications that can be benefit from fractal antennas. Examples of these types of applications include personal hand-held wireless devices such as cell phones and other wireless mobile devices such as laptops on wireless LANs and PDAs. Thus, a possible avenue for future work is to investigate other types of fractals for antenna applications. A novel and intriguing development is the use of fractal patterns for antenna arrays.

References

[1] Y. J. Sung, T. U. Jang, and Y.-S. Kim, "A Reconfigurable Microstrip Antenna for Switchable Polarization" *IEEE Microwave and Wireless Components Letters,* Vol. 14, No. 11, November 2004, pp. 534-536.

[2] Faruque, S., "High capacity cell planning based on fractional frequency reusewith optimum trunking efficiency", *Proceedings of Vehicular Technology Conference*, 1998, Volume 2, 18-21 May 1998, pp. 1458 – 1460.

[3] Saraydar, C.U.; Yener, A., "Adaptive cell sectorization for CDMA systems Selected Areas in Communications", *IEEE Journal*, Volume 19, Issue 6, Jun 2001, pp. 1041 - 1051

[4] Bellofiore, S.; Balanis, C.A.; Foutz, J.; Spanias, A.S., "Smart-antenna systems for mobile communication networks - Part 1 -Overview and antenna design", *IEEE Antennas and Propagation Magazine*, Volume 44, Issue 3, Jun 2002, pp. 145 – 154.

[5] M. Tangemann, C. Hoek, R. Rheinschmitt, "Introducing Adaptive Array Antenna Concepts in Mobile Communications Systems", *Proceedings RACE Mobile Telecommunications Workshop*, Amsterdam, May 17-19, 1994, Volume 2, pp. 714-727.

[6] M. Haardt, J. A. Nossek, "Unitary ESPRIT: How to obtain an Increased Estimation Accuracy with a Reduced Computational Burden." *IEEE Trans. Signal Processing*, vol. 43, no. 5, May1995, pp. 1232-1242.

[7] J. H. Winters, "Signal Acquisition and Tracking with Adaptive Arrays in the Digital Mobile Radio System IS-54 with Flat Fading" *IEEE Trans. Vehicular Technology*, vol. 42, no. 4**,** November 1993, pp. 377-384.

[8] J. Kennedy and M. C. Sullivan, "Direction Finding and Smart Antennas Using Software Radio Techniques", *IEEE Communications Magazine*, Vol. 33, No. 5, May 1995, pp. 62-68.

[9] S. C. Swales, M. A. Beach, D. J. Edwards, J. P. Mc Geehan, "The Performance Enhancement of Multibeam Adaptive Base-Station Antennas for Cellular Land

Mobile Radio Systems", *IEEE Trans. on Vehicular Technology*, vol. 39, no. 1, February 1990, pp. 56-67.

[10] A. R. Lopez, "Performance Predictions for Cellular Switched-Beam Intelligent Antenna Systems*", IEEE Communications Magazine*, October 1996, pp. 152-154.

[11] G. V. Tsoulos, M. A. Beach, "Capacity Enhancement for Current and Future Cellular Systems with Adaptive Multibeam Antennas", *Proceedings COST 231*, Belfort, France, January 1996.

[12] J. Bahl and P. Bhartia, *Microstrip Antennas,* Artech House, 1980

[13] J. R. James and P.S. Hall, *Handbook of Microstrip Antennas,* Vol. I and II, Peter Peregrinus Ltd., 1989.

[14] R. A. Sainati, *CAD of Microstrip Antennas .for Wireless Applications,* Artech House, London, 1996.

[15] H. F. Lee and W. Chen, *Advances in Microstrip and Printed Antennas,* John Wiley and Sons, Inc., New York, 1997.

[16] D. M. Pozar, Microstrip antennas, *Proc IEEE,* Vol. 80, 1992, pp. 79-81.

[17] Girish Kumar and K. P. Ray, "*Broadband Microstrip Antennas*", Artech House.

[18] Ramesh Garg, Prakash Bhartia, Inder Bahl, Apisak Ittipiboon, "*Microstrip Antenna Design Handbook",* Artech House.

[20] Greg Swick, "Overview of Several Multiple Element Microstrip Patch Antennas".

[21] David M. Pozar "A Review of Aperture Coupled Microstrip Antennas: History, Operation, Development, and Applications", May 1996

[22] J. F. Zurcher, "The SSFIP: A global concept for high performance broadband planar antennas", *Electronics Letters*, vol. 24, pp. 1433-1435, November 1988.

[23] S. Targonski and D. M. Pozar, "Design of wideband circularly polarized aperture coupled microstrip antennas", *IEEE Trans. Antennas and Propagation*, vol. 41, pp. 214-220, February 1993.

[24] F. Croq and A. Papiernik, "Large bandwidth aperture coupled microstrip antenna", *Electronics Letters*, vol. 26, pp. 1293-1294, August 1990.

[25] F. Croq and A. Papiernik, "Stacked slot-coupled printed antenna", *IEEE Microwave and Guided Wave Letters*, vol. 1, pp. 288-290, October 1991.

[26] F. Croq and D. M. Pozar, “Millimeter wave design of wide-band aperture coupled stacked microstrip antennas”, *IEEE Trans. Antennas and Propagation*, vol. 39, pp. 1770-1776, December 1991.

[27] M. Edimo, P. Rigoland, and C. Terret, “Wideband dual polarized aperture coupled stacked patch antenna arrayoperating in C-band”, *Electronics Letters*, vol. 30, pp. 1196-1197, July 1994.

[28] S. D. Targonski and R. B. Waterhouse, “An aperture coupled stacked patch antenna with 50% bandwidth”, *IEEE International Symposium on Antennas and Propagation*, Baltimore, MD. 1996.

[29] EIE332 Electromagnetics, “Microstrip Patch Antennas”.

[30] D. H. Schaubert, F. G. Farrar, A. Sindoris, and S. T. Hayes, “Microstrip antenna with frequency agility and polarization diversity,” *IEEE Trans. Antennas Propagation,*, vol. AP-29, pp. 118–123, Jan. 1981.

[31] A. Petosa, P. K. Mongia, A. Ittipiboon, and J. S. Wight, “Switchable LP/CP ferrite disk resonator antenna,” *Electronic Letters*, vol. 31, pp. 148–149, Feb. 2, 1995.

[32] F. Yang and Y. Rahmat-Samii, “A reconfigurable patch antenna using switchable slots for circular polarization diversity,” *IEEE Microwave Wireless Compon. Letters*, vol. 12, pp. 96–98, Mar. 2002.

[33] P. M. Haskins and J. S. Dahele, “Varactor-diode loaded passive polarisation-agile patch antenna,” *Electronic Letters.*, vol. 30, pp. 1074–1075, June 23, 1994.

[34] M. Boti, L. Dussopt, and J. M. Laheurte, “Circularly polarised antenna with switchable polarisation sense,” *Electronic Letters*, vol. 36, pp. 1518–1519, Aug. 31, 2000.

[35] M. K. Fries, M. Grani, and R. Vahldieck, “A reconfigurable slot antenna with switchable polarization,” *IEEE Microwave Wireless Compon. Lett.*, vol. 13, pp. 490–492, Nov. 2003.

[36] M. H. Ho, M. T. Wu, C. G. Hsu, and J. Y. Sze, “An RHCP/LHCP switchable slotline-fed slot-ring antenna,” *Microw. Opt. Technol. Lett.*, vol. 46, pp. 30–33, Jul. 5, 2005.

[37] Y. J. Sung, T. U. Jang, and Y. S. Kim, "A reconfigurable microstrip antenna for switchable polarization," *IEEE Microwave Wireless Compon. Letters*, vol. 14, pp. 534–536, Nov. 2004.

[38] John D. Kraus, "*Antennas*", Second edition, McGraw Hill.

[39] Schaubert, D. H., et al., "Microstrip Antennas with Frequency Agility and polarization Diversity", *IEEE Trans. Antenna and Propagation*, Vol. AP-29, 1981, pp. 1182-123.

[40] K. T. V. Reddy and G. Kumar, "Sequentially rotated nearly square microstrip antennas for broadband circularly polarized radiation", *Proceedings of National conference on Microwaves, Antennas and Propagation, MICROWAVE-200*1, Jaipur, India, pp.134-137, Nov. 2001.

[41] M. Kara, "Formulas for the computation of the physical properties of rectangular microstrip antenna elements with various substrate thickness," *Microwave and Optical Technology Letters,* vol. 12, pp.1360-1363, 1996

[42] M. I. Aksun, S. L. Chuang and Y. T. Lo, "On slot-coupled microstrip antennas and their applications for to CP operation", *IEEE Transactions on Antennas and Propagation,* vol 38, pp.1244-1230, 1990.

[43] J. R. James and P.S. Hall, "*Handbook of Microstrip Antennas",* vol. I and II, Peter Peregrinus Ltd., 1989

[44] R. Garg, et aI., *Microstrip Antenna Design Handbook,* Artech House, 2001.

[45] M. Himdi, J. P. Daniel and C. Terret, "Analysis of aperture-coupled microstrip antenna using cavity model", *Electronics letters,* vol. 25, pp. 391 - 392, 1989.

[46] Kosiavas, G., et.al., "The C patch small microstrip element", *Electronics Letters*, vol. 25, 1989.

[47] N. Herscovici "Suspended three dimensional microstrip radiators," *U. S. Patent application 08/669, 047*, April1995.

[48] E. Nishiyama, M. Aikawa and S. Egashira, "Stacked micro strip antenna for wideband and high gain", *IEE Proceedings-Microwave*, vol. 151, No. 2 April 2004.

[49] James, J. R., and P. S. Hall, "*Handbook of Microstrip Antennas", V*ol. I, Peter Peregrinus, Ltd., London, 1989.

[50] Gupta, K. C, and Bennella, F., "M*icrostrip Antennas Theory and Design",* Artech House, Norwood. MA, 1988.

[51] Pozar, D. M., and D. H. Schaubert, "*Microstrip Antennas: The Analysis and Design of Microstrip Antennas and Arrays",* IEEE Press, New York, 1995.

[52] Sainati, R. A., "*CAD of Microstrip Antennas for Wireless Applications",* Artech House, Norwood, MA, 1996.

[53] Lee, H. F. and W. Chen, "*Advances in Microstrip and Printed Antennas*John Wiley & Sons, Inc., New York, 1997.

[54] Damiano, J. P., J. Bennegueouche, and A. Papiernik, "Study of Multilayer Antennas with Radiating Elements of Various Geometry", *Proc. IEE Microwave, Antennas Propagation,* Part H, Vol. 137, No. 3, 1990, pp. 163-170.

[55] Sabban, A., "A New Broadband Stacked Two Layer Microstrip Antenna", *IEEE AP-S International Symposium Digest,* June 1983, pp. 63-66.

[56] Ali M., "Design of a wideband microstrip patch antenna on a PBG type substrate", Proceedings IEEE, 2002 Page(s): 48 – 51

[57] J. R. James, P. S. Hall, and C. Wood, "*Microstrip Antenna Theory and Design*", Peter Peregrinus, London, U.K., 1981.

[58] F.-S. Chang, K.-L. Wong, and T.-W. Chiou, "Low-cost broadband circularly polarized patch antenna," *IEEE Transactions on Antennas and Propagation*, Vol. 51, Oct. 2003, pp. 3006–3009.

[59] F. Yang and Y. Rahmat-Samii, "A reconfigurable patch antenna using switchable slots for circular polarization diversity", *IEEE Microwave Wireless Com. Lett.*, Vol. 12, March 2002, pp. 96–98.

[60] M. K. Fries, M. Grani, and R. Vahldieck, "A reconfigurable slot antenna with switchable polarization," *IEEE Microwave Wireless Com. Lett.*, Vol. 13, November 2003, pp. 490–492.

[61] K. C. Gupta and P. S. Hall, "*Analysis and Design of Integrated Circuit Antenna Modules*", Wiley, New York, 2000.

[62] P. M. Haskins, P. S. Hall, and J. S. Dahele, "Polarization-agile active patch antenna," *Electronic Letters,* Vol. 30, Jan. 1994, pp. 98–99.

[63] Xiao-Hai Shen, Guy A. E., Vandenbosch and Antoine R. Van de Capelle, "Study of Gain Enhancement Method for Microstrip Antennas Using Moment Method", *IEEE Transactions on Antennas and Propagation,* Vol. 43, No. 3, March 1995.

[64] Young Ju Lee, Wee Sang Park, Junho Yeo and Raj Mittra, "Directivity Enhancement of Printed Antennas Using a Class of Metamaterial Superstrates", *Electromagnetics*, Volume 26, Issue 3 & 4, July 2006, pages 203 – 218.

[65] Wood, C., "Improved bandwidth of microstrip antennas using parasitic elements" *Proc. IEE*, Part H*,* vol. 127, 180, pp. 231-234.

[66] James J. R., and P. S. Hall, "Handbook of Microstrip Antennas", vol. 1, Peter Peregrinus, London, 1989.

[67] Lee, H. F., and W. Chen, *"Advances in microstrip and printed antennas"*, John Wiley & sons, New York, 1997.

[68] Sainati, R. A., "*CAD of Microstrip Antennas for Wireless Applications",* Artech House, 1996.

[69] Pozar D. M., and B. Kaufman, "Increasing Bandwidth of a Microstrip antenna by Proximity Coupling," *Electronics letters,* Vol. 23, No. 8, 1987, pp. 368-369.

[70] Roy, J. S., et al., "Some Experimental Investigations on Electromagnetically Coupled Microstrip Antennas on Two Layer Substrate", *Microwave and Optical Technology Letters,* Vol. 4, No. 9, 1991, pp. 49-50.

[71] Pozar D. M. "Microstrip Antenna Aperture-Coupled to a Microstrip Line," *Electronics letters,* Vol. 21, No. 2, 1985, pp. 49-50.

[72] Pozar D. M. and S. D. Targosnski, "Improved Coupling for Apeture-Coupled Microstrip Antennas", *Electronics Letters,* Vol. 27, No. 13, 1991, pp. 1129-1131.

[73] Rathi V., G. Kumar, and K. P. Ray, "Improved Coupling for Apeture-Coupled Microstrip Antennas," *IEEE Transactions on Antennas and Propagation*, Vol. AP-44, No. 8, 1996, pp. 1196-1198.

[74] MacKinchan, J. C., et al., "A Wide Bandwidth Microstrip Sub-array for Array Antenna Application using Aperture Coupling", *IEEE AP-S Int. Symp. Digest,* 1989, pp. 878-881.

[75] Menzel, W., and W. Grabherr,"Microstrip Patch Antenna with Coplanar Feed Line", *IEEE Microwave and Guided Wave letters,* Vol. 1, No. 11, 1991, pp. 340-342.

[76] Menzel, W. and Grabherr, W., "A microstrip patch antenna with coplanar feed line", *Microwave & Guided Wave Letters,* November 1991, pp. 340-342.

[77] Harokopus, W. P. and Katehi, P. B., "Microstnp antennas fed by a coplanar waveguide feeding structure", Proc., 1991, pp. 360.

[78] Aksun, M**.** I., Chuang, S. L. and Lo, Y. T., "Coplanar waveguide-fed microstrip antennas', *Microwave & Guided Wave Letters***,** July 1991, pp. 292-295.

[79] Smith R. L. and J. T. Williams, "Coplanar Waveguide Feed For Microstrip Patch Antenna", *Electronics Letters,* Vol. 28, No. 25, 1992, pp. 2272-2274.

[80] Reference: I. J. Bahl and D. K. Trivedi, "A Designer's Guide to Microstrip Line", *Microwaves,* May 1977, pp. 174-182.

[81] R.J.P. Douville and D.S. James, Experimental Characterization of Microstrip Bends and Their Frequency Dependent Behavior, 1973 IEEE Conference Digest, October 1973, pp. 24-25.

[82] R.J.P. Douville and D.S. James, "Experimental Study of Symmetric Microstrip Bends and Their Compensation", *IEEE Transactions on Microwave Theory and Techniques*, Vol. MTT-26, March 1978, pp. 175-181.

[83] Cristal, E.C., "Meander-line and hybrid meander-line transformers", *IEEE Trans. Microw. Theory Tech.,* 1973, Vol. 21, No. 2, pp. 69-75

[84] Matthaei, *C* L., Young, L. and Jones, E.M.T., "Microwave Filters, Impedance-matching Networks and Coupling Structures", McGraw-Hill, New York, 1964.

[85] HP Eesof, Libra, v. 6.1, 1996.

[86] D.M.Pozar, S.D. Targonski and H.syrigos, "Design of millimeter wave microstrip reflectarrays", *IEEE Transactions on Antennas and Prorogation*, Vol.45, No.2, February 1997, pp.287-295.

[87] R D Javor, Xiao-Dong Wu and Kai Chang, "Design and Performance of a Microstrip Reflectarray Antenna", *IEEE Trans. on Antennas and Propagation* Vol. 43, No. 9, September 1995, pp. 932-939.

[88] J Huang and Ronald J Pogorzelski , "A Ka Band Microstrip Reflect Array With Elements Having Variable Rotation Angles", IEEE *Trans. on Antennas and Propagation,* Vol. 46, No.5, May 1988, pp. 650-656.

[89] J.Huang, "Bandwidth Study Of Microstrip Reflectarray Antenna and a Novel Phased Reflectarray Concept", *Proceedings of IEEE International Symposium Antenna and Propagation*, Newport Beach, C A , June 1995, pp. 582-585.

[90] D.M. Pozar and S.D. Targonski, "A microstrip reflectarray using crossed dipoles", *IEEE Int. Symposium Antenna and Prorogation*, Atlanta, GA, July 1998, pp.1008-1011.

[91] P.N. Chine and Girish Kumar, "Three Dimensional, Efficient, Directive Microstrip Antenna Arrays," IEEE *International Symposium on Antenna and Propagation,* Washington DC, July 2005.

[92] P.N.Chine, "Design and Development of Space fed Microstrip Antenna Array," *M. Tech. Thesis*, IIT Bombay, 2005.

[93] C.A. Balanis, *"Antenna Theory: Analysis and Design"*, John Wiley & Sons, Inc., 2002.

[94] G. Kumar and K.P. Ray, "*Broadband Microstrip Antennas",* Artech House, Norwood, MA, 2003.

[95] IE3D release 12.0, *Zeland software Inc.*, Fremont, CA., USA, 2005.

[96] H. Legay and L. Shafai, "A new stacked microstrip antenna with large bandwidth and high gain," *Proc. IEEE AP-S Int. Symp. Digest*, Jul. 1993, pp. 948–951.

[97] S. D. Targonski, R. B. Waterhouse, and D. M. Pozar, "Design of wide-band aperture-stacked patch microstrip antennas," *IEEE Trans. Antennas Propag.*, vol. 46, no. 9, Sep. 1998, pp. 1245–1251.

[98] R. B. Waterhouse, "Stacked patches using high and low dielectric constant material combinations," *IEEE Trans. Antennas Propag.*, vol. 47, no. 12, Dec. 1999, pp. 1767–1771.

[99] R. Li, G. Dejean, M. Maeng, K. Lim, S. Pinel, M. M. Tentzeris, and J. Laskar, "Design of compact stacked-patch antennas in LTCC multilayer packaging modules for wireless applications," *IEEE Trans. Adv. Packag.*, vol. 27, no. 4, Nov. 2004, pp. 581–589.

[100] E. Nishiyama, M. Aikawa, and S. Egashira, "Three-element stacked microstrip antenna with wide-band and high-gain performances," *IEEE AP-S Symp. Dig.*, vol. 2, Jun. 2003, pp. 900–903.

[101] T. Seki, K. Nishikawa, and K. Cho, "Multi-layer parasitic microstrip array antenna on LTCC substrate for millimeter-wave system-on-package," *Proc. 33rd Eur. Microwave Conf.*, Oct. 2003, pp. 1393–1396.

[102] T. Seki, N. Honma, K. Nishikawa, and K. Tsunekawa, "High efficiency multilayer parasitic microstrip array antenna on Teflon substrate," *Proc. 34th Eur. Microwave Conf.*, Oct. 2004, pp. 829–832.

[103] B. B. Mandelbrot, The Fractal Geometry of Nature, *Freeman,* 1983.

[104] Tian Tiehong; Zhou Zheng; "A novel multi-band antenna: fractal antenna", *Communication Technology Proceedings ICCT, 2003*.

[105] Ji-Chyun.Liu, Yi-Je.Liu, Dau-Chyrh Chang, Chung-Chi Chang and Ching Cheng "Fractal Multiband Antennas Based on Lotus –Pod Patterns" *Microwave and Optical Technology Letters*, Wiley Periodicals, Inc.

[106] Agilent Technologies, "Advanced Design System".

[107] Addison S Paul, "Fractal and Chaos An illustrated course", 2005, pp. 1-24.

[108] J. Gianvittorio, "Fractal Antennas: Design, Characterization and Applications".

[109] James Gleick, "Chaos: Making a New Science", pp. 91-115.

[110] H.O. Peitgen, H. Jurgens, and D.Saupe, "Chaos and Fractals: New Frontiers of Science", 1992.

[111] *http://www.fractenna.com/faq/faq.html*

[112] N.Cohen, "Fractal Antenna Applications in Wireless Telecommunications".

[113] Elkamchouchi, H.M., Abouelseoud, G., "A compact broadband Sierpinski gasket patch microstrip antenna", *Proceedings of the Twenty-First National Radio Science Conference*, 16-18 March 2004, pp. B1 - 1-8.